EFFECTS OF POLYTETRAFLUOROETHYLENE MICRO–PARTICLES ON MECHANICAL AND TRIBOLOGICAL PROPERTIES OF GLASS FIBER REINFORCED POLYOXYMETHYLENE

JASBIR SINGH A/L KUNNAN SINGH

FACULTY OF ENGINEERING
UNIVERSITY OF MALAYA
KUALA LUMPUR

2020

EFFECTS OF POLYTETRAFLUOROETHYLENE MICRO–PARTICLES ON MECHANICAL AND TRIBOLOGICAL PROPERTIES OF GLASS FIBER REINFORCED POLYOXYMETHYLENE

JASBIR SINGH A/L KUNNAN SINGH

THESIS SUBMITTED IN FULFILMENT OF THE REQUIREMENTS FOR THE DEGREE OF DOCTOR OF PHILOSOPHY

FACULTY OF ENGINEERING
UNIVERSITY OF MALAYA
KUALA LUMPUR

2020

UNIVERSITY OF MALAYA
ORIGINAL LITERARY WORK DECLARATION

Name of Candidate: **JASBIR SINGH A/L KUNNAN SINGH**

Matric No: **KHA140045**

Name of Degree: **DOCTOR OF PHILOSOPHY**

Title of Project Paper/Research Report/Dissertation/Thesis ("this Work"):

EFFECTS OF POLYTETRAFLUOROETHYLENE MICRO–PARTICLES ON MECHANICAL AND TRIBOLOGICAL PROPERTIES OF GLASS FIBER REINFORCED POLYOXYMETHYLENE

Field of Study: **MECHANICAL ENGINEERING**

I do solemnly and sincerely declare that:

(1) I am the sole author/writer of this Work;
(2) This Work is original;
(3) Any use of any work in which copyright exists was done by way of fair dealing and for permitted purposes and any excerpt or extract from, or reference to or reproduction of any copyright work has been disclosed expressly and sufficiently and the title of the Work and its authorship have been acknowledged in this Work;
(4) I do not have any actual knowledge nor do I ought reasonably to know that the making of this work constitutes an infringement of any copyright work;
(5) I hereby assign all and every right in the copyright to this Work to the University of Malaya ("UM"), who henceforth shall be owner of the copyright in this Work and that any reproduction or use in any form or by any means whatsoever is prohibited without the written consent of UM having been first had and obtained;
(6) I am fully aware that if in the course of making this Work I have infringed any copyright whether intentionally or otherwise, I may be subject to legal action or any other action as may be determined by UM.

Candidate's Signature Date: 12 May 2020

Subscribed and solemnly declared before,

Witness's Signature Date: 12 May 2020

Name:

Designation:

ABSTRACT

Reinforcing polyoxymethylene (POM) with glass fibers (GF) enhances its mechanical properties, but at the expense of tribological performance. Formation of a transfer film to facilitate tribo–contact is compromised due to the abrasiveness of GF. As a solid lubricant, for example, polytetrafluoroethylene (PTFE) significantly improves friction and wear resistance. The effects of chemically etched PTFE micro–particles on the fiber–matrix interface of POM/GF/PTFE composites have not been systematically characterized. This research investigated the effects of PTFE micro–particles on mechanical and tribological properties of POM/GF/PTFE composites. Since PTFE is immiscible with most polymers, the surface was etched using sodium naphthalene salt dissolved in tetrahydrofuran to increase its surface energy. The porous etching layer, characterized using Scanning Electron Microscopy (SEM) and Fourier Transform Infra–Red (FTIR) techniques promoted mechanical interlocking as the matrix melt filled these surface imperfections. The effects of two variables, namely PTFE content and PTFE etch time, on the mechanical properties of the composite were studied. Experiments were designed in accordance to response surface methodology (RSM) using central composite design (CCD). Samples were prepared with different contents of PTFE (1.7, 4.0, 9.5, 15.0, or 17.3 wt.%) at different PTFE etch times (2.9, 5.0, 10.0, 15.0, or 17.1 min). Four mechanical properties of the POM/GF/PTFE composites, that is, strength, stiffness, toughness, and hardness, were characterized as a function of two studied variables. The dependency of these mechanical properties on the PTFE etch conditions was analyzed using analysis of variance (ANOVA). Overall desirability, D global index, was computed based on the combination of these mechanical properties for POM/GF/PTFE composites. A continuous three–dimensional response surface plot with D global index as z–axis and the PTFE contents and PTFE etch times as x– and y–axis permitted a visual representation where desirability can be maintained at a high level over a range of the two predictors.

The D global index was found to be 87.5%, when PTFE content and PTFE etch time were 6.5% and 10 min, respectively. Good correlation between experimental and RSM models was obtained using normal probability plots. These mechanical properties were evaluated by analyzing the fractured surfaces using SEM and the degree of crystallinity using Differential Scanning Calorimetry (DSC). Knowing these optimum conditions, tribological performance was characterized for POM/GF/PTFE composites as a function of micro–PTFE blended by weight percentage. Samples were prepared by different contents of PTFE (0, 1.7, 4.0, 9.5, 15.0 and 17.3 wt.%). The surface energy of PTFE micro–particles was increased by etching for 10 min using sodium naphthalene salt in tetrahydrofuran. Tribological performance was characterized through simultaneous acquisition of the coefficient of friction and wear loss on a reciprocating test rig in accordance to Procedure A of ASTM G133–95. Friction and wear resistance improved as the micro–PTFE weight ratio was increased. Morphology analysis of worn surfaces showed transfer film formation, encapsulating the abrasive GF. Energy dispersive X–ray spectroscopy (EDS) revealed increasing PTFE concentration from the GF surface interface region (0.5, 1.0, 1.5, 2.0, 2.5 µm).

Keywords: DOE; RSM; coefficient of friction; wear; POM/GF/PTFE composites

ABSTRAK

Apabila polyoxymethylene (POM) diperkuatkan dengan gentian kaca (GF), sifat mekaniknya meningkatkan, tetapi ia memberi kesan negatif kepada prestasi tribologi. Pembentukan filem pemindahan untuk memudahkan tribo–contact dikompromi disebabkan oleh kekasaran GF. Sebagai pelincir pepejal, contohnya, polytetrafluoroethylene (PTFE) dapat mengurangkan geseran dan kehausan permukaan. Kesan permukaan zarah mikro PTFE, yang diaktifkan secara kimia, ke atas sempadan gentian–matriks di dalam komposit POM/GF/PTFE belum pernah dikaji secara sistematik. Kajian ini menyiasat kesan–kesan zarah mikro PTFE terhadap sifat mekanikal dan tribologi bagi komposit polimer POM/GF/PTFE. Oleh kerana PTFE tidak serasi dengan kebanyakan polimer, permukaannya perlu diaktifkan menggunakan garam natrium naftalena dalam larutan tetrahydrofuran untuk meningkatkan tenaga permukaannya. Lapisan poros yang dianalisis menggunakan teknik Scanning Electron Microscopy (SEM) dan Fourier Transform Infra–Red (FTIR) didapati menggalakkan jaringan mekanikal apabila matriks dalam bentuk cecair meliputi ketidaksempurnaan permukaan ini. Kesan dua pembolehubah, iaitu kandungan PTFE dan masa pengaktifan PTFE, ke atas sifat mekanik komposit itu telah dikaji. Eksperimen telah direka mengikut Response Surface Methodology (RSM) menggunakan reka bentuk Central Composite Design (CCD). Sampel disediakan dengan komposisi PTFE yang berbeza (1.7, 4.0, 9.5, 15.0, atau 17.3 peratus berat) dan masa pengaktifan PTFE yang berbeza (2.9, 5.0, 10.0, 15.0, atau 17.1 min). Empat sifat mekanikal komposit POM/GF/PTFE, iaitu kekuatan tensile (tensile strength), modulus elastisiti (elasticity modulus), ketahanan (toughness), dan kekerasan permukaan (hardness), diperolehi sebagai fungsi yang bergantung kepada dua pemboleh ubah yang dikaji. Kebergantungan sifat–sifat mekanik ini pada mikro–PTFE dianalisis menggunakan analisis varians (ANOVA). Keupayaan keseluruhan yang diwakili oleh D global indeks, dikira berdasarkan kombinasi sifat–sifat mekanikal ini untuk komposit POM/GF/PTFE. Graf permukaan tiga dimensi yang berterusan dengan indeks D global sebagai paksi–z dan kandungan PTFE dan masa PTFE etch sebagai paksi–x dan paksi–y membenarkan perwakilan visual, di mana keinginan dapat dikekalkan pada tahap yang tinggi melalui pelbagai dua peramal yang dikaji. Indeks D, iaitu 87.5%, diperolehi apabila kandungan PTFE sebanyak 6.5% dengan masa pengaktifan zarah mikro PTFE selama 10 min. Hubungan yang baik antara model eksperimen dan RSM diperolehi dengan menggunakan carta kebarangkalian normal. Ciri–ciri mekanikal ini dinilai dengan menganalisis permukaan retak sampel selepas ujian tensile dengan menggunakan teknik SEM dan darjah kristalografi menggunakan Differential Scanning Calorimetry (DSC). Setelah mengetahui keadaan optimum ini, prestasi tribologi untuk komposit POM/GF/PTFE dikaji secara terperinci sebagai fungsi mikro–PTFE yang dicampur dengan peratusan berat. Sampel disediakan dengan komposisi yang berbeza PTFE (0, 1.7, 4.0, 9.5, 15.0, atau 17.3 peratus berat). Tenaga permukaan zarah mikro PTFE ditingkatkan dengan pengaktifan selama 10 min menggunakan garam natrium naftalena dalam larutan tetrahydrofuran. Prestasi tribologi telah dikaji melalui pengambilan data serentak bagi pekali geseran dan tahap kehausan permukaan meggunakan kaedah ujian ulang–alik berpandukan Prosedur A, ASTM G133–95. Geseran dan kehausan permukaan bertambah baik apabila nisbah berat mikro–PTFE meningkat. Analisis morfologi permukaan memperlihatkan pembentukan filem pemindahan yang dapat meliputi permukaan GF yang kasar. Spektroskopi sinaran sinar–X (EDS) mendedahkan peningkatan PTFE dari kawasan permukaan permukaan GF (0.5, 1.0, 1.5, 2.0, 2.5 μm).

Kata kunci: DOE; RSM; pekali geseran; darjah kehausan; komposit POM/GF/PTFE

ACKNOWLEDGEMENTS

First and foremost, I would like to express my deepest gratitude and most sincere thanks to my supervisor, Associate Professor Ir. Dr. Ching Yern Chee, who have been extremely helpful in providing guidance for this project. Her suggestions have so often initiated a push for me to seek further knowledge in relation to complete this project. Special thanks to my co-supervisors Dr. Shaifulazuar Razali and Professor Gan Seng Neon for their support.

My thanks to the teaching staff of Faculty of Engineering, University Malaya for their dedication to the academic field, especially for being teachers and permitting use of laboratories. They patiently answered my questions regardless of how trivial they may seem. Also, thanks to my working colleagues for their cooperation and help throughout this project.

In addition, my special thanks to my wife, Fiona Ang, my children, Arvindher Singh and Jasvindher Kaur and also to my mother, brothers and sisters for their support and being a constant source of encouragement.

TABLE OF CONTENTS

CHAPTER 3: METHODOLOGY 68

CHAPTER 4: RESULTS AND DISCUSSION 86

LIST OF FIGURES

LIST OF TABLES

LIST OF SYMBOLS AND ABBREVIATIONS

1D : One Dimensional

2D : Two Dimensional

3D : Three Dimensional

AAm : Acrylamide

ABS : Acrylonitrile Butadiene Styrene

AFM : Atomic Force Microscopy

Al_2O_3 : Alumina

ANOVA : Analysis of Variance

AF : Aramid Fiber

AP : Aramid Particles

BSD : Backscatter Diffraction

CAGR : Compounded Annual Growth Rate

CCD : Central Composite Design

CF : Carbon Fiber

CF–PP : Carbon Fiber/Polypropylene Matrix

CFRP : Carbon Fiber Reinforced Composite

CH_2Cl_2 : Dichloromethane

CNT : Carbon Nanotube

COF : Coefficient of Friction

CTE : Coefficient of thermal expansion

DCM : Dichloromethane

DOE : Design of Experiments

DMA : Dynamic Mechanical Analysis

DMM : Dimethoxymethane

DSC : Differential Scanning Calorimetry

EBF : Eucalyptus Bleached Fiber

EDS : Energy Dispersive Spectroscopy

EP : Engineering Plastic

ESCA : Electron Spectroscopy for Surface Analysis

EVA : Ethylene–vinyl Acetate

FE–SEM : Field Emission Scanning Electron Microscope

FTIR : Fourier Transform Infra–red

GF : Glass fiber

HIPS : High Impact Polystyrene

HRR : R–scale Rockwell Hardness

IPN : Interpenetrating Network

KF : Kenaf Fiber

KPIV : Key Process Input Variable

KPOV : Key Process Output Variable

MoS_2 : Molybdenum Disulphide

MWCNT : Multi–walled Carbon Nanotube

NF : Natural Fiber

OVAT : One–Variable–At–a–Time

PDMS : Polydimethylsiloxane

PEG : Polyethylene Glycol

PEO : Polyethylene Oxide

PET : Polyethylene Terephthalate

PLA : Polylactic Acid

PMMA : Polymethyl Methacrylate

PMC : Polymer Matrix Composite

POD	:	Pin on Disk
POM	:	Polyoxymethylene
POM525GR	:	Polyoxymethylene Reinforced with 25% Glass Fiber
PP	:	Polypropylene
PPS	:	Polyphenylene Sulfide
PSU	:	Polysulfide
PTFE	:	Polytetrafluoroethylene
PU	:	Polyurethane
RH	:	Relative Humidity
ROI	:	Return on Investment
RSM	:	Response Surface Methodology
SC CO_2	:	Supercritical Carbon Dioxide
SCF	:	Short Carbon Fiber
SEM	:	Scanning Electron Microscope
SGF	:	Short Glass Fiber
SiC	:	Silicon Carbide
SiO_2	:	Silica
SPC	:	Statistical Process Control
SWCNT	:	Single–walled Carbon Nanotube
TEM	:	Transmission Electron Microscope
XPS	:	X–ray Photoelectron Spectroscopy
xGnP	:	Expanded Graphene Nano Particles
ZnO	:	Zinc Oxide

d	:	Individual Desirability
D	:	Optimum Overall Desirability, Global Desirability Index
ø	:	Diameter
γ_{lv}	:	Surface Energy of Solid–Vapor Interface
γ_{sl}	:	Surface Energy of Solid–Liquid Interface
γ_{sv}	:	Surface Energy of Solid–Vapor Interface
R^2	:	Coefficient of Determination, Correlation Coefficient
R^2_{adj}	:	Adjusted R^2
θ	:	Contact Angle Between Solid and Liquid
x_i	:	i–th factor
vol.%	:	Volume Percentage or Fraction
W_s	:	Specific Wear Rate
wt.%	:	Weight Percentage or Fraction
X_c	:	Degree of Crystallinity
Y	:	Response
Y_i	:	i–th Response

LIST OF APPENDICES

CHAPTER 1: INTRODUCTION

1.1 Research Background

The discovery of thermoplastics revolutionized the development of engineering plastics. This does not only include research on new materials but also modification of existing polymers with additives to improve material properties (Marturano, Cerruti, & Ambrogi, 2017). The large variety of additives allow diversification of product portfolios, enabling novel opportunities for the plastic product market. Generally, additives are sometimes grouped into four main functional categories, namely, property modifiers, property stabilizers, property extenders and processing aids. The largest market segment is the material property modifiers. The top six categories with largest market demand are plasticizers, flame retardants, impact modifiers, antioxidants, antimicrobials and UV stabilizers. In 2011, the global market for plastic additives was worth USD40B and expand to USD48B in 2016 (Fried, 2014). On a compounded annual growth rate (CAGR) basis, it is in a growing phase of 4.4% annual expansion from 2013 to 2020 and the growth is expected to accelerate in the future (Clark, 2014).

Figure 1.1: Global plastics additives market size and forecast, 2012–2020 in million USD (Clark, 2014)

The use of engineering plastics as an alternative material to metals has grown significantly in recent decades. The application includes pharmaceutical, automotive, home appliances, computer and data storage related industries. Research interest has been shifting from monolithic materials to composites using additives such as fibers and/or fillers. Modifications of polymers to meet specific requirement is one of the reasons why their use has widened. This allows properties of polymers to be customized to specific application, usually carried out by varying atomic makeup of repeat structure, molecular weight, flexibility of adding a chain by the presence of side branching and degree of crystallinity modification (Harper, 2000). Due to these advances, different choices of plastics are easily available for users.

1.2 Problem Statement

Polyoxymethylene (POM) is an excellent engineering thermoplastic well known for its superior tribological properties with a good balance of mechanical, thermal characteristics and dimensional stability. POM resins are also known for better creep, fatigue, strength, toughness, stiffness and water resistance performance than other unreinforced plastics. Homopolymers possess slightly better mechanical properties and higher melting point compared to copolymers of POM.

However, use of POM is limited to conditions of low sliding speed and low load. By depending on its own inherent properties, neat POM may not be appropriate in applications requiring superior mechanical and tribological properties. Attempt to improve one of these properties usually results in deterioration of another (Zsidai et al., 2002). Modification of mechanical and tribological properties are typically carried out by blending of other polymers, fibers, inorganic particles, liquid lubricant and micro or nano sized particles. Undeniably, POM based composites are excellent replacements for metals that have been proven in medical, consumer and industrial applications. This research involves modification of glass fiber (GF) reinforced POM through addition of polytetrafluoroethylene (PTFE) micro particles as second dispersed phase to improve its tribological properties with minimal impact to mechanical properties.

GF are usually surface treated and/or coated during the manufacturing process, prior to mixing with the matrix. This type of coating is called sizing. Typically, fibers are sized using an aqueous formulation containing an adhesion promoter which acts as a film former and protective compound containing emulsifier and a lubricant. This effectively reduces flaws in GF. When these fibers are compounded, the film former diffuses into matrix and the matrix is also expected to diffuse to form the interphase. In order for this to happen, the film former must be compatible with the matrix.

Mechanical properties of reinforced composites depend on the ability to dissipate energy throughout the bulk material. The composite will be brittle with low impact strength if the energy is concentrated on small areas within the bulk material. Impact strength is affected by stress concentrations that occur at fiber ends, areas of poor adhesion and regions where fiber to fiber contact occur. To improve energy dissipation, the nucleophilic adhesion and mechanical friction between fibers and matrix plays an important role to aid stress transfer.

Matrix selected for this research was POM reinforced with 25% glass fiber (POM525GR) from Du Pont. The main considerations for selecting this material were its tensile strength, elasticity modulus and coefficient of thermal expansion (CTE). POM525GR were melt blended with PTFE, in the form of micro particles, to alter its mechanical and morphological properties. Their weight fractions and process controls were vital to produce POM composites with consistent properties.

Since PTFE is a hydrophobic polymer with low surface free energy, it was necessary to etch its surface to increase the surface free energy. The surface changes on non–etched and etched PTFE was studied prior to melt mixing with the matrix. The effects of adding PTFE to the composite's properties were investigated through systematic experimentation design to characterize mechanical, tribological and morphological properties. For thermoplastics, the type of process utilized for mixing additives to matrix may result in slightly different properties. In this work, polyoxymethylene/glass fibers/polytetrafluoroethylene (POM/GF/PTFE) composite samples were fabricated using injection moulding process based on preliminary studies that revealed the advantages of this process over isostatic hot press.

1.3 Scope of Research

This research is divided into three phases. During the initial phase, preliminary experiments were performed to determine the parameters for injection moulding process using POM525GR. This phase involved review of material data sheets, operation manual of injection moulding machine and literature search. The injection moulding process comprised of three main processes, namely, filling, plasticizing and holding. Once the process parameters were identified, initial samples were produced to visually inspect for presence of flashes, sink marks, material flow, dimensional variations, etc. Further refinement to the process parameters were needed based on the appearance and dimensional consistency. Using the refined process settings, Design of Experiments (DOE) approach was employed to determine significance of the processing conditions to tensile strength and elasticity modulus. Ideally, the mechanical characteristics must be independent of the process variables and comparable to the typical properties published by the resin manufacturers.

Comparison were made against compression moulding process, i.e. isostatic hot press. Although it is the most economical, simplest process for polymer processing and samples have lower stresses due to resin flows over short distance, the major disadvantage was found to be sustaining consistent mould temperature to increase reaction time of the resin. As such, plastic injection moulding process was preferred. Based on the results of characterization DOE, range of process parameters that demonstrated similar mechanical properties as the published product information for POM525GR were selected.

Second phase of this research involved chemical etching of PTFE microparticles and investigation of mechanical properties when blended with POM/GF matrix. In the first part of second phase, effects of chemical etching on the surface of micro–PTFE were characterized through morphology studies. In addition, Fourier Transform Infra–red (FTIR) analysis was utilized to determine presence of new functional groups. In the second part of this phase, effects of chemical etching time on micro–PTFE and its weight fractions on mechanical properties, i.e. tensile strength, elasticity modulus, hardness and toughness were individually characterized using response surface methodology (RSM). Then, optimization of the POM composite's mechanical properties defined as a function of PTFE etch time and its weight composition. A region of desirable mechanical properties for POM/GF/PTFE composite was successfully defined.

The third and final phase was to determine the effects of micro–PTFE blended with POM/GF matrix on tribological properties in accordance to different amount of weight percentage, 0 wt.%, 1.7 wt.%, 4.0 wt.%, 9.5 wt.%, 15.0 wt.% and 17.3 wt.% with constant PTFE etch time of 10 min. These POM composites were subjected to tribology testing on a reciprocating rig to understand the behavior of coefficient of friction (COF) and wear loss. The influence of micro–PTFE on worn surfaces were evaluated using optical, scanning electron microscopy (SEM) and FTIR analysis. In the last part of this stage, Field Emission Scanning Electron Microscope (FE–SEM) and Energy Dispersive X–ray Spectroscopy (EDS) analysis at the fiber–matrix interface region quantified the presence micro–PTFE based on weight percentage of fluorine atoms. The three phases of the research scope are shown in Figure 1.2.

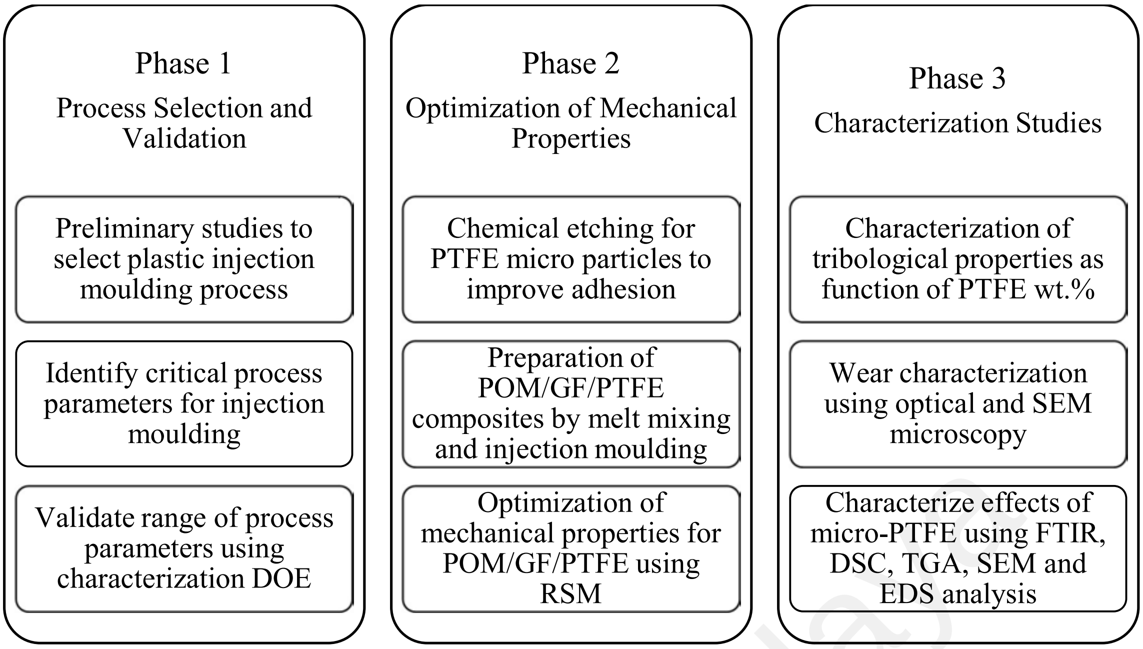

Figure 1.2: Block diagram for the scope of research

Hence, the ultimate goal of the present research is to study the effects of PTFE micro particles on mechanical and tribological properties of POM/GF/PTFE composites. It is known mechanical properties will be compromised through addition of a tribological modifier such as PTFE particulates. The reinforcement effects of GF allow acceptable losses in mechanical properties in order to gain the tribological enhancement as a result PTFE. This would be ideal for metal replacement applications where both of these properties are of equal importance.

1.4 Research Objectives

The objectives of the present research are as follow;

- To determine injection moulding process parameters that significantly affects tensile strength and elasticity modulus and the specifications for fabrication of POM composite samples.
- To characterize the effects of chemical etching on the surface of PTFE microparticles using SEM and FTIR techniques.

- To optimize mechanical properties, i.e. tensile strength, elasticity modulus, hardness and toughness of the engineered POM/GF/PTFE composites as a function of PTFE etch time and mass fraction.
- To evaluate tribological properties of the engineered POM/GF/PTFE composites.
- To study the effects of micro–PTFE in the formation of transfer films that enhances tribological properties of POM/GF/PTFE composites.
- To map the presence of PTFE at the matrix–fiber interface region.

1.5 Structure of the Thesis

In chapter 2, literature review on POM and its composites are addressed in general. The effects of various types of reinforcements on mechanical and tribological properties are presented. Subsequently, a general literature on matrix–fiber interphase and interface involving strategies for interface modification is extensively discussed. Theories on wetting of polymer solids and surface etching of PTFE have been reviewed in detail. This chapter provides a good view of the existing studies on POM composites reinforced with GF and PTFE conducted by various researchers. More importantly, the manner of how my research complements the current body of knowledge on the mechanical and tribological properties of POM/GF/PTFE composites is clarified.

Chapter 3 provides a detailed description of the experimental techniques such as surface etching of PTFE micro particles, melt mixing, and injection moulding. The selection of injection moulding process parameters using DOE approach and the optimization of mechanical parameters for POM/GF/PTFE composites using RSM are clarified. Chemical etched PTFE micro particles characterization using SEM microscopy and FTIR spectroscopy are described. POM/GF/PTFE composite samples characterization such as tensile strength, elasticity modulus, toughness, hardness, COF, and wear loss are discussed. Further characterization studies of POM/GF/PTFE composite samples involve surface morphology analysis using SEM on fractured surfaces after tensile test, FE–SEM and EDS for mapping of fiber–matrix interface and FTIR spectroscopy to determine presence of new functional groups. In addition, thermal analysis using Differential Scanning Calorimetry (DSC) and Thermogravimetric Analysis (TGA) are further discussed in this chapter.

The experimental findings and discussion are presented and comprehended in Chapter 4. This chapter is structured into three broad areas comprising; procedure and justification for selecting injection moulding process parameters, statistical data analysis to optimize the mechanical properties of POM/GF/PTFE composites and characterization studies that lead to the understanding of improved tribological properties by blending PTFE micro particles in POM/GF matrix.

Lastly, Chapter 5 draws conclusions from the current research findings and suggestion for future work.

CHAPTER 2: LITERATURE REVIEW

2.1 Introduction

Engineering plastics (EP) are commonly used as metal replacement owing to their good strength, dimensional stability and good electrical and chemical properties. Their application involves electrical and electronic, construction, automobile, consumer products and industrial machinery. In order for EPs to be commercially viable, their properties are enhanced by blending with other materials. Polymer mixtures can be broadly categorized as polymer blends, polymer alloys and polymer composites (Utracki, 1990). Polymer blends are miscible polymer systems whereas polymer alloys are immiscible polymer systems.

Polymer composites are physical mixtures of a polymer, known as the matrix, and a reinforcing filler, called the dispersed phase. The latter is added to modify mechanical, tribological, thermal, electrical or other properties. It is common to mix more than one type of filler in a polymer composite system. These reinforcing fillers can be organic or inorganic, in the form of fibers or particles. Thermoplastics and thermosets are the two types of matrix used in these class of composites. The important types of polymer matrix composites (PMCs) contain fibers, particles, or a combination of both (Brostow, Lobland, Hnatchuk, & Perez, 2017). The matrix and reinforcement are separated by an interphase, a term introduced in the 1970s (Papanicolaou, Paipetis, & Theocaris, 1978). Recent advancements in fiber/matrix interphase tailoring for fiber–reinforced polymer composites were reviewed by Karger–Kocsis et al. (Karger-Kocsis, Mahmood, & Pegoretti, 2015). This study investigates PMCs of polymer matrices blended with fibers and particles as reinforcing fillers.

The mechanical properties of PMCs are dependent on the affinity between the polymer and filler. There are several techniques to improve the bond between these phases. Among them are activation of filler surface, modification of the matrix or addition of a compatibilizer to promote a good bond between filler and matrix. When fillers are blended into polymers, the resulting bond can be mechanical interlocking, chemical bond or a combination of both.

The use of thermoplastics as the matrix for PMCs has an advantage because processing can be carried out by injection molding, compression molding, or extrusion techniques. These processes are very economical for manufacturing components that require good precision, low cost, and high volume. As such, PMCs are widely used in automotive, aviation, marine, computer and construction industries.

Fibers are used as a reinforcement to improve mechanical properties such as tensile strength and elasticity modulus. Decreased fiber dimension lowers the probability of flaws or imperfections, thus making them significantly stronger and stiffener. The matrix transfers the load to these fibers and stresses are distributed among them. Stress transferred from matrix to fiber and fiber to fiber is dependent on the interphase. The matrix also allows positioning of fibers and protects the fibrous reinforcement from the environment in which these composites are used.

Fiber–reinforced PMCs are widely used in tribological designs owing to their light weight and excellent mechanical, self–lubricating, and wear resistance properties. These polymer composites are usually grouped based on the type of reinforcing fibers and matrices. The appearance of these reinforcing fibers can be classified as discontinuous, continuous, or aligned. They are further categorized into organic and inorganic. High strength inorganic fibers such as glass, carbon, and ceramic fibers are used to improve mechanical properties.

Polymer tribology is vastly different from traditional tribology, which was originally developed for metals. The main differences between polymers are the viscoelasticity, time dependent properties and absorption of liquid lubricants (Brostow, Deborde, Jaklewicz, & Olszynski, 2003; Brostow, Kovačević, Vrsaljko, & Whitworth, 2010). It is important to understand polymer tribology and select an appropriate test methodology to simulate the service life of components produced using PMCs (Nirmal, Hashim, & Lau, 2011). Polymeric materials manufacturers usually maintain confidentiality on the actual composition of resins. Therefore, designers depend on catalogue information and academic literature when selecting the appropriate material to be used in applications. The vast amount of dispersed and scattered data force designers to conduct their own lab–scale experiments to gain confidence in their design solution (De Baets, Glavatskih, Ost, & Sukumaran, 2014; Myshkin, Pesetskii, & Grigoriev, 2015).

In this research, the mechanical and tribological properties of POM/GF/PTFE composites were studied. Among the mechanical properties characterized were tensile strength, elasticity modulus, toughness and hardness. As for tribological properties, the characterization was performed on a reciprocating test rig. The test utilized a flat POM composite specimen and a stainless–steel ball as the upper specimen that slides against the stationary composite sample. The effects of surface etched PTFE micro particles were studied based on morphology of worn surfaces, formation of new functional groups and the presence of PTFE at the interface region.

2.2 Polyoxymethylene (POM)

POM, sometimes known as acetal or polyformaldehyde, may be the first universal polymer. In 1987, gas clouds of Halley's Comet showed presence of POM using mass spectral analysis. As man–made polymer, it is obtained through the anionic or cationic polymerization of formaldehyde or by ring opening polymerization of trioxane shown in

Figure 2.1. It comprises of highly ordered chain structure contributing to its excellent crystallinity and chemical resistance (Fried, 2014).

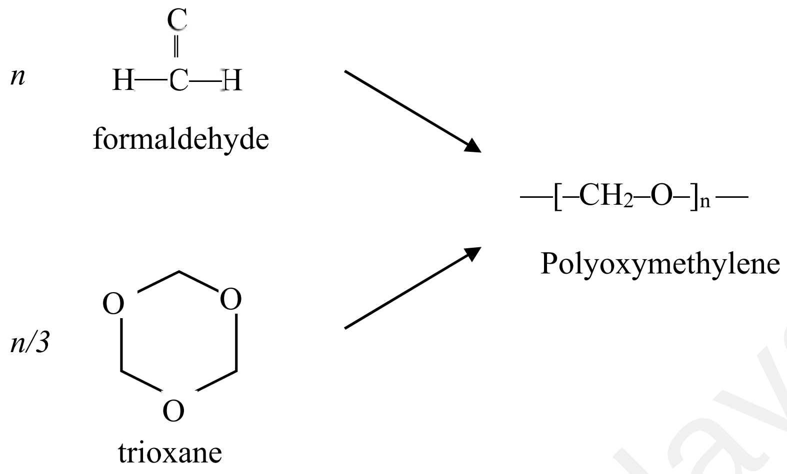

Figure 2.1: Two routes for the synthesis of polyoxymethylene (Fried, 2014)

Hermann Staudinger first studied POM formed from polymerization of formaldehyde in the 1920s. Due to thermal stability issues, commercialization of POM did not occur until the early 1950s. Only in 1952, thermally stable materials were available when researchers at Du Pont developed Delrin. Thermal degradation of POM occurs by unzipping with the release of formaldehydes (V. M. Archodoulaki, Lüftl, & Seidler, 2004; V. M. Archodoulaki, Luftl S., Koch T., Seidler S., 2007). The thermal stability increase is due to esterification of the hydroxyl ends with acetic anhydride (Z. Liu, Zeng, Yang, & Yang, 2015). An alternative method to increase the thermal stability is copolymerization with a second monomer such as ethylene oxide. This copolymer prepared by cationic methods developed by Celanese and marketed under the trade name Celcon. Hostaform is another copolymer marketed by Hoescht. The presence of the second monomer reduces the tendency for the polymer to degrade by unzipping (Harper, 1999).

POM is an engineering plastic with outstanding tribological properties and a good balance of mechanical and thermal properties. It is widely used in industries for various applications as an alternative to metal. About two thirds of worldwide POM production is used in the automotive, electrical and electronic applications (Ebewele, 2000). The excellent tribological, mechanical and thermal properties of POM make it a better option compared to other engineering plastics. POM, being a thermoplastic material, is easily injection moulded to the required shape and dimension. In addition, this provides cost reduction opportunity to component manufacturers. During the injection moulding process, avoidance of overheating is important as production of formaldehyde may cause pressure build up. The polymer should be purged from the machine before shut down to avoid excessive heating during start up.

Among other properties are good dimensional stability because of negligible water absorption. This allows POM to be used in gears and machine parts. Modified grades such as rubber–toughened POM is used where higher impact strength, flexural strength and tensile fracture resistance are critical to function.

POM resin is a crystalline polymer due to its special molecular structure. It tends to crystallize easily to form large spherulites during injection or extrusion moulding. These spherulites, usually ranging from a few micrometers to millimeters, are likely to cause stress concentration when products made of POM are subjected to the external impact. It appears that POM is very sensitive to notch and has a low notched impact strength in nature. This presents a limitation to meet the requirement of mechanical properties in many relevant fields (Gao, Sun, He, Wang, & Wu, 2011). As such, modifications of neat POM by incorporating an appropriate reinforcement is necessary.

POM has good self–lubricating characteristics with a low coefficient of friction and high wear resistance (Samyn, De Baets, Schoukens, & Quintelier, 2007). However, by depending on its own inherent properties, pure POM may not be appropriate in applications requiring superior mechanical and tribological properties (Benabdallah & Olender, 2006; Poulios, Drago, Klit, & De Chiffre, 2014; M. Wang, Zhang, & Wang, 2017). Therefore, these properties must be improved to extend its range of applications. Numerous studies have reported the development of POM composites as self–lubricating materials in applications related to engineering, automotive, bearings, electronic appliances, and building materials (De Santis, Gnerre, Nobile, & Lamberti, 2017; Kalacska, 2012). This has been achieved by blending with fibers, and micro– or nano–sized particles. These modifiers were organic and non–organic (Sun, Yang, & Li, 2008b; Wacharawichanant, Thongyai, Phutthaphan, & Eiamsam-ang, 2008).

On the contrary, POM has very poor compatibility with other materials. Compatibilizers are often used as additives to obtain the desired properties of its composites (C. Y. Huang, Kuo, & Roan, 2016). Improving the compatibility of immiscible polymers results in improved morphology and properties of the composite (J. Chen, Cao, & Li, 2006). It is often challenging to disperse fillers effectively in the matrix polymer of a composite. Development of compatibilization technologies are crucial for the polymer industry to reap the full benefits of such approaches to obtain materials with optimum performance and cost characteristics.

2.3 POM Based Composites

POM is a highly crystalline, typically 75% crystalline, with a melting point of 180 °C. Its high melting point is due to the chains are packed closer together. The high degree of crystallinity does not only yield excellent mechanical properties, but also imparts good solvent resistance. It is a strong and stiff thermoplastic with good fatigue, creep, stiffness, water resistance and dimensional stability. Typically, the CTE is modified through addition of GF, making POM/GF based composites as a good alternative to metals in various applications.

Addition of fillers and reinforcement into POM is known to alter its mechanical, thermal, tribological and other properties. These additives can be organic and inorganic, in the form of solid or liquid lubricant. Soft particles, in micro or nano size, are commonly used as solid lubricant. (Sun, Yang, & Li, 2008a). Generally, nano–sized particles are more effective to achieve the intended properties such as tensile strength, elasticity modulus, flame retardant capability, decrease CTE and increased solvent resistance. However, synergistic effect of nano particles and other fillers or reinforcements to matrix material is not well understood.

The effects of interface modification using macro sized additives in the form of fibers or particles into POM matrix requires surface treatment to change their surface energy (C. Y. Huang et al., 2016). The reinforcement efforts by incorporating fibers in a POM matrix enhances its mechanical properties, provided that a stable interface layer is formed between the fibers and matrix. This determines the fiber–matrix adhesion, which eventually affects the load transfer capability from the matrix to reinforcing fibers. Depending on the types of fibers, tribological properties can either improve or deteriorate. For an example, addition of PTFE fibers improves frictional and wear properties (C. Y. Huang & Tseng, 2000) whereas GF have negative effects on the tribological properties (Unal, Mimaroglu, & Demir, 2010).

Dry friction between neat polymeric materials is primarily due to local adhesion between asperities and the subsequent shear yielding or ruptures of the material with lowest shear strength under these local conditions (Laursen et al., 2009). Tribological properties are improved through reduction of POM adhesion to the counterpart material during tribo–contact. There are various strategies employed to achieve this, such as increasing hardness, stiffness and compressive strength and blending of a lubricating filler in the POM composites. The latter approach improves wear resistance when these fillers decompose and generate reaction products which enhance the bonding between transfer film and mating surfaces (Mergler, Schaake, & Huis in't Veld, 2004). There are other fillers that decreases wear resistance due to generation of more discontinuities in the material (Gao et al., 2011).

The usage of an additive to improve tribology properties for friction and wear may negatively affect mechanical properties. Typically, tribology properties are enhanced by blending POM with solid lubricants such as molybdenum disulfide (MoS_2) (J. Wang, Hu, Xu, & Hu, 2008), alumina (Al_2O_3) (Sun et al., 2008b) and polytetrafluoroethylene (PTFE) in micro or nano sized particles (T. Huang et al., 2011). Other polymeric materials such as polyethylene oxide (PEO) (Bai & Wang, 2012), polylactic acid (PLA) (Guo, Zhang, & Huang, 2015), poly(ethylene glycol–co–cyclohexane–1, 4–dimethanol terephthalate) (PETG) (Lam, Abu Bakar, & Mohd Ishak, 2004), etc. have been sought in to improve the mechanical and tribological properties of POM based composites.

The next section reviews literature published on POM based composites and the contribution of this research to the development of POM based composites with superior mechanical and tribological properties.

2.4 Mechanical Properties for POM Based Composites

Significant research has been devoted to improve the mechanical strength of neat POM by incorporating reinforcements and fillers. Addition of reinforcing fibers result in POM composites with increased strength and stiffness, provided these fibers are capable of undertaking the stress introduced onto the POM matrix. The resultant mechanical properties of the POM composites depend on the stress transfer capability from matrix to fibers, independent of the fibers' length. This can be accomplished only if the bond between the two phases is good, which can be mechanical interlocking, chemical bond or a combination of both. Therefore, fiber–matrix interface determines the mechanical and physical properties of the composite.

Incorporation of fillers, in the form of particulates improve the processability and mechanical properties, especially toughness. These particulate fillers are usually added as second dispersed phase into the matrix, forming a three–phase composite material.

When added to matrix, improvements realized in fracture properties of the composite material may not be in the same order as the filler itself. It is suggested that the constraint imposed by the fibers suppresses the toughening mechanism (Prabhakar, Debnath, Ganesan, & Palanikumar, 2018). Particulate reinforcement can cause deterioration in the mechanical properties. The size, shape, surface area, surface chemistry and loading of particles are some of the factors that determine the effects of these fillers on mechanical properties of the POM composites.

2.4.1 GF Reinforcement

The addition of GF to POM as reinforcement has been one of the approaches to improve strength, stiffness and hardness. The change of these properties is mainly due to the strength of GF holding POM matrix together and the bond of GF to POM matrix. When impacted or loaded, the energy absorbed by the reinforcement makes the polymer composite not only tougher, but also stronger. This is evident when comparing the morphology of fractured surface for filled versus reinforced after impact testing. Addition of GF to POM negatively affects the wear resistance and COF because of its abrasive characteristics (Benabdallah, 2003).

During melt mixing, the dispersion of GF can be restricted through formation of a microphase boundary around the surface of GF. As a result, the mechanical properties of POM/GF composites can be significantly compromised. The performance is greatly enhanced by application of surface treatment and/or coating on the GF during their manufacturing process. This type of coating is commonly known as sizing. The difference between conventional coating and sizing is the composition, where coating involves incorporation of nanofillers. To prevent fracturing, GFs are commonly sized immediately after spinning. The sizing compound contains an adhesion promoter, a film former, an emulsifier and a lubricant (Karger-Kocsis et al., 2015).

Mohan Babu et al. (2014) compared mechanical properties of POM reinforced with 25% GF by adding 1%, 3% and 5% nanoclay against POM/GF and neat POM. The surface of GF was treated with a silane coupling agent whereas the nanoclay were left untreated. As shown in Table 2.1, addition of nanoclay deteriorated tensile strength. SEM images of fractured surfaces shown in Figure 2.2 reveals non–homogenous dispersion of fiber and nanoclay and more fibers were pulled out. The immiscibility of nanoclay with POM and GF is due to absence of a compatibilizer and absence of surface treatment for nanoclay resulting in nonuniform mixing. Consequently, this caused a microphase boundary to form around the GF surface resulting in inferior mechanical performance when compared to POM/GF composite without nanoclay.

Table 2.1: Mechanical properties of POM reinforced with 25% GF and filled with 1%, 3% and 5% nanoclay (Mohan Babu & Mettilda, 2014)

Material	Tensile Strength (MPa)	Flexural Strength (MPa)	Impact Strength (Charpy test) (kg/m^2)	Impact Strength (Izod test) (kg/m^2)
POM Neat	60.27	86.57	10.823	7.191
POM/GF	70.34	96.37	6.352	4.967
POM/GF with 1% nanoclay	66.15	102.10	6.303	4.042
POM/GF with 3% nanoclay	57.83	89.76	4.625	4.082
POM/GF with 5% nanoclay	55.21	78.74	6.460	3.859

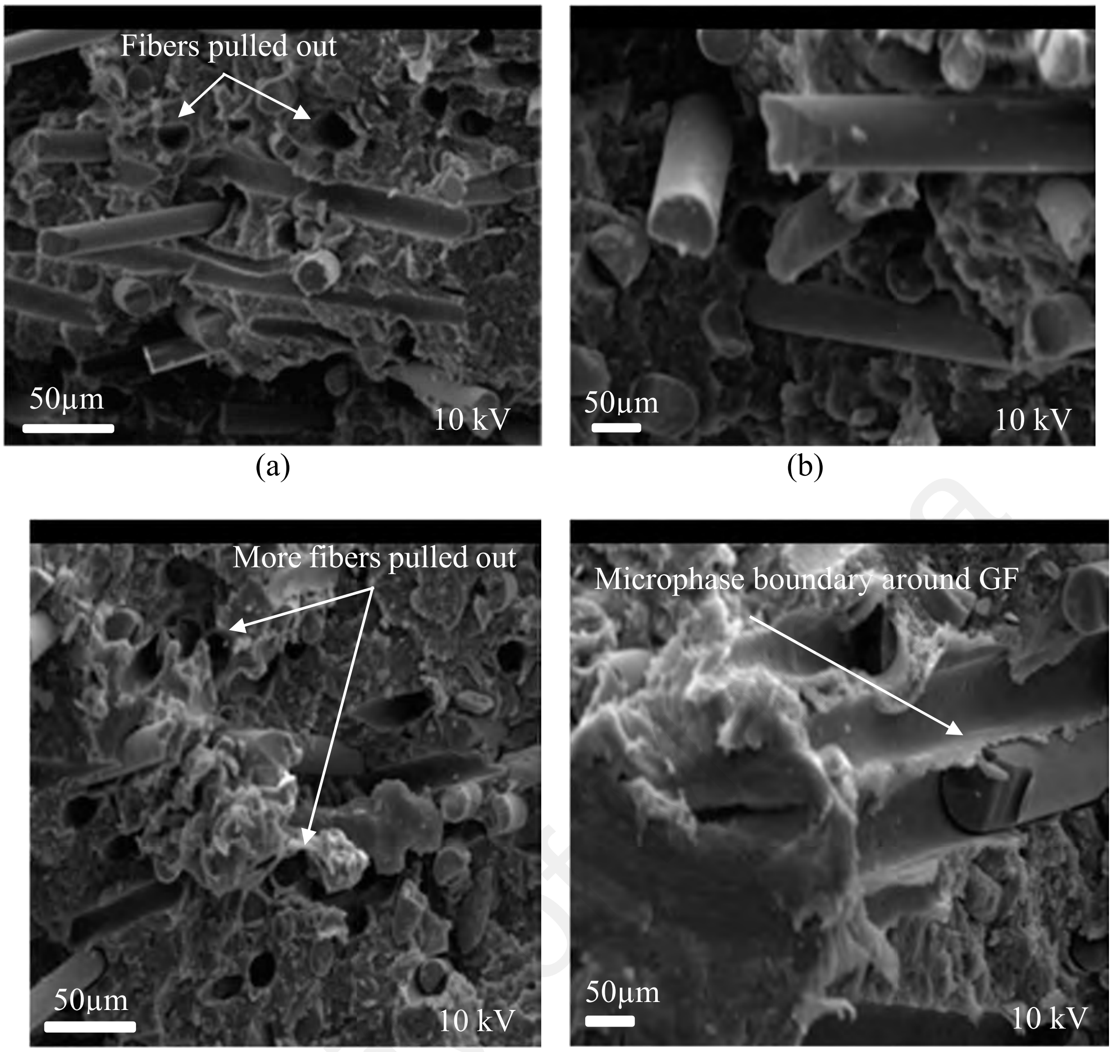

(a) (b)

(c) (d)

Figure 2.2: SEM micrographs of fractured surfaces (a), (b) POMGF with 1% nanoclay (c), (d) POMGF with 5% nanoclay (Mohan Babu & Mettilda, 2014)

The adhesion between GF and POM matrix is influenced by the type of sizing. The reaction of surface hydroxyl groups on GF and the sizing compound determines the type of bond. The final structure can be said as a semi interpenetrating network (IPN) because the film former in the sizing compound is usually a linear polymer while the silane coupling agent is a cross–linked polymer. With the diffusion of film former into the matrix, and vice versa, it is expected that matrix to diffuse into the semi IPN. Therefore, the film former and matrix should be highly compatible (Jones, 2012). Figure 2.3 illustrates the semi IPN structured interphase on GF.

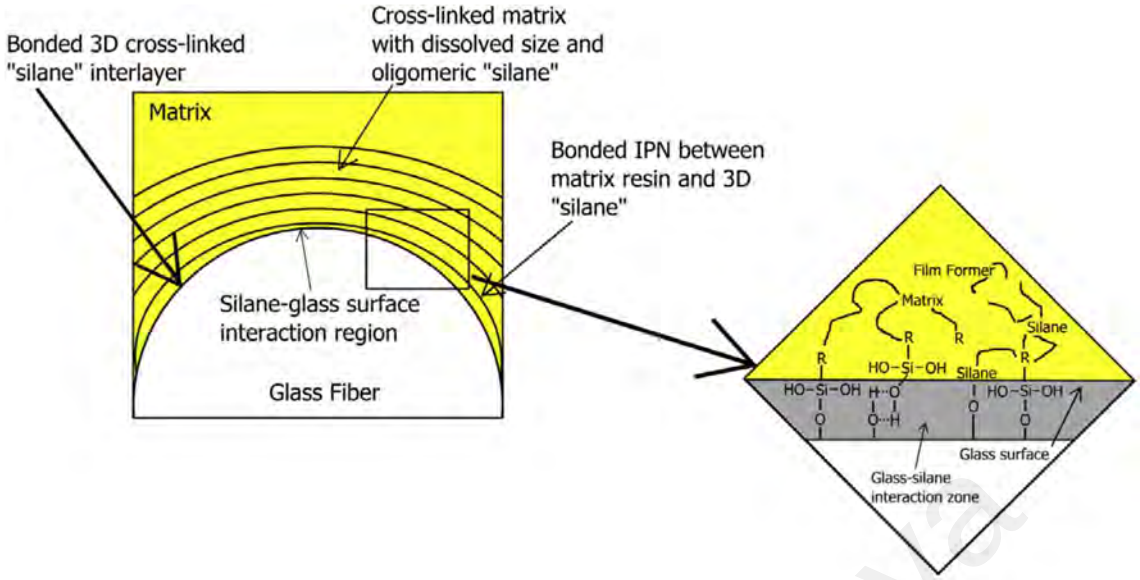

Figure 2.3: Scheme of the semi IPN structured interphase on GF. Note: The scheme highlights the effects of silane coupling agent and film former (Jones, 2012)

Presence of defects or cracks on GF affects the fiber's mechanical strength. An appropriate coating is important to rectify these surface flaws and alter the surface properties of GF. This is usually achieved by formation of single or multiple molecular layers on the GF. Biswas et al. (2014) studied the influence of four different types of polymer coatings on the tensile properties of GF itself. Table 2.2 shows the type of coating and the corresponding tensile properties of coated GF compared to uncoated GF. Their study revealed difference in coating recipes greatly affected the tensile properties of GF. As such, selection of an appropriate GF coating needs to take into account its effects on GF and also its compatibility to the matrix.

Table 2.2: Comparison of GF tensile strength with different types of coating (Biswas, Cherif, Hund, Shayed, & Hossain, 2014)

Substrate	Polymer coating (wt.%)	Chemical type	Solvent (wt.%)	Tensile strength (MPa)
GF	–	–	–	1200
GF	Silikophen P80/MPA (15)	Phenylmethyl polysiloxane resin	Acetic acid ester (85)	2000
GF	Silres K (20)	Methyl silicone resin	Acetic acid ester (80)	1850
GF	Silres IC836 (15)	Phenyl polysiloxane	Acetic acid ester (85)	1650
GF	KiON® HTT 1800 (15)	Polysilazane	Acetic acid ester (85)	1700

Chiang et al. (1999) experimented mechanical properties of POM/GF composites with different types of polymer coatings and by varying composition of GF. Four types of polymer coating, comprising of polyurethane (PU), ethylene–vinyl acetate (EVA), acrylonitrile–butadiene–styrene (ABS) and high impact polystyrene (HIPS) was applied on GF. POM/GF composite samples with 10%, 20% and 30% GF were prepared and subjected to mechanical testing. For all types of coatings, tensile strength was enhanced when compared to POM/GF with uncoated GF because of better interfacial adhesion between GF and POM. As expected, steady improvement in tensile strength was noted as the GF content was increased (Figure 2.4). The degree of improvement in mechanical properties for GF after coating compared to blending these coated GF into POM matrix was vastly different as a result of the adhesion at the interfacial boundary between GF and POM. Although the coated GF easily dispersed into the matrix because of better affinity to POM, mechanical properties of the composites was influenced by its adhesive properties.

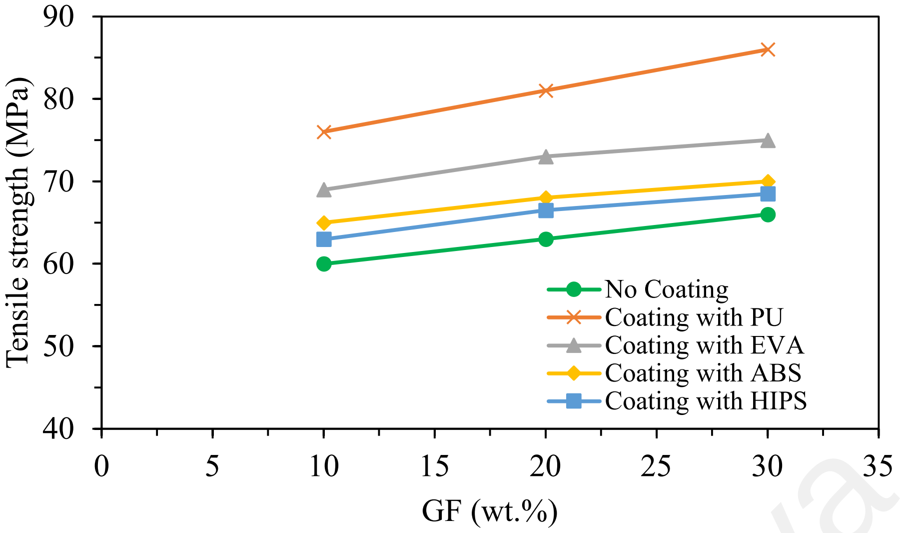

Figure 2.4: Tensile strength vs. GF content for POM/GF composites (Chiang & Luor, 1991)

Kuciel et al. (2019) evaluated the possible reinforcing effects of POM by GF and carbon fibers (CF). Mechanical and fatigue properties were determined by preparing POM/GF and POM/CF composites with varying weight percentage of fiber content between 5% and 40%. The geometry of GFs used was 10 µm and 13 µm in diameter with length of about 150–200 µm whereas CFs were 7 µm and 3 mm in diameter and length respectively. The type of surface treatment or coating on these fibers were not reported in their research.

Figure 2.5 shows the elasticity modulus of these POM/GF and POM/CF composites. The differences in the mechanical properties for POM/CF composite are discussed in section 2.4.2. The stiffness of POM/GF composite doubled when GF weight was between 10% and 20%. Further increase of GF content did not reveal similar improvement. This observation indicates approximately 25% GF may be sufficient for enhanced stiffness in products manufactured with POM/GF composites.

Figure 2.6 illustrates the relationship between tensile strength and different weight ratio of fibers in the POM composites. Steady increment in tensile strength observed as the content of GFs increased is due to fibers' adhesion to POM matrix. Forces occurring at the fiber/matrix interface determines the adhesion strength. These forces are determined by the chemical structure of the filler and polymer matrix forming the composite. Mechanism of fiber/matrix interface are discussed in detail in section 2.6.

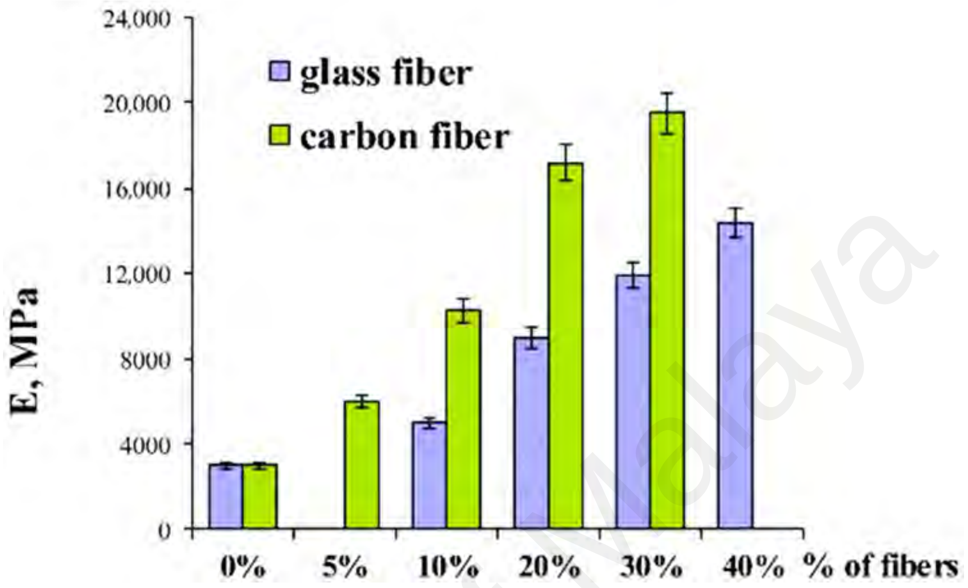

Figure 2.5: Changes in elasticity modulus for POM/GF and POM/CF with different weight ratio of fibers (Kuciel, Bazan, Liber-Knec, & Gadek-Moszczak, 2019)

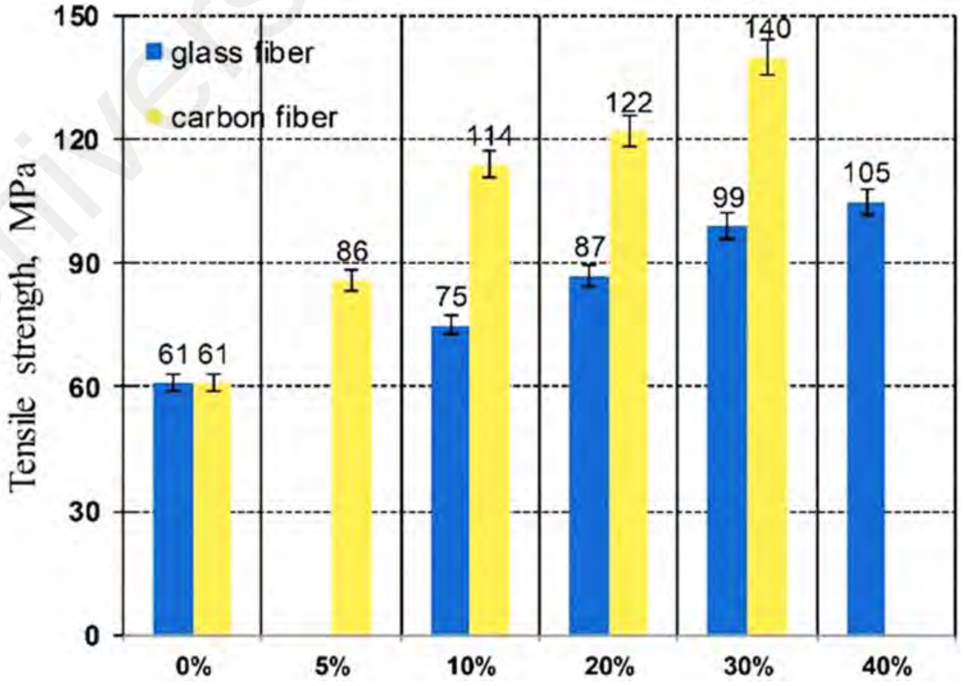

Figure 2.6: Changes in tensile strength for POM/GF and POM/CF with different weight ratio of fibers (Kuciel et al., 2019)

Kuciel et al. also presented the effects of fiber geometry on the mechanical properties. POM composites were prepared with two different GF diameter, 10 µm and 13 µm, and the content of GF maintained at 25 wt.%. Table 2.3 shows the difference in mechanical properties as a function of fiber diameter. Larger diameter and more developed GF surface improved its adhesion to polymer matrix and enhanced the composite's strength.

Table 2.3: Comparison of mechanical properties for POM composites with GF 25 wt.% and diameters of 10 µm vs. 13 µm (Kuciel et al., 2019)

Diameter of GF	Ø = 10 µm	Ø = 13 µm
Young's Modulus E, MPa	10500	12200
Tensile Strength, MPa	80.0	85.0
Strain at Break, %	1.0	1.0
Energy at P_{max}, J	0.80	0.85
Unnotched Impact Strength, kJ/m^2	9.6	11.3

2.4.2 CF Reinforcement

CFs have excellent properties, such as high tensile strength, elasticity modulus, and outstanding wear resistance and are widely used to reinforce advanced composite materials. CFs can be continuous, long, and short CFs (SCFs) depending on the its length (Yao, Jin, Rhee, Hui, & Park, 2018). Carbon fiber reinforced polymer composites (CFRP) have several exceptional characteristics: good chemical resistance, outstanding mechanical properties at low density, and customizable strength based on load requirement. In CFRP, the polymer usually acts as the continuous phase or the matrix, while CFs serve as the discontinuous phase. Their applications are in the fields of aerospace, transportation, and sporting goods (Forintos & Czigany, 2019).

Fu et al. (2012) investigated the effects of CF content on the mechanical properties of POM/CF composites. Tensile strength and elasticity modulus improved as the CF vol.% increased. Both of these properties obeyed the rule of mixture, except for the POM/CF composite with more than 25 vol.% revealed sharp increase in tensile modulus.

The difference in elasticity modulus and tensile strength of POM/CF against POM/GF composites observed in Figures 2.5 and 2.6 is likely caused by the different fiber geometry of CF and GF. The longer (3 mm) and smaller diameter (7 µm) CF compared to GF (10–13 µm in diameter and length of 150–200 µm) with the same weight fractions may have resulted in a larger contact surface between the fiber and the matrix. Thus, POM/CF composites revealed better mechanical properties compared to POM/GF composites. Assessment of the size and type of reinforcement is vital as it affects other material properties for POM composites, such as, tribological, chemical, thermal, etc.

2.4.3 Carbon Nanotubes (CNT)

CNTs have a unique one–dimensional (1D) structure and a perfect hexagonal shape, possessing extremely high strength in the same order of C–C bond. CNTs have been considered as an ideal replacement for conventional nanofillers used in polymer nanocomposites because of their superior characteristics such as nanometer in size, high aspect ratio, superior mechanical strength and thermal conductivity. Homogenous dispersion of CNTs within a polymeric matrix is a major challenge as they entangle or aggregate into bundles. Various strategies have been designed to improve its dispersion stability and quality (Bose, Khare, & Moldenaers, 2010).

Blending multi–walled carbon nanotubes (MWCNTs) functionalized with polyethylene glycol (PEG) revealed strong affinity with POM due to similarity in the molecular structure (Zhao & Ye, 2011a). The POM/MWCNT composites exhibited higher mechanical strength and stiffness with 0.1 to 1 wt.% loading of MWCNTs. Evidence of an obvious nucleation on POM lead to the increase in crystallization temperature, crystallization rate. The morphology of fractured surface correlated with the mechanical properties, where the surface transitioned from rough to smooth when the MWCNTs loading was higher (Zhao & Ye, 2011b).

Yu et al. (2010) successfully wrapped POM on single–walled carbon nanotubes (SWCNTs) using supercritical carbon dioxide (SC CO_2). This fluid has rare properties such as low viscosity, non–zero surface tension and highly diffusible. It is easily soluble in most organic solvents but weak solubility for many polymers. SC CO_2 performs as an antisolvent to improve the absorption of polymers on the surface of CNTs (Yu, He, Ren, & Xu, 2011). Molecular interactions of C–H groups using spectroscopy techniques ascertained the polymer adsorption on the surface of CNTs. SEM and Transmission electron microscope (TEM) further validated presence of POM with a few nanometers in thickness.

2.4.4 Natural Fibers (NF)

In recent years, natural fibers have shown good potential as replacement for synthetic fibers for their superior mechanical properties, light weight, recyclability and biodegradability (Yan, Chouw, & Jayaraman, 2014). There has been an increasing use of natural fibers as reinforcement to POM to enhance the mechanical and tribological properties. These group of fibers are renewable source of reinforcing materials. In applications, natural fibers are less abrasive and considered as less harmful to the machinery (Ho et al., 2012).

2.4.4.1 Abaca and Cellulose Fibers

Abaca fibers have high tensile strength, resistant to rotting and specific flexural strength comparable to glass fibers. It is the first to meet stringent quality requirements for components used on the exterior of road vehicles; the under–floor protection for Daimler Chrysler passenger cars. Cellulose fibers are industrially produced as well as naturally occurring in plants. Its properties depend on the processing methods. Some of the advantages are, less abrasive to processing equipment, high strength, stiffness in the fiber direction and more importantly, the recyclability.

Bledzki et al. (2012) investigated two separate POM composites loaded with 30% abaca fibers and 30% cellulose fibers to develop a value–added engineering material. As depicted in Figure 2.7, the elasticity modulus increased by 90% and 105% with the addition of abaca and cellulose fibers, respectively when compared against neat POM material. Similarly, flexural modulus of abaca fiber reinforced POM improved by 120% whereas cellulose fiber reinforced POM resulted in 90% better stiffness compared to neat POM. Figure 2.8 shows the tensile and flexural strength for the composites. Tensile strength for POM reinforced with abaca fibers reduced by 18% while POM reinforced with cellulose fibers showed an enhancement of 90% compared to neat POM. The lower strength caused by the single fiber packages for abaca fibers whereas cellulose fibers bundled with hemicellulose and lignin served as a natural composite. Flexural strength for both composites improved significantly (Bledzki, Mamun, & Feldmann, 2012)

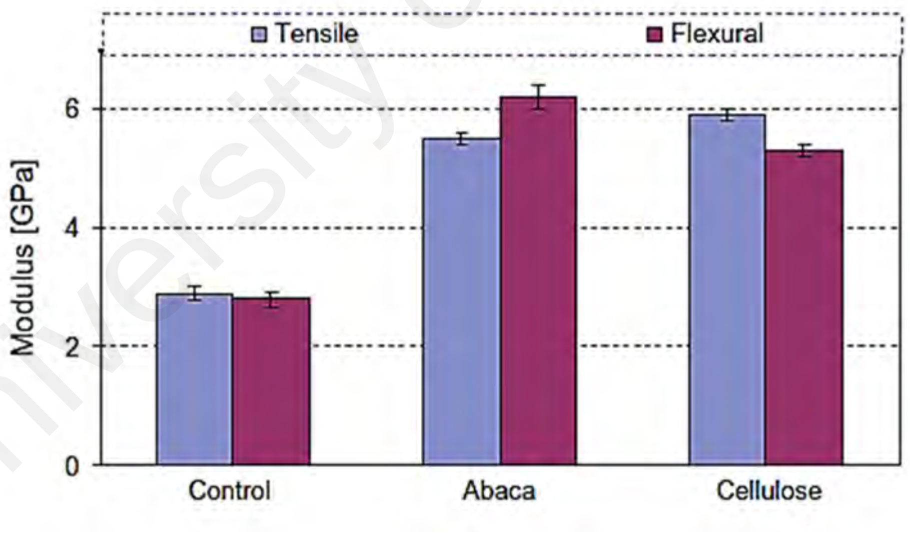

Figure 2.7: Elasticity modulus of POM composites with abaca and cellulose fibers (Bledzki et al., 2012)

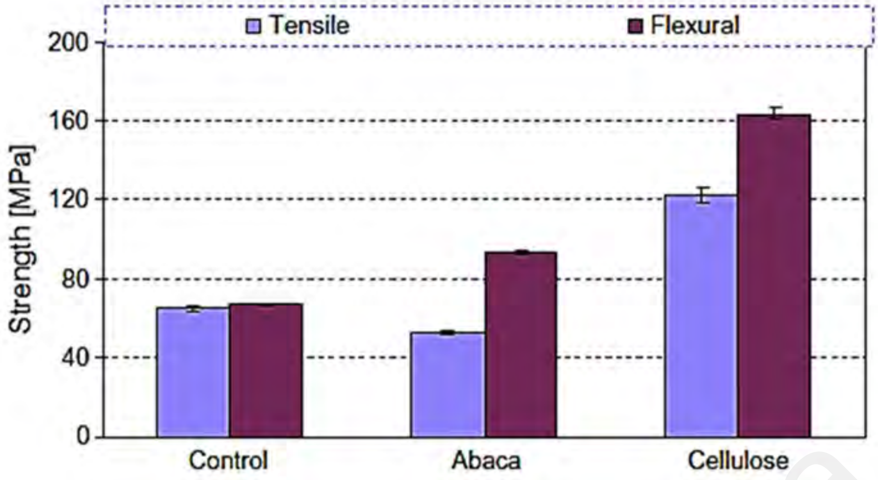

Figure 2.8: Tensile strength of POM composites with abaca and cellulose fibers (Bledzki et al., 2012)

2.4.4.2 Eucalyptus bleached fibers (EBF)

Besides its conventional use in paper industry, EBFs are also used as natural reinforcement. The lignocellulosic fibers extracted from Eucalyptus have an advantage over other fibers. Their reproducibility properties in a large–scale production of cloned Eucalyptus species arise from cultivation under controlled conditions. Similar to other vegetal fibers, these Eucalyptus extracted fibers are a lignocellulosic material, comprising of cellulose, hemicellulose and lignin (Gadioli, Morais, Waldman, & De Paoli, 2014). POM/EBF composites show good tensile properties due to mechanical interlocking or anchoring of EBFs in POM matrix with seemingly low chemical interaction. The EBFs were found dispersed individually but require more research to attain better fiber matrix interface (Espinach et al., 2017).

2.4.4.3 Kenaf fibers (KF)

Kenaf is another natural fiber used as reinforcement in PMCs. Its superior toughness and high aspect ratio compared to other fibers makes it a potential reinforcing fiber in thermoplastic composites (Saba, Paridah, & Jawaid, 2015). KF is well known source of cellulose with economic and ecological advantages. It is able to grow under a wide range of weather conditions within three months after sowing the seeds. Presently, the use of

KF in paper production is very limited (Akil et al., 2011). Yakubu et al. investigated tensile properties (Dan-mallam, Abdullah, & Yusoff, 2019) and impact strength (Dan-Mallam, Abdul Majid, & Abdullah, 2015) of POM reinforced with short and long KF. The tensile strength of continuous POM/KF composites increased significantly with 70/30 wt.% and 80/20 wt.% compared to neat POM. The impact strength of POM reinforced with long KF was better than the short KF reinforcement. In summary, tensile, flexural and impact properties of continuous POM/KF composites were substantially enhanced in comparison with the short fiber composites.

2.4.5 POM–Polymer Blends

2.4.5.1 POM/PETG

PETG is an amorphous copolyester that is unable to crystallize during heating due to the presence of cyclohexanedimethylene. These units lead to the destruction of its chain regularity. One of its advantage is related to broader range of processing parameters than other crystallizable polycondensation. POM/PETG own a dual phase and interpenetrating structure suitable for applications requiring superior impact strength. This property is dependent on both constituents. Parameters related to ductility and toughness are usually lower than the neat POM and PETG as a result of incompatibility, causing poor adhesion between phases and rough morphology. However, equal mix of both constituents yield better ductility and toughness parameters because of a co–continuous morphology instead of a dispersed one. Other properties such as tensile and flexural stiffness obey the rule of mixture (Lam et al., 2004).

2.4.5.2 POM/Elastomers

Although POM has excellent mechanical properties, its brittleness is a limiting factor of its applications. Blending with elastomers is another strategy to enhance its toughness (Dziadur, 2001). Elastomers in the form of particulates are preferred as dispersion plays an important role to determine the mechanical properties. Karger–Kocsis et al. (2008) developed a novel method of toughening and reinforcing of POM simultaneously by blending POM with PU and alumina particles (Siengchin, Karger-Kocsis, & Thomann, 2008). The reduction of stiffness caused by PU was partly compensated by alumina. The technique utilized to prepare the composite samples affected the mechanical properties. This was caused by the nonhomogeneous dispersion of particulates.

2.5 Tribological Properties for POM Based Composites

Polymer composites are commonly used under dry sliding conditions in various motion systems owing to their light weight and self–lubricating properties. POM is one of the semi crystalline polymers that is preferred due to its good sliding properties (Benabdallah & Olender, 2006). Depending on the type of counter surface, the rate at which friction builds up and stabilizes can be very different. When rubbing against metal surfaces, transfer of a polymeric layer determines the characteristics of friction and generation of wear debris (Bahadur, 2000). One of the strategies commonly adopted to promote transfer layer formation is by increasing polymer adhesion on the counter–surface, especially by filling the surface asperities through generation of debris.

The development of nanotechnology has motivated many researchers to explore the function of nanoparticles in polymer nanocomposites. The role of nanoparticles is mainly to improve tribological properties. Since the size of these particles are similar to surface asperities, tribo–contact promote development of an effective transfer film. Another advantage of introducing nanoparticles in polymer composites is the ability to react with molecular chain, either chemically or mechanically. This enhances the interactions among the macromolecular chains after blending them into a polymer matrix (Pesetskii, Bogdanovich, & Myshkin, 2013).

2.5.1 PTFE

PTFE is a solid lubricant often used for wear and COF reduction in thermoplastics through formation of a transfer layer during sliding (T. Xie, Feng, Qi, & Cui, 2018). PTFE transfers onto the counterpart of the sliding pair to form a layer of adhesive coating. There are several roles for the transfer layer, i.e. to change the tribo–contact state of the frictional surfaces, protection of surfaces and ultimately reducing friction. For sliding systems comprising of PTFE and metals, the transfer layer will be formed instantly on the metal surface during sliding and change the friction interaction of metal–polymer into polymer–polymer, thus reducing friction and wear.

Other advantages of PTFE include its resistance to organic and inorganic solvents, its hydrophobic properties, and its electrical and thermal insulating capabilities. Its composites are typically processed using melt mixing process. Since the surface energy of PTFE is low, melt mixing process leads to poor distribution and nonhomogeneous dispersion. In composites where PTFE is added as second or third phase, mechanical properties may be compromised depending on the matrix material (Gao et al., 2011). As such, surface modification of PTFE is required to enhance compatibility to matrix (Ebnesajjad, 2015; Hunke, Soin, Shah, Kramer, Witan, et al., 2015). The disadvantage of using PTFE as a reinforcing phase is its low free surface energy. This causes weak molecular interactions between the composite components. The free energy of PTFE can be increased by either coarsening its surface or imparting new chemical groups on the surface layer. This task is fulfilled through surface modification to enhance its compatibility to the matrix.

Naturally, adhesion between POM and PTFE is poor due to incompatibility between these two polymers. PTFE has very low wettability and bond ability due to its low surface energy and non–stick properties (Chiang & Huang, 1999). Its chemical stability and inertness make the surface modification of PTFE very challenging. In order to impart polar functional groups to form hydrogen, oxygen or other bonds to its carbon backbone chain, the surface needs to be altered. Generally, the strategy applied is to etch its surface (Hunke, Soin, Shah, Kramer, Witan, et al., 2015). Chemical etching (Ebnesajjad, 2015) , plasma treatment (Vesel, Kovac, Zaplotnik, Modic, & Mozetic, 2015) or electron beam irradiation (Rahman et al., 2016) are among the methods frequently employed to alter its mechanical and/or chemical structure.

Huang et al. (2016) reported improvement in the compatibility between PTFE fibers and POM through plasma grafting polymerization using acrylamide (AAm) monomers to modify the surface of PTFE fibers. Morphology analysis using SEM was performed on PTFE fibers fabricated under different concentrations of monomers and process conditions. The surface morphology of neat PTFE, plasma treated PTFE and plasma grafting polymerization PTFE with different concentrations of AAm is presented in Figure 2.9. The surfaces of PTFE fibers with plasma treatment and plasma grafted polymerization revealed rougher texture compared to neat PTFE fibers.

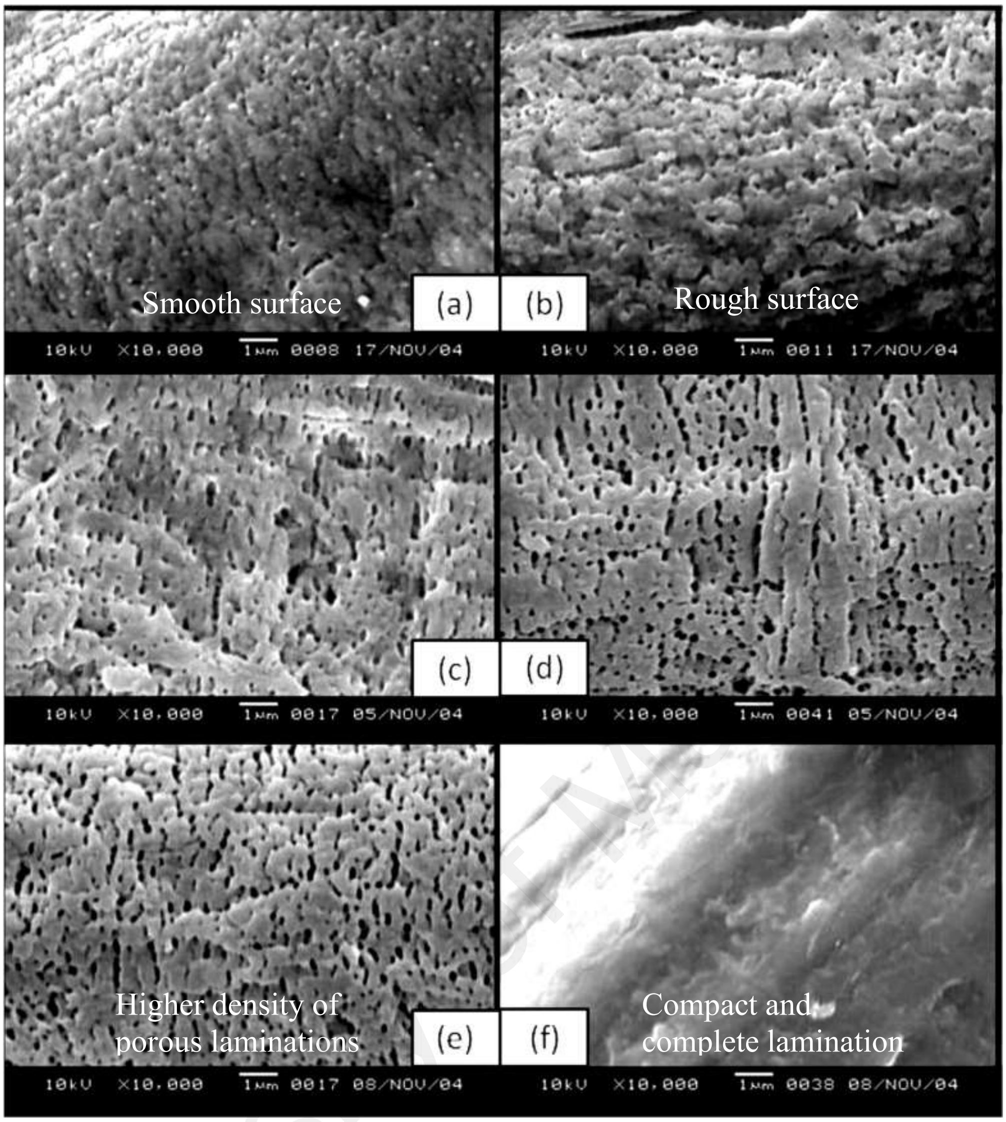

Figure 2.9: SEM photographs of the various PTFE fibers: (a) pure PTFE; (b) PPTFE (20 W and 30 min); (c) AAm_5–PTFE; (d) AAm_{10}–PTFE; (e) AAm_{15}–PTFE; (f) AAm_{20}–PTFE (C. Y. Huang et al., 2016)

Subsequently, POM was melt–blended with PTFE fibers and then subjected to mechanical tensile testing. The process conditions, concentrations of AAm during plasma grafting and the corresponding mechanical properties are shown in Table 2.4. With the addition of AAm during plasma treatment, stress, strain and impact strength improved significantly as a result of surface modification. Plasma grafting polymerization enhanced the compatibility of POM and PTFE fibers.

Table 2.4: POM/PTFE composites, process conditions, AAm concentration and the corresponding mechanical properties (C. Y. Huang et al., 2016)

Samples	POM (wt.%)	PTFE (wt.%)	AAm (wt.%)	Plasma Time (min)	Stress (MPa)	Strain (%)	Impact Strength
POM$_{100}$/PTFE$_{0}$	100	0	–	–	54.24	16.75	4.923
POM$_{85}$/PTFE$_{15}$	85	15	–	–	29.81	6.65	6.078
POM$_{85}$/PTFE$_{15}$	85	15	–	30	28.87	7.22	8.352
POM$_{85}$/AAm$_{5}$–PTFE$_{15}$	85	15	5	30	35.44	10.27	8.010
POM$_{85}$/AAm$_{10}$–PTFE$_{15}$	85	15	10	30	33.96	11.01	7.985
POM$_{85}$/AAm$_{15}$–PTFE$_{15}$	85	15	15	30	33.14	10.41	7.286
POM$_{85}$/AAm$_{20}$–PTFE$_{15}$	85	15	20	30	33.97	9.01	8.061

One of the strategies widely used to increase toughness for polymers is through incorporation of PTFE in the form of particulates. One of the mechanisms of toughness improvement is through crack pinning. When the dispersed phase pins the crack front, there is a subsequent lengthening and bowing of the crack front, increasing the fracture energy. Other mechanisms include bridging effects by the particles, yielding of these particles while remain bonded with matrix (cavitation) and formation of dilatational shear bands (Jesson & Watts, 2012). Such modifications require processing conditions to be thoroughly investigated and the effects to other mechanical properties. It is possible that an increase in toughness could be because of a reduction in tensile strength. A polymer is usually filled with particulates when the properties of interest are wear, fire retardancy, optical, etc. and is often added as a third phase.

Huang et al. (2011) compared the effects of blending micro and nano PTFE particles in POM matrix. As expected, PTFE enhanced tribological properties, but deteriorated tensile properties. Nano–PTFE was more effective in reducing frictional coefficient and wear. Table 2.5 summarizes the tensile properties and crystallinity for various POM/PTFE composites. With the addition of nano–PTFE, tensile strength and breaking elongation reduced only slightly. Once the nano–PTFE was higher than 2 wt.%, the mechanical properties fall sharply. This may be caused by agglomeration of nano–PTFE, weakening the interactions among POM macromolecular chains. Decrease crystallinity indicate the interaction between nano–PTFE and POM was poor; thus, adsorption of POM was difficult and nucleation with nano–PTFE did not occur.

Table 2.5: Mechanical and thermal properties of POM composites filled with micro– and nano–PTFE (T. Huang et al., 2011)

Samples	Tensile strength (MPa)	Breaking elongation rate (%)	Crystallinity, X_c (%)
Pure POM	63.50	49.82	52.9
POM/1% nano–PTFE	60.32	45.02	51.1
POM/2% nano–PTFE	59.04	44.15	47.0
POM/4% nano–PTFE	26.87	19.25	45.4
POM/2% micro–PTFE	57.08	39.89	–
POM/5% micro–PTFE	54.02	29.53	–
POM/10% micro–PTFE	49.35	28.17	–

As depicted in Figures 2.10 and 2.11, frictional coefficient and wear rate improved with higher mass fractions of PTFE particulates. Nano–PTFE was found to be more effective compared to micro–PTFE, where POM/PTFE with 2 wt.% nano–PTFE achieved similar tribological performance as POM/PTFE with 10 wt.% micro–PTFE. The smaller nanoparticles with high surface energy filled the rougher surface and wear scratches of its counterpart, forming a homogenous and compressed transfer film. Beyond the 2 wt.% nano–PTFE and 10 wt.% micro–PTFE, the tribological properties plateaued.

Two important observations can be deduced from this study. First, there is an optimum mass fraction of PTFE particulates to attain the good tribological performance. Beyond this optimum, mechanical properties will be compromised significantly. Second, with higher mass fraction of micro–PTFE, the reduction rate in mechanical properties is lesser compared to nano–PTFE. This is crucial when PTFE is added as second dispersed in POM composites comprising of an abrasive reinforcement, such as GF.

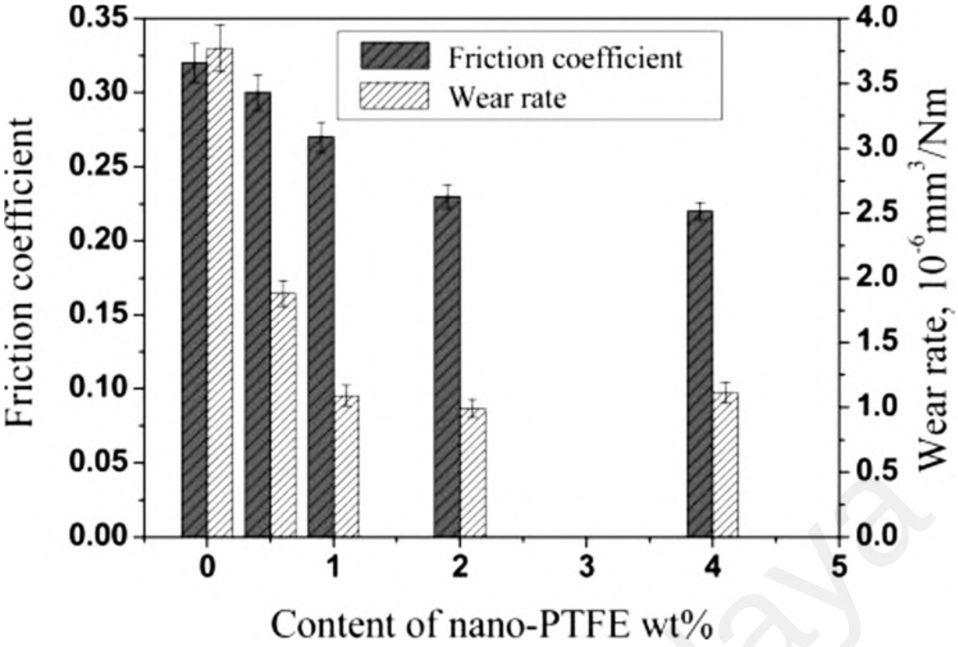

Figure 2.10: Friction coefficient and wear rate of POM/PTFE nanocomposites against concentration of nano–PTFE particles (T. Huang et al., 2011)

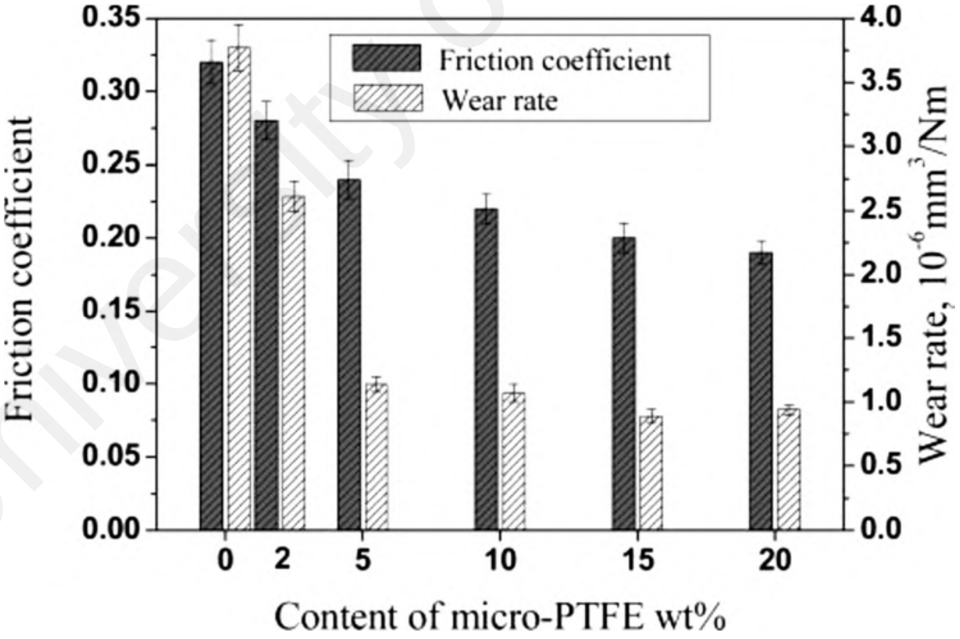

Figure 2.11: Friction coefficient and wear rate of POM/PTFE micro composites against concentration of micro–PTFE particles (T. Huang et al., 2011)

2.5.1.1 Aramid Fibers (AF) and Particles (AP)

AF is commonly used as organic reinforcement owing to its good stiffness to weight ratio, high thermal stability, stable frictional force and good wear performance. The effects of aspect ratio is important in enhancing tribological properties of aramid reinforced composites (Cai, Li, Wang, & Wang, 2015). When blended with POM, aramid in the form of fibers and particles enhanced friction and wear properties under dry frictional conditions. Due to anchoring of fibers within the matrix, POM composites reinforced with aramid fibers have better mechanical properties compared to aramid particles reinforcement (Huawei Zou et al., 2015). Addition of silica nanoparticles as second dispersed phase did not further improve COF and wear of aramid reinforced POM composites. However, tribological performance can be drastically improved by incorporating PTFE in conjunction with aramid. Figures 2.12 and 2.13 demonstrate the effects of these fillers on COF and specific wear rate, W_s (in mm^3/Nm) for POM based composites.

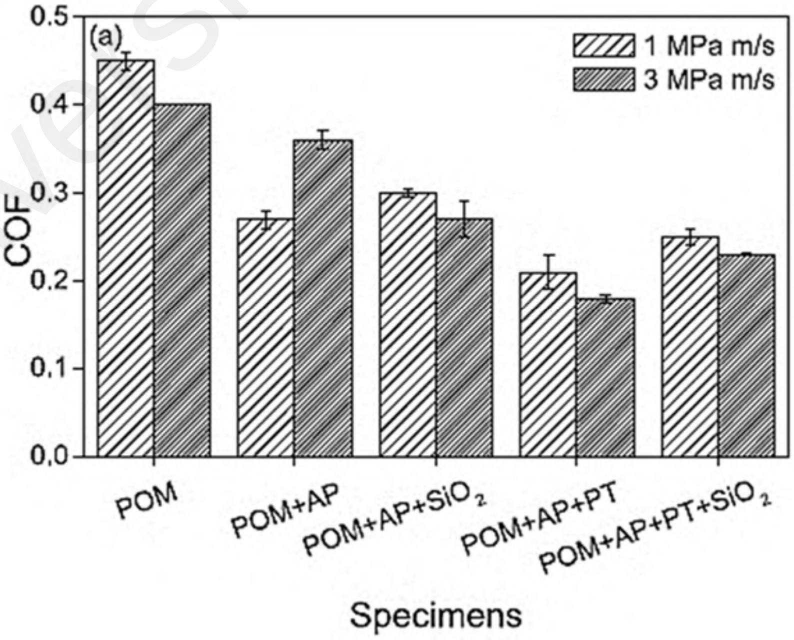

Figure 2.12: Frictional coefficient of neat POM and aramid reinforced POM composites (L. Zhang et al., 2017)

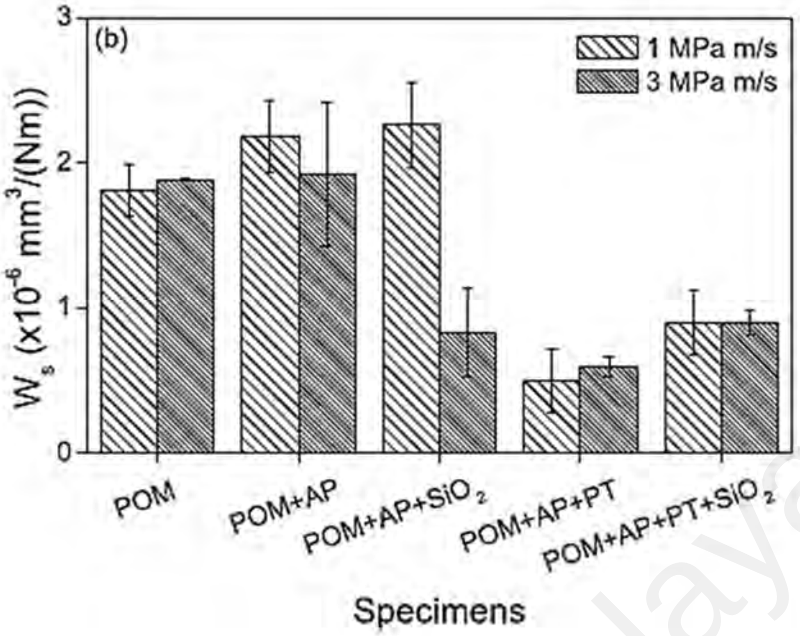

Figure 2.13: Specific wear rate of neat POM and aramid reinforced POM composites (L. Zhang et al., 2017)

2.5.2 Particulate Fillers

2.5.2.1 Alumina (Al_2O_3)

In the last three decades, many researchers have been attracted to the field of polymer nanocomposites (B. Liu, Pei, Wang, Wang, & Sun, 2012). Al_2O_3 is a nano–sized solid lubricant typically blended with POM to improve elasticity modulus, but negatively affects tensile strength. These nano–sized particles with high specific surface area and surface energy react with the macromolecular chains to enhance the interactions between them. The drawback of these small particles is the tendency to agglomerate and form bigger particles initiating stress concentration in composites. An area with more stress concentration affects the tensile strength. Addition of Al_2O_3 as solid lubricant further enhances tribological properties under oil lubrication condition over dry sliding condition (Sun et al., 2008b).

2.5.2.2 Molybdenum Disulfide (MoS_2)

MoS_2 is another solid lubricant commonly used to improve tribology properties of POM composites by enhancement of its stiffness. Its laminar structure is composed of strong S–Mo–S covalent bonds inside layers and weak van der Waals force between layers. Its superior lubricity is associated with these layered compounds that eases the sliding. Generally, nano–sized MoS_2 has better tribological properties; both lower COF and wear resistance compared to micro–sized MoS_2. During long sliding cycles of squared shaped POM/MoS_2 samples, stable self–lubricating properties were associated to the formation of debris and followed by reparation of surface asperities by these debris (Hu et al., 2009).

2.5.2.3 Silica (SiO_2)

Silica is commonly found in nature as sand and known for its superior hardness properties. SiO_2, as nanoparticles, are selected as a stabilizer because it exhibits high surface energy and can be functionalized to form a functional shell for core shell structured composites. Blending of nano–SiO_2 into POM and CF improved the tensile properties of the composites because of better interfacial adhesion (Fu et al., 2012). Although not reported, these abrasive particulates will deteriorate tribological properties.

2.5.2.4 Zinc Oxide (ZnO)

ZnO particles contribute to improved tribological properties by altering thermal conductivity of nanocomposites. ZnO modified PP showed lower COF and better wear resistance of the PP/ZnO nanocomposites. However, the effect of ZnO addition on the COF and surface roughness strongly depends on the dispersion quality of the nanofiller within the polymer matrix (Kreivaitis et al., 2015). When blended with POM matrix, tensile strength reduced slightly but significant improvement in elasticity modulus can be realized. Smaller nanoparticles result in better stiffness of POM/ZnO nanocomposites (Wacharawichanant et al., 2008).

2.5.3 POM–Polymer Blends

2.5.3.1 PEO

PEO has —(CH_2–CH_2–O)— repeat unit is also a well–known linear crystalline polymer. Presence of a methyl group in the repeat units differentiates PEO and POM. POM/PEO blend is a rare crystalline/crystalline system with good compatibility, which forms multi–scale and multilevel structures during liquid to solid process (Z. Chen et al., 2012). PEO as modifier increases notched impact strength and decrease COF and wear resistance. POM and PEO have good compatibility at amorphous and melting states as revealed by dynamic mechanical analysis (DMA) results and viscosity measurements. This polymer blend has 100 °C difference between crystallization temperature and melting point. PEO, when added to POM/PTFE fiber composite enhances the formation of transfer films on the mating surfaces during sliding contact, thus improving the COF and wear (B. Liu et al., 2012).

2.6 Interface and Interphase of Fiber–Matrix in Polymers

Polymer interfaces can be divided into non–interpenetrated and interpenetrated. Generally, non–interpenetrated interface occurs between polymers and impenetrable solids such as metals or glass or between a polymer melt and a polymer glass. Transfer of stresses at the interface happens via the type of bond between the two polymers, e.g. covalent bond, van der Waals forces or any other types of interactions. In the case of interpenetrated interface, certain amount of chain interpenetration occurs between two polymers. Chain entanglements is key for stress transfer. The interface of the two polymers is diffused and is better described as interphase instead of interface.

An adhesive bond between fiber and polymer matrix in liquid form starts with the latter spreading over the fiber's surface, triggering the interfacial molecular contact. Once this occurs, the molecules can then diffuse to form an interfacial zone with preferential conformations to trigger chemical reaction and the formation of chemical bonds across the interface. Ideally, the surface of fiber should be completely wetted by the melt polymer to minimize total free energy of the fiber–matrix system. The bond strength or adhesion between the two phases is determined by the extent of chemical interaction. For a fiber reinforced composite, its mechanical properties, such as tensile strength and elasticity modulus, are dependent on the properties of fibers used as reinforcement. Among them are, tensile properties, volume or mass fractions, orientation relative to load direction and length. As such, the interfacial properties determine the quality of a fiber–matrix composite.

The interphase of fiber–matrix comprises of finite interlayer. It has distinct physico–chemical properties of fiber and matrix. The finite and functional interlayer should improve compatibility of the system via formation of strong link between both phases. According to Drzal's concept as mentioned by Cech et al. (Cech, Palesch, & Lukes, 2013), the interphase is a three–dimensional region that include contact area with some finite thickness extending on both sides of interface in the fiber and matrix. Figure 2.14 illustrates the composite interphase with a cross section of fiber reinforced composite and a detail view of fiber surface.

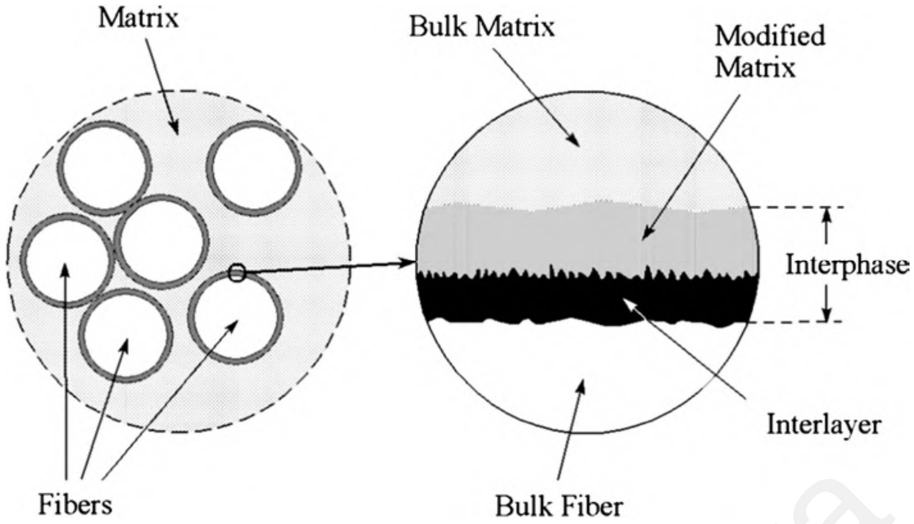

Figure 2.14: Schematic illustration of a composite interphase (Cech et al., 2013)

Performance of a composite is highly dependent on the interphase. As such, its design has attracted interest from both the academia and industry. It is important to customize interphase's properties based on the application parameters such as local stress fields, environmental conditions, temperature, etc. Since the primary cause of failure modes in fiber–reinforced polymers are usually de–bonding under transverse direction to fiber orientation and stress concentrations at the vicinity of fibers, interphase customization provides new strategies for improvement. Karger–Kocsis et al. introduced the term "Interphase Engineering" for the development of this engineering field (Karger-Kocsis et al., 2015).

2.6.1 Strategies for Interphase Customization

In general, the interphase customization can be carried out through surface modification of dispersed phase or from the matrix side. For any fiber reinforced polymer composite, the fiber's surface is etched and/or coated during their manufacturing process, referred as sizing (Luo, Zhao, Duan, & Du, 2011). However, there are differences between sizing and coating where the latter can incorporate fillers. For GF, sizing is carried out immediately after spinning process for surface fracture protection. An adhesion promoter, usually of silane–based coupling agent forms a film former along with an emulsifier and a lubricant. For fiber/matrix adhesion, effects of film former cannot be neglected because of its capability to diffuse into the matrix. As such, the film former should be highly compatible with the matrix (Karger–Kocsis et al., 2015). The alternate approach is to influence the interphase from the matrix side. The composition and microstructure of matrix can affect the fiber–matrix interphase resulting in changes to the performance of composite. Two common approaches are by addition of fillers and structuring of the bulk matrix.

In recent years, modification of fiber–matrix interphase via incorporation of micro– or nano–sized particles has been investigated widely (Cerclé & Favis, 2012). The approach has an advantage, as the properties are altered without any change of processing conditions. Well–dispersed particulate fillers fit between fibers, improving the interfacial shear strength and, thereby, the mechanical properties of fiber–reinforced composites (X. Xie, Mai, & Zhou, 2005). However, the influence of these particles on the fiber–matrix adhesion has shown inconsistent results.

Arao et al. (Arao et al., 2013) reported improved mechanical properties by incorporating nanofillers into carbon fiber/polypropylene (CF–PP) matrix. The interfacial shear strength remarkably improved between GF and PP by dispersing expanded graphite nanoplatelets (xGnP) based on the investigation by Pegoretti et al. (Pedrazzoli & Pegoretti, 2014). On the contrary, Zhang et al. (J. Zhang et al., 2013) found that inclusion of nano–silica particles in carbon fiber/epoxy did not affect the interfacial bonding behavior between fibers and the matrix. By characterizing transverse fiber bundle test and finite element analysis to determine thermal residual stresses, it was concluded that addition of silica nanoparticles in epoxy did not affect the interfacial bonding.

Shear and radial stresses at the interphase provide an insight for the design of engineered interfaces/interphases. Kumar et al. (Upadhyaya & Kumar, 2015) developed a micromechanical model to predict the stress transfer through the interphase of fiber–reinforced composites. To characterize the interphase of fiber–reinforced composites, different approaches have been reported. Cech et al. (Cech et al., 2013) successfully determined a region of 0.5 μm thickness in the periphery of glass fiber using atomic force microscopy (AFM) and DMA. A nano–scratch method reported by Schoneich et al. (Schöneich, Zamanzade, & Stommel, 2015) distinguished the fiber, matrix, and the interphase layer. Olmos et al. (Olmos, Arroyo, & González-Benito, 2012) revealed gradual phase separation at the interphase depending on the distance of glass fiber surface and epoxy modified with polymethylmethacrylate (PMMA) matrix. The PMMA domains were removed by immersing in dichloromethane (CH_2Cl_2) for one day before SEM morphology and calculation of PMMA particle density analysis from the fiber surface. Other indirect methods, such as the pull–out test, the microbond test, and the single fiber fragmentation test were reviewed by Graupner et al. (Graupner, Rößler, Ziegmann, & Müssig, 2014).

2.6.2 Wetting of Polymer Solids

In order to stain a solid surface, it needs to be wetted by the staining liquid. Therefore, wetting of surfaces directly involve surface free energies caused by unbalanced forces of molecules at the surface. This term, also called surface tension, is tied to the concept that the surface stays under tension. Surface tension or surface free energy, γ can be viewed as force per unit length (mN/m or N/m). Wetting is the ability of a liquid to spread over a solid surface depending on the attraction forces of liquid and solid surface (Drelich & Miller, 1995). Figure 2.15 illustrates the wetting phenomenon and Equation 2.1, known as Young's equation, describes the equilibrium contact angle for the three–phase system, i.e. solid filler, the melt state of matrix and the interface between two.

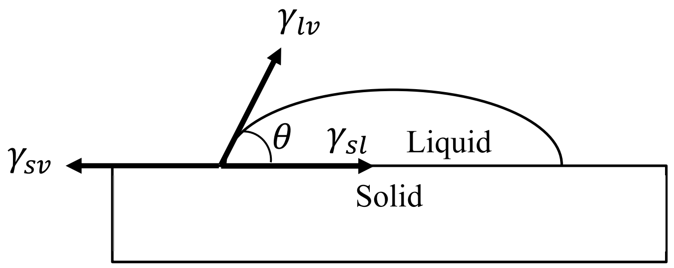

Figure 2.15: Wetting of liquid on a solid surface

$$\cos\theta = (\gamma_{sv} - \gamma_{sl})/\,\gamma_{lv} \tag{2.1}$$

where γ_{sv} is the surface energy of solid–vapor interface, γ_{sl} is surface energy of solid–liquid interface, γ_{lv} is the surface energy of liquid–vapor interface and θ is the contact angle between solid and liquid, i.e. filler and matrix. The contact angle, θ is a measure for degree of wetting (Sauer & Carney, 1990).

When $\theta = 0°$, the liquid spreads into a thin film and the solid is considered to be fully wetted out by the liquid. Based on Young's equation, this condition is fulfilled with high value of γ_{sv} and low values of γ_{sl} and γ_{lv}. This indicates when the molecular attraction between solid and liquid is more than the attraction between the liquid molecules, complete wetting would take place resulting in low contact angle. On the other hand, when $\theta \rightarrow 180°$, which is considered to be a limiting case, the attraction of between liquid molecules is greater than between liquid and solid molecules, liquid droplet will be formed over the solid surface. The high contact angle causes poor wetting of the solid surface.

In general, the solid is considered to be wetted the liquid when $0° < \theta < 90°$, although not completely. The solid favors to be covered by the liquid instead of the gas. When $90° < \theta < 180°$, the liquid does not wet the solid as the latter has much lower surface energy compared to the liquid (Van de Velde & Kiekens, 2000).

2.6.3 Surface Etching of PTFE

Fluorinated polymers are known to have low surface energies. These types of material can only be wetted by liquids that have equally low surface tension. PTFE has very low surface energy that wetting it is almost impossible using any commercial solvents or adhesives. There are some solvents with lower surface energy than PTFE but are highly toxic and expensive. When wetted by adhesives, its inertness prevents the formation of hydrogen bonds.

For POM based composites with PTFE as tribological enabler, two approaches can be taken. First, surface treatment of PTFE in order to increase the surface energy to facilitate wetting by the POM matrix. The second approach would be to wet with matrix that have low surface tension. As this research involve composite with three components, the former approach is preferred. The approach to increase the PTFE surface energy may also possibly enhance its adhesion to GF. This will reduce the stress concentrations at the ends of GF, thus improving mechanical properties of the composite.

Table 2.6 shows the surface energies and contact angles for PTFE, POM and GF (Ebnesajjad & Morgan, 2012). By increasing the surface energy of PTFE through surface modification, compatibility between PTFE and POM will improve interfacial adhesion to GF. The resulting effect is less deformation of GF which reduces matrix strain at the vicinity of GF. The challenges are adhesion and cohesion of phases. The ends of discontinuous fibers are high stress concentration sites which affect mechanical properties of the polymer composite.

Table 2.6: Surface energy and contact angle of matrix and reinforcement (Ebnesajjad & Morgan, 2012)

Material	Surface energy, γ (mN/m)	Contact angle, θ (°)
PTFE	20	109.2
POM	37	76.8
GF	70	75.0

As mentioned in section 2.5, one of the strategies to increase the surface energy of PTFE is through chemical etching. This is achieved by reduction of fluorine and increase of oxygen, carbon or other elements in surface composition. Etched PTFE surface will consist only small amount of fluorine. Etching depth on polymer surface using chemical etching can extend up to 300nm (Rye & Arnold, 1989). A highly porous surface structure is obtained, which promotes mechanical interlocking as the adhesion mechanism.

Surface chemistry of PTFE is greatly altered after etching. PTFE surface prior to etching is similar to a conducting wire with insulation where the carbon backbone is the wire whereas the fluorine atoms are the insulation. During etching, fluorine is removed to form free radicals on the carbon backbone. This allows other elements to react with these free radicals. After etching, elements such as oxygen, nitrogen, hydrogen replaces the fluorine atoms. Figure 2.16 shows the surface chemistry changes during etching process.

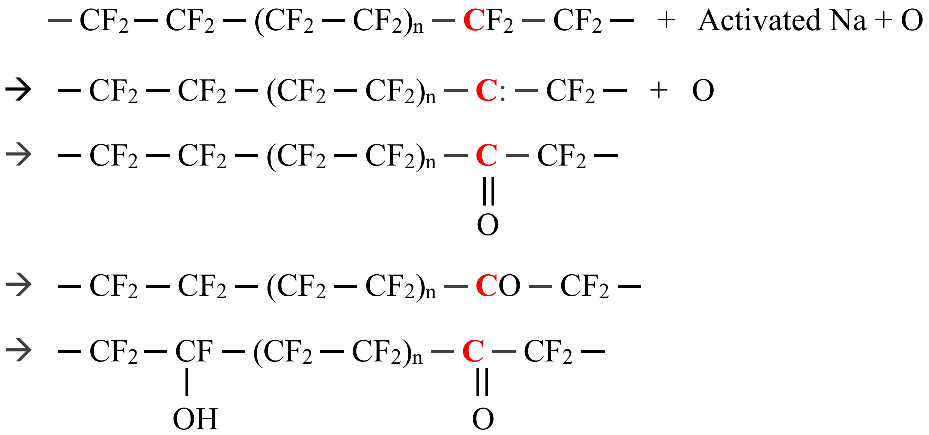

$$-CF_2-CF_2-(CF_2-CF_2)_n-CF_2-CF_2- \; + \; \text{Activated Na} + O$$
$$\rightarrow -CF_2-CF_2-(CF_2-CF_2)_n-C:-CF_2- \; + \; O$$
$$\rightarrow -CF_2-CF_2-(CF_2-CF_2)_n-\underset{\underset{O}{\|}}{C}-CF_2-$$
$$\rightarrow -CF_2-CF_2-(CF_2-CF_2)_n-CO-CF_2-$$
$$\rightarrow -CF_2-\underset{\underset{OH}{|}}{CF}-(CF_2-CF_2)_n-\underset{\underset{O}{\|}}{C}-CF_2-$$

Figure 2.16: Surface chemistry changes for PTFE during etching (Ebnesajjad, 2015)

2.7 POM/GF/PTFE Composites

In some applications, both mechanical and tribological properties needs to be better than neat POM. Blending with a suitable particulate filler to aid frictional and wear characteristics and selection of fiber with good strength and stiffness to enhance the mechanical properties is often preferred. It is known that toughening of polymer composites by addition of fillers in the form of particulates usually results in reduction of strength and stiffness. To obtain a high–performance POM based composite, the dependency of mechanical and tribological properties against the variation of fibers and fillers is vital.

Significant research has been dedicated to develop POM composites to achieve a low frictional coefficient and better wear resistance, as well as excellent tensile strength and elasticity modulus (Cho & Park, 2011; Kalacska, 2012; Krishna, Suresha, Kallesh, & Hemanth, 2016). Transfer films formed by solid lubricants, such as PTFE, play an important role in stabilizing COF, but at the expense of mechanical properties. On the contrary, high strength reinforcing fibers, such GF, have negative effects to tribological performance. It is well established that tribology is a system behavior influenced by complex tribo–chemical and tribo–physical actions taking place at the interface of sliding counterparts. Based on the literature reviewed in earlier sections, extensive studies have been carried out on the effects of reinforcing fillers or fibers on POM based composites independently. It can be concluded that the lubricating properties of PTFE as reinforcing fillers are one of the main influencing factors in transfer film formation whereas high strength GF, when coated with a coupling agent to promote adhesion with POM matrix, governs the mechanical properties. However, only limited literature can be found on the combined effects of GF and PTFE as second and third dispersed phase in POM matrix.

Zhang et al. (2017) systematically experimented the properties of reinforcing fillers on the transfer film structure on POM–fiber composites. POM composites were reinforced with aramid particles (AP), short carbon fibers (SCF) and short glass fibers (SGF). As tribological enablers, the composites were filled with PTFE micro particles of 4 µm average dimeter and silica nanoparticles of 20 nm average diameter. Samples were prepared in accordance to Table 2.7 and subjected to tribology testing using Pin–On–Disc (POD) tribometer with normal pressures of 1 MPa and 3 MPa and sliding speed of 1 m/s. Correlation between tribological properties and how the properties of fillers affect transfer film formed on the steel counterpart was established. This led to greater understanding into tribological characteristics of POM hybrid composites with various reinforcements.

Table 2.7: Compositions of POM composites studied (L. Zhang et al., 2017)

Composites	Compositions (vol.%)					
	POM	AP	SCF	SGF	PTFE	SiO_2
POM+AP	85	15	–	–	–	–
POM+AP+SiO_2	83	15	–	–	–	2
POM+AP+PTFE	65	15	–	–	20	–
POM+AP+PTFE+SiO_2	63	15	–	–	20	2
POM+SCF	90	–	10	–	–	–
POM+SCF+SiO_2	88	–	10	–	–	2
POM+SCF+PTFE	70	–	10	–	20	–
POM+SCF+PTFE+SiO_2	68	–	10	–	20	2
POM+SGF	90	–	–	10	–	–
POM+SGF+SiO_2	88	–	–	10	–	2
POM+SGF+PTFE	70	–	–	10	20	–
POM+SGF+PTFE+SiO_2	68	–	–	10	20	2

Figures 2.17 and 2.18 shows the COF and W_s (mm^3/Nm) Addition of silica nanoparticles (SiO_2) to POM/GF did not ameliorate the tribological properties but blending PTFE micro particles into POM/GF significantly enhanced the coefficient of friction and wear rate. Evidence of a uniform PTFE–based transfer film formation on the steel counter surface was reported.

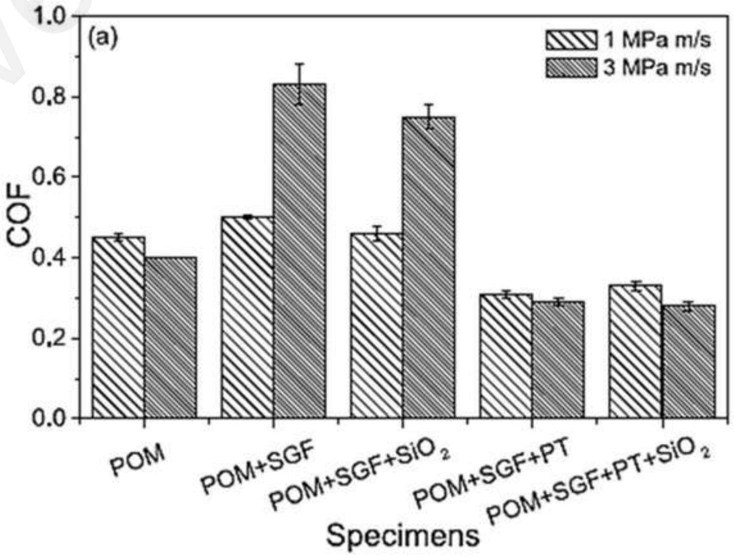

Figure 2.17: COF of POM composites SGF–reinforced and filled with PTFE and SiO_2 (Zhang et al., 2017)

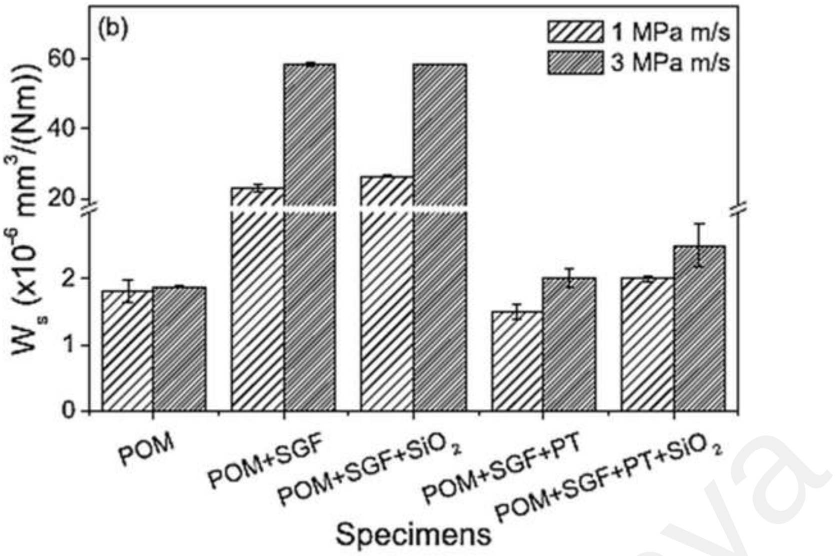

Figure 2.18: W_s of POM composites SGF–reinforced and filled with PTFE and SiO_2 (Zhang et al., 2017)

Suresha et al. (Suresha, Hemanth, & Sekar, 2014) reported that the addition of PTFE particles into neat POM deteriorated the tensile strength by 23%. Addition of glass fibers improved the strength of POM/GF/PTFE composite by 20%. Tribology characterization was not reported. Benabdallah (Benabdallah, 2003) reported that POM filled with 20% GF resulted in deterioration of COF and wear resistance. On the other hand, when POM was filled with 20% PTFE micro particles, COF and wear resistance improved significantly. Franklin et al. (Franklin & de Kraker, 2003) conducted a detailed study investigating the relationship between the characteristics of a transfer layer formed by POM filled with 20% PTFE and the counter face surface topography. Wear rate was influenced by the counter face surface topography and the characteristics of the transfer layer. Mechanical properties such as tensile strength, elasticity modulus, elongation at break, and impact strength can be improved as a result of better compatibility of POM and PTFE. This is evident in the work carried out by Chiang et al., where increasing PTFE particles composition up to 15% steadily improved tensile properties. Beyond 15%, the strength of POM/PTFE composite deteriorated. With surface modification of PTFE particles through chemical etching, superior mechanical properties were achieved.

2.8 Design of Experiments (DOE)

Researchers are interested on system or process investigations where several variables affect a particular response of interest. These investigations are usually centered around manipulating multiple process variables or factors simultaneously to observe the corresponding changes to the process output or response. Often, not only the individual changes produced by the variables are of interest, but their interactions as well. Traditionally, in an investigation, experiments are planned to study the effects of a single variable of a process. However, the combined study of multiple factors represents a way to determine the main effects, as well as the interaction effects among the factors underlying the process. In engineering, experimentation is important in development of new products, manufacturing processes and continuous process improvement. In many cases, the goal is to develop a robust process, where it has minimal impact when exposed to external sources of variability.

DOE refers to the process of planning an experiment in order to collect appropriate data that can be analyzed using statistical methods. It is a framework of statistical techniques, such that the results produce valid and objective conclusions. Data analysis using statistical methods allow the researcher to draw meaningful conclusions, particularly when the data are susceptible to experimental errors. As such, there are two important aspects of DOE, i.e. the design of the experiment and the statistical analysis of the data. Both of these are related as the choice of design determines the analysis method to be utilized. Ultimately, the researcher being knowledgeable in his/her field, must be able to extract valuable information from the experimental data (Montgomery, 2013).

DOE was developed originally for agriculture and later became a quality improvement tool during World War II. Its application encompassed statistical process control (SPC). Chemical, food and pharmaceutical industries mainly used DOE prior to 1980s. With the great success of modern electronics, automobiles and personal computers, SPC and DOE were widely adopted by these industries. In fact, statistically designed experiments have been used in all areas of science and engineering. There has been an extensive use of designed experiments in numerous areas, including the business service sector, financial services, government operations, e–commerce and many nonprofit business sectors.

Sir Ronald A. Fisher pioneered the development of DOE in 1920s and early 1930s. At Rothamsted Agricultural Field Research Station in London, Fisher was responsible for statistical data analysis. Field experiments were carried out to determine the effects of fertilizers on various agricultural lands. It was found that the final condition of the crop was dependent primarily on fertilizers. However, other factors such as condition of soil, soil's moisture content, etc. were also affecting the crop. The DOE was able to differentiate the effect of fertilizer and the effect of other factors successfully. Since then, DOE have been extensively applied in agricultural fields and also in many other industries (Patrick & Mark, 2005).

Scientific experiments involve a sequence of activities as below;

- Hypothesis – An assumption that motivates the experiment
- Experiment – Series of tests conducted to investigate the hypothesis
- Analysis – Involves understanding the nature of data and performing statistical analysis of the data
- Interpretation – Understanding the results
- Conclusion – Verifies whether the original hypothesis is true or false

The systematic experimentation strategy starts with a standard two level fractional factorial design, mathematically designated as "2^{k-p}", where k is the number of process variables and p is the fraction. At this phase, the goal is to discover the variables that produce statistically significant effects to the process. In general, minimum number of experiments are preferred since the objective is screen the vital few factors from the trivial many. By reducing the number of experiments, the ability of the design to discover higher order interactions between factors declines.

Once the influence of vital factors and effects of the trivial many are known, the experiment enters breakthrough phase where interactions become evident. Hence, designs with higher resolution are selected as it generates huge return–on–investment (ROI) at this breakthrough phase. Experimenters can expect 80% or more of all that can be gained in the response might be at this point by investing only 20% of the overall experimental work. The specification for these vital factors is defined by determining the change in the response when one or more factors are adjusted.

The information obtained from the breakthrough phase can be used to determine the direction of adjustment for the vital factors to obtain best possible response. Usually, some of these vital factors may influence the output more than others through reduction of variability. Statistically, these benefits can be obtained if a curvature is detected. The remaining 20% gain can be obtained through optimization of processes involving these vital factors. This is the point where RSM comes into play. It is necessary to perform another experiment to develop a statistical model representing an accurate estimate of the operating conditions for vital factors (Patrick & Mark, 2005).

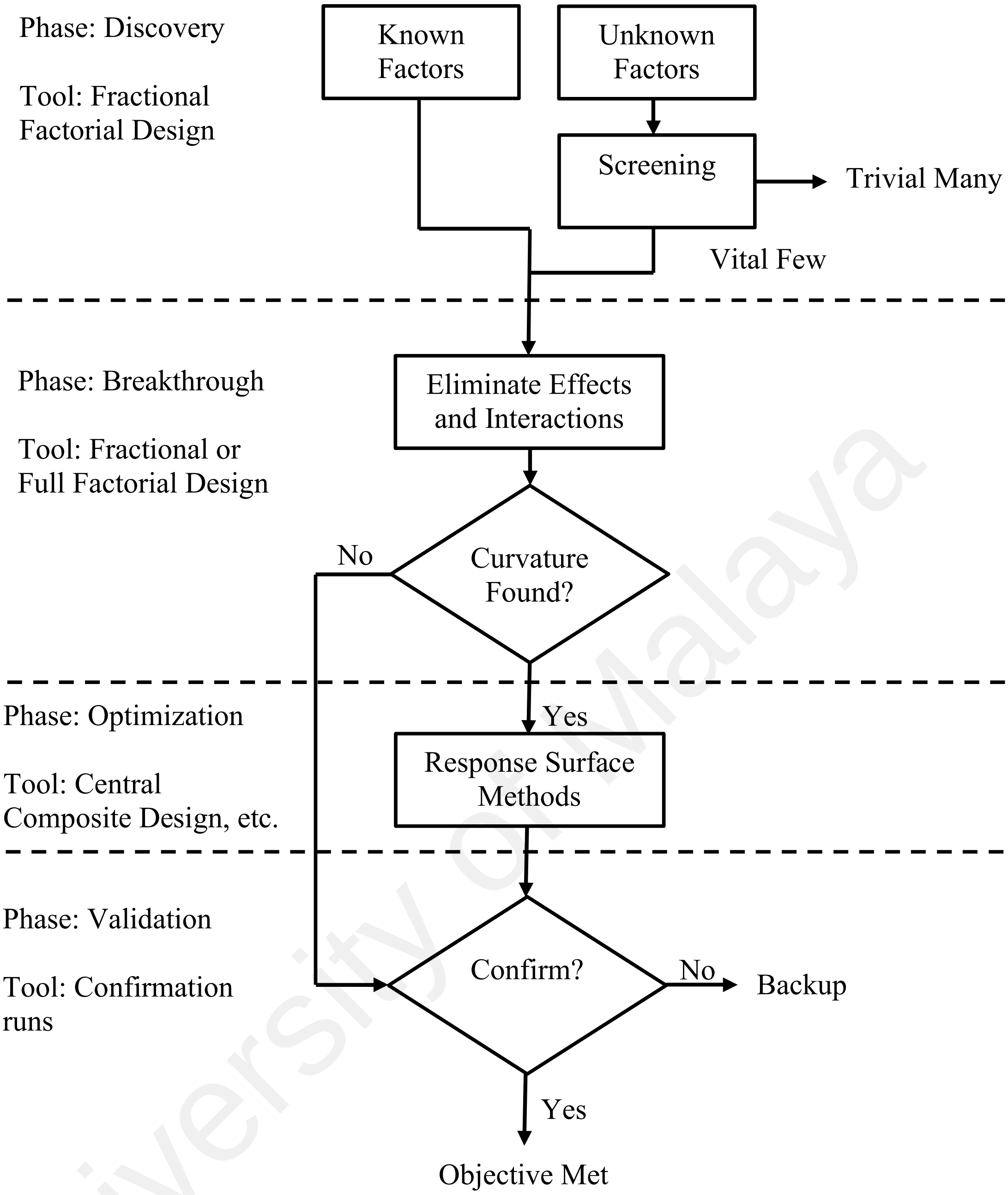

Figure 2.19: Strategy of experimentation using DOE (Patrick & Mark, 2005)

DOE methodology has been highly successful in the verification, improvement and reduction of process variability. In addition to product quality being predictable in the early development phases, this effectively improves development cost and time. A relevant class of DOE techniques is called factorial design, where the goal is to study and analyze the results (effects) produced by multiple variables of a process. The beginning of a factorial design is a careful selection of a fixed number of levels for each set of factors. The experiments should be performed with all combination's factors and levels.

For example, if there are l_1 levels to the first variable, l_2 for the second, ..., l_k for the $k\text{–}th$ factor, the full array of l_1, l_2, …, l_k plays will be classified as factorial design $l_1 \times l_2 \times \ldots \times l_k$. The default schema for designs with two levels uses the notation "–" (negative) and "+" (positive) to denote the low and high levels of each factor, respectively. For example, a 2 × 2 factorial design with two factors (x_1 and x_2) and two levels (low and high), requires four experimental runs.

2.8.1 Full Factorial Design

When all combinations of factors are running at the same number of times for each level, the experiment is classified as 2^k full factorial design. The most intuitive approach to study such factors would be varying the factors of interest in a full factorial design, i.e. trying all possible combinations of settings. For example, a 2^3 full factorial with three factors (x_1, x_2, and x_3) at two levels requires eight experiments, while to study five factors at two levels, the number of runs would be $2^5 = 32$, and $2^6 = 64$, and so on. So, the number of runs required for 2^k full factorial design grows geometrically as k increases, and therefore even the number of factors is small, a full factorial design can increase the number of experiments significantly. In these circumstances, it is recommended to use fractional factorials designs.

2.8.2 Fractional Factorial Design

Fractional factorial designs represent one way where only a fraction of appropriate combinations required for 2^k full factorial designs is selected for execution. Fractional designs are commonly used when one wants to investigate k factors with smaller number ($2^{k–p}$) of experiments, where p is the reduction factor. For example, the 2^3 full factorial design can be re–written as a fractional factorial design $2^{3-1} = 2^3/2 = 4$, where 4 is the number of experiments.

This design is described as 2^{3-1} design of resolution III. This means that the overall $k = 3$ factors, however, one half of those factors were generated from the interactions of $2^{[(3-1) = 4]}$ full factorial design. There are main and interaction effects that confound with each other. However, fractional designs require a smaller number of experiments as compared to the full factorial design, but with the assumption that higher–order interactions do not matter. Therefore, greater than two–way interactions may escape detection.

Design resolutions provide information of how the main and interaction effects in a fractional factorial design are aliased. One or more effects are confounded, where estimating them separately from each other is not possible. It is a good practice to employ a highest possible resolution for a fractional factorial design. For example, it is beneficial to select a design where the main effects confound with three–way interactions (Resolution IV) as an alternative to a design where main effects are confounded with two–way interactions (Resolution III). Fractional factorial designs of resolution III, IV, and V are important (Anderson & Whitcomb, 2015). The definitions of these designs are as follow;

- Resolution III – No main effects are aliased with any other main effect, but main effects are aliased with two–factor interactions.
- Resolution IV – No main effects are aliased with any other main effects and two–factor interactions, but some two-factor interactions are aliased with other two–factor interactions and main effects are aliased with three–factor interactions.
- Resolution V – No main effects or two–factor interactions are aliased with any other main effects or two–factor interactions, but two–factor interactions are aliased with 3–factor interactions and main effects are aliased with four–factor interactions.

2.9 Response Surface Methodology (RSM)

The development of RSM started since the publication of an article by Box and Wilson entitled "On the experimental attainment of optimum conditions" (Box & Wilson, 1951). The need for a systematic strategy of experimentation continued where it became common industrial practice in UK and other countries. Du Pont US became the leader for making effective use of DOE and RSM where engineers, scientist and quality personnel were trained extensively. Presently, RSM is commonly adopted in industries and academia as a statistical modelling tool.

RSM is a statistical design method that lead to peak process performance. It is useful for modelling and analyzing applications where the response is influenced by several variables and the goal is to optimize this response. Such response surface plots represent on a surface graph in a three–dimensional environment as depicted in Figure 2.20. To visualize its shape, the response surface's contour as illustrated in Figure 2.21 is utilized. In the x_1 and x_2 plane, constant response lines are drawn and each contour corresponds to a response surface particular height. Experimenters obtain the most value from these maps along with the mathematical equations and statistics utilized to generate the plot.

The relation between the response and independent variables is unknown in most of RSM problems. Thus, RSM's first step is to find an adequate rapprochement to the real relationship between the response and independent variables. In general, a polynomial of low order is applied to some areas for the independent variables. If a linear model is sufficient to establish their relationship, then the transfer function will be first–order model. If a curvature exists, then a higher degree polynomial must be used, such as second–order model.

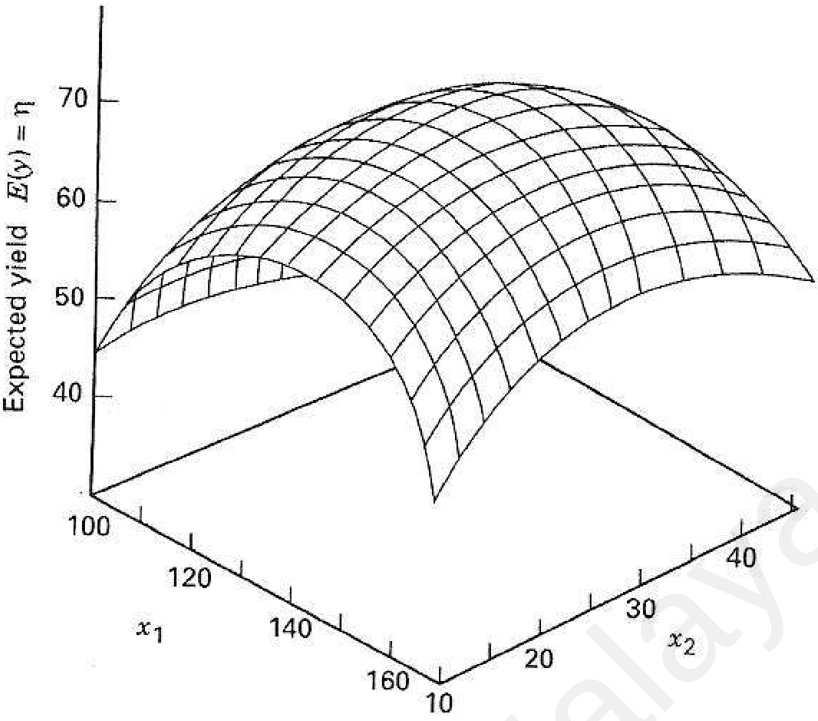

Figure 2.20: A three–dimensional response surface showing an expected response, E(y) as a function of x_1 and x_2 (Montgomery, 2013)

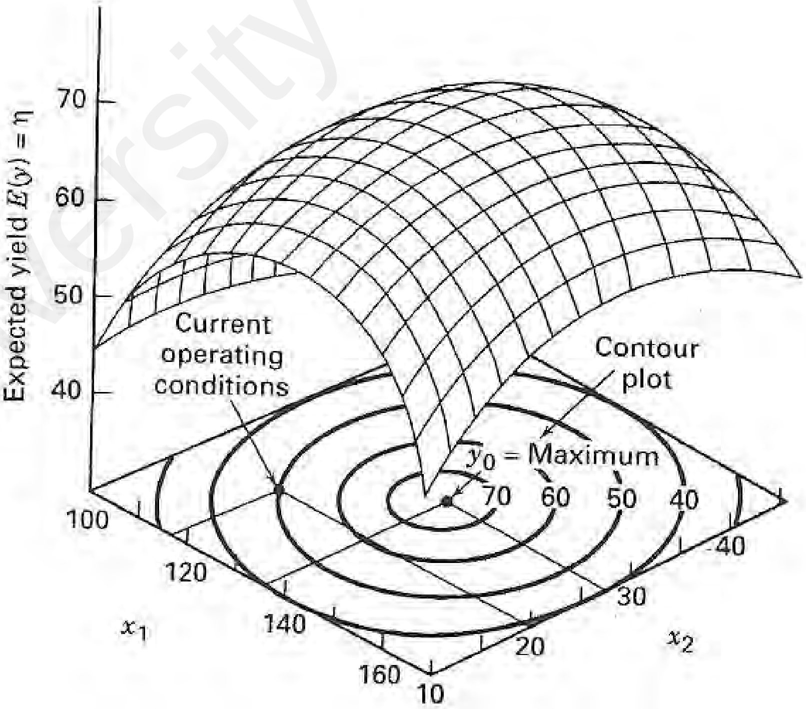

Figure 2.21: A two–dimensional contour plot of a response (Montgomery, 2013)

One or both of these models are used in almost all RSM applications. Realistically, it is not feasible that a polynomial model could be a reasonable rapprochement to a real functional relationship of the whole independent variables' environment. However, when the interest is only limited to a relatively small area or a certain boundary conditions, these models usually work quite well.

To estimate parameters to establish a mathematical model through derivation of a polynomial, the minimum squares method is used. Response surface analysis is then performed in terms of adjusted surfaces. If the adjusted surface is an adequate representation of the response's true functions, the adjusted surfaces will be almost equivalent to the real system analysis. The model parameters can be estimated most effectively if a proper experimental design is used for data collection. A design for adjusted response surface is called response surface design (Montgomery, 2013).

RSM is usually performed sequentially. When the location of response surface is far from optimum, e.g. such as the current operating conditions in Figure 2.22, there is very little curvature in the system and first–order model will be appropriate. The goal is to efficiently lead the experimentalist to optimum surroundings. Once the optimum region has been found, a more elaborate model, such as second–order model may be applied. Analysis may be performed to locate the optimum.

In Figure 2.22, the analysis of a response surface can be seen as "climbing a hill" where the top of the hill represents maximum response. If an optimum is a point of minimum response, then it is as "going down a valley".

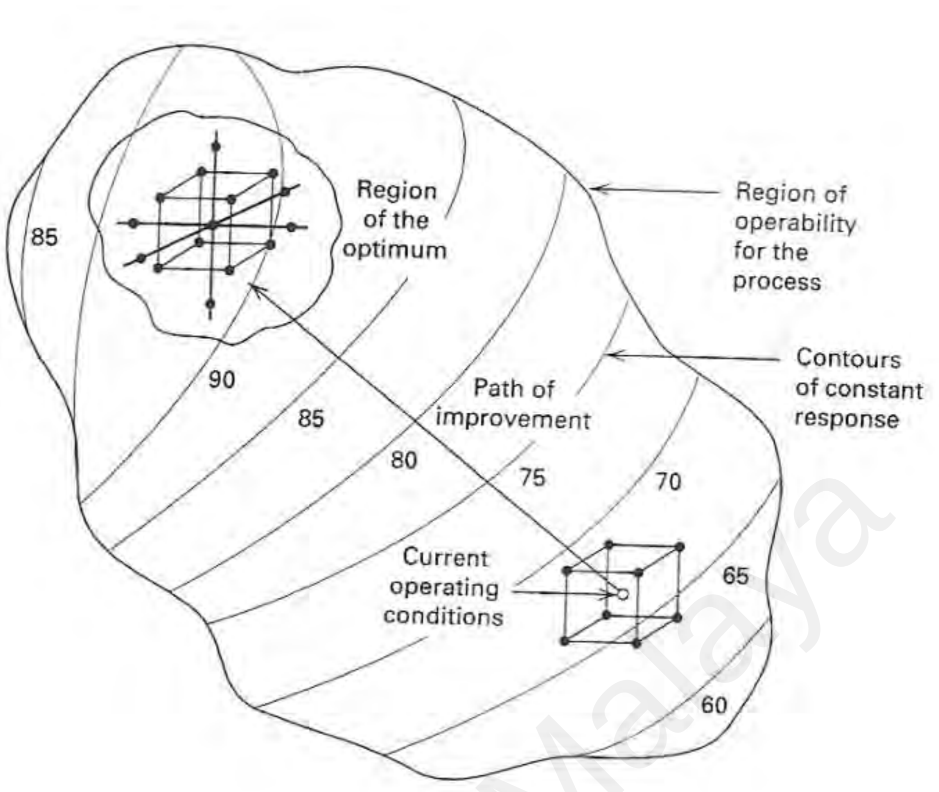

Figure 2.22: The sequential nature of RSM (Montgomery, 2013)

2.10 Fabrication of POM/GF/PTFE Composites

2.10.1 Plastic Injection Moulding

Injection molding is one of the processing methods to convert thermoplastics, in the form of pellets or powder, into a specific shape of products. This concept was first developed in the 1870s as a result of billiard balls as an alternate to ivory. In 1868, Phelan and Collender Company, a manufacturer of billiard balls offered a lucrative reward for a suitable replacement of ivory. John Wesley Hyatt successfully invented celluloid (cellulose nitrate) which became the first synthetic resin to be commercially produced for billiard balls and dentures. Subsequently, he patented the extrusion devise which used the basic concept in modern injection moulding machines.

The injection molding process begins with the heating of pellets or powder to its melting point. Then, the melt is injected precisely into a mold consisting of a retractable and a fixed partner. The mold temperature is usually regulated through a water–based cooling system. The molten plastic is held inside the mold under pressure until the material solidifies. Subsequently, the mold retracts and the product is ejected. Hence, the injection molding machine must perform three essential functions. First, melt the pellets so that it can flow under pressure. Second, injection of the melt plastic precisely into the mold through an opening, known as the gate. And third, keep the melt inside the mold until it solidifies and then eject the solid plastic to the shape of final product out of the mold. All of these functions must be carried out through an automated process that is capable of manufacturing a product of good quality and low cost.

Injection moulding is commonly used to manufacture reinforced POM composites because of short production cycle and ease of moulding into complex forms. This enables precision components to be manufactured in high volume with reasonable cost. Process conditions for injection moulding influence the tensile properties of POM/GF composites. Some of these injection moulding parameters are melt temperature, filling time, mould temperature and packing pressure (Hsu, Hwang, & Ting, 2010). Mechanical properties are also dependent on amount, orientation, thickness and distribution of GF within POM matrix. Hence, identification and controlling these parameters are crucial to ensure components meet the intended mechanical properties (Y. Wang, Kim, & Song, 2014). In reality, managing process controls for injection moulding has been a major concern of the plastics manufacturing industry (Singh & Verma, 2017). Newer approaches for process monitoring based on process and product fingerprints over the conventional metrology efforts to determine process stability and part quality monitoring reveal exciting opportunities (Giannekas, Zhang, & Tosello, 2018).

Figure 2.23 shows a reciprocating screw injection moulding machine. Two main components that perform the cyclical steps during injection molding process are the injection unit and the clamping unit. Resin is placed inside the hopper and fixed volume is fed into the rotating screw. The solid resin is then plasticized by the screw and forms a constant volume of homogenous melt. Heaters located on the barrel accurately control the temperature of the melt polymer. The rotation stops and the screw then acts as a ram and thrust forward to inject the melt under high pressure using hydraulically driven cylinder. A sprue is the thick section which the molten resin is forced from the nozzle first enters the mould, which can be of single of multiple cavities depending on the size and shape of samples. Once the mould is filled, it is cooled and opened to release the moulded sample (Fried, 2014).

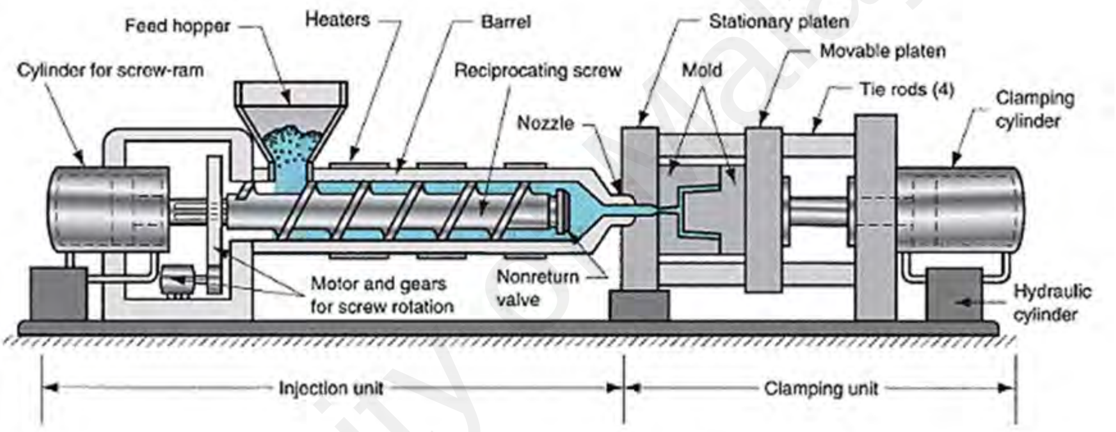

Figure 2.23: Typical reciprocating screw injection moulding machine and mould

The process parameters for injection molding can affect the mechanical and thermal properties of POM composites. Bai et al. (2012) reported injection speed influenced phase morphology, crystallization properties and mechanical properties for POM/PEO composites. Increasing injection speed decreased the PEO size and positioned PEO towards the crystal lamella resulting in better impact strength (Bai & Wang, 2012). Higher injection speed can expand the POM–rich phase into wider area. Improvement in the distribution of this phase enhanced the mechanical properties of POM/PLA composites (Mathurosemontri, Auwongsuwan, Nagai, & Hamada, 2014).

2.10.2 Isostatic Hot Press

Isostatic hot press falls under the category of compression moulding process. It is the most economical and simplest for polymer processing. The process to produce samples uses a press consist of upper and lower dies with built–in heat elements. These dies are initially apart and mould of certain shape is then placed on the lower die. The resin is placed into the mould which is open and heated by the heaters built in the lower die. Next, the upper die is lowered until it contacts the lower die. The pressure, time and temperature are controlled parameters used to completely fill the molten resin inside mould cavity. Flashes are common due the excess resin is forced to flow out of mould.

The advantages of isostatic hot press method are samples having lower stresses due to resin flows over shorter distances, mould design is fairly simple with low maintenance and cost. The resin is placed in a mould, heated to its melting point to form the required specimen. This not only leads to weakness points in a moulding, but also has a major disadvantage in sustaining consistent mould temperature to increase reaction time of the resin. Poor moulding can be caused by short curing time of resin at localized areas in the mould and cause inhomogeneous pressure.

2.11 Summary

POM is an important engineering plastic widely used in automotive, aerospace and electronics industries due to its good mechanical, tribological and thermal properties. As its application continues to expand, there is a need to further enhance its composites by incorporating reinforcements. For an example, in automotive industry, POM based composites are primarily used to improve fuel efficiency through reduction of vehicle weight. There are not many other engineering plastics that can replace POM without compromising quality, performance and cost.

Incorporating GF as reinforcement is one of the most effective ways to strengthen POM. Compared to other class of fibers, it is cheaper and less brittle when used in polymer composites. Therefore, POM reinforced with GF are very strong and relatively lightweight. In tribological applications under high load and sliding speed such as bearings and gears, the performance of POM/GF is compromised because of the abrasive characteristics of GF.

As such, addition of a second disperse phase is necessary. The shape consideration of this filler is crucial as the mechanical properties enhanced as a result of GF reinforcement may be compromised. PTFE is an excellent solid lubricant to enable better rubbing properties of polymer composites. PTFE fibers are effective in enhancing mechanical properties but tribological properties, especially wear, may not be optimized due to generation of debris. On the other hand, PTFE particles improve tribological properties but at the expense of mechanical properties. It is known that an optimum mass fraction of PTFE particulates exists to accomplish good tribological performance with negligible loss of mechanical characteristics. Beyond this, mechanical properties are compromised significantly. Given the same mass fractions, mechanical properties deteriorate more with nano–PTFE compared to micro–PTFE.

Theoretically, PTFE nanoparticles can produce composites with superior mechanical properties because it provides a larger surface area for stress transfer mechanism. However, they tend to agglomerate because of high surface energy. The clustering forms agglomeration and weak bond between these agglomerates causes failure when matrix–filler debonding occurs. In addition, stiffness of polymer composites also reduces due to nonhomogeneous dispersion.

As such, PTFE microparticles are selected. The disadvantage of using PTFE as reinforcing phase is its low free surface energy. This causes weak molecular interactions between the composite components. The surface free energy of micro–PTFE micro is increased by either coarsening its surface or imparting new functional chemical groups on the surface layer. This task has been fulfilled through surface modification using chemical etching to enhance its compatibility to matrix. This is achieved by preparation of an etch solution using sodium naphthalene salt dissolved in tetrahydrofuran. Stirring the micro–PTFE in the etch solution effectively roughened the surface.

In this work, POM/GF is used as a matrix where GF acts as the reinforcement phase. The composition of GF is unchanged at 25% of mass fraction. Surface modified PTFE micro particles are melt–blended with the matrix. Samples are prepared using injection moulding process. The POM/GF/PTFE composites' strength, stiffness, toughness, and hardness are characterized with PTFE content and PTFE etch time as control variables. Response surface methodology (RSM) is employed to determine the dependency of these mechanical properties against PTFE content and PTFE etch time (Kunnan Singh, Ching, Abdullah, et al., 2018). The aim of this work is to identify a stable region where the mechanical properties for POM/GF/PTFE composites are optimal. Based on the literature search, there is no information available on any optimization of mechanical properties involving POM/GF/PTFE composites using the statistical modeling approach.

The effects of these surface etched micro–PTFE on the fiber–matrix interface are also studied by characterizing the coefficient of friction, wear loss, morphology of worn surfaces, and the chemistry of the interface layer (Kunnan Singh, Ching, Liu, et al., 2018). The aim of this work is to characterize the tribological properties of POM/GF/PTFE composites as a function of micro–PTFE content. There have been several studies on tribological performance of POM composites blended with various reinforcing fillers. Reviewing existing publications, it was established that the effects of surface etched micro–PTFE at the fiber–matrix interface of POM/GF/PTFE composites have not been systematically studied.

CHAPTER 3: METHODOLOGY

3.1 Introduction

The effects of PTFE micro particles on POM reinforced with GF were thoroughly investigated in this research. The micro–PTFE was chemically etched using sodium naphthalenide solution prior to melt blending into POM/GF matrix. Samples were prepared using injection moulding process. As process parameters may influence the material properties, an important step of the experimentation involved identification and control of these vital process parameters.

3.2 Materials

POM with 25% GF reinforcement, commercially known as POM525GR, used as the matrix was purchased from Du Pont (Kuala Lumpur, Malaysia). It is a homopolymer with density of 1.6 g/cm^3 and melting temperature of 178 °C. The filler, PTFE, in the form of micro particles with an average particle size of 12 µm, density of 0.425 g/cm^3 and specific surface area of 1.5–3.0 m^2/g were also acquired from Du Pont (Kuala Lumpur, Malaysia). The etch solution was prepared in the lab by dissolving sodium naphthalene salt in tetrahydrofuran obtained from J.T. Bakker (Kuala Lumpur, Malaysia). The density of sodium salt was 0.45 g/cm^3.

3.3 Preparation of Etch Solution for PTFE Micro Particles

Preparation of the etch solution was carried out using a magnetic stirrer. Sodium naphthalene salt was added directly to tetrahydrofuran. The mixture, comprising 5% sodium naphthalene to 95% tetrahydrofuran, was stirred at 25 °C for 5 min with stirring speed of 350 rpm. A dark brown saturated solution was formed. Next, 30 g of PTFE micro particles was added to the etch solution and stirred at 25 °C for 10 min with stirring speed of 525 rpm. Upon completion of the stirring cycle, the sediments were left to settle for about 1 min. The solid sediment, comprising sodium salt and micro–PTFE, settled at the bottom. The upper liquid was then poured away carefully.

The sediment was subjected to a wash cycle using 200 cm^3 of acetone. The mixture was stirred for 5 min at 525 rpm. Upon completion, the sediment was left to settle for 3 min. The upper liquid was discharged before subjecting the residue to two further wash cycles. All wash cycles utilized the same volume of acetone and stirring conditions.

The solid was then rinsed in 200 cm^3 of distilled water. A total of 5 rinse cycles were repeated, each cycle consisting of 2 min stirring at 525 rpm speed. After each rinse cycle, the solid was left to settle for 3 min. The upper portion, consisting of dissolved sodium salt in distilled water, was poured away before repeating the next rinse cycle. These rinse cycles effectively separated the PTFE micro particles from the sodium salt. The slurry PTFE micro particles were then poured into a 150 mm diameter petri dish that formed a layer approximately 1 mm thick. The petri dish was placed in an incubator maintained at 40 °C for 48 h to remove the water. Lastly, the dry micro–PTFE was removed from the petri dish, transferred into a lab container and stored in a dark environment to prevent exposure to light.

SEM analysis using Phenom ProX (Phenom-World B.V., Eindhoven, The Netherlands) and FTIR spectroscopy utilizing PerkinElmer Spectrum 400 FTIR spectrometer unit (PerkinElmer, Waltham, MA, USA) were employed to characterize the micro–PTFE etched for 0 min, 10 min and 17.1 min. These samples represent the extreme high and low as well as nominal conditions of the chemical etching time. This allowed the effects of etching on PTFE micro particles to be easily distinguished.

Figure 3.1 illustrates precise representation of the experimental steps along with characterization of surface etched PTFE using SEM and FTIR techniques.

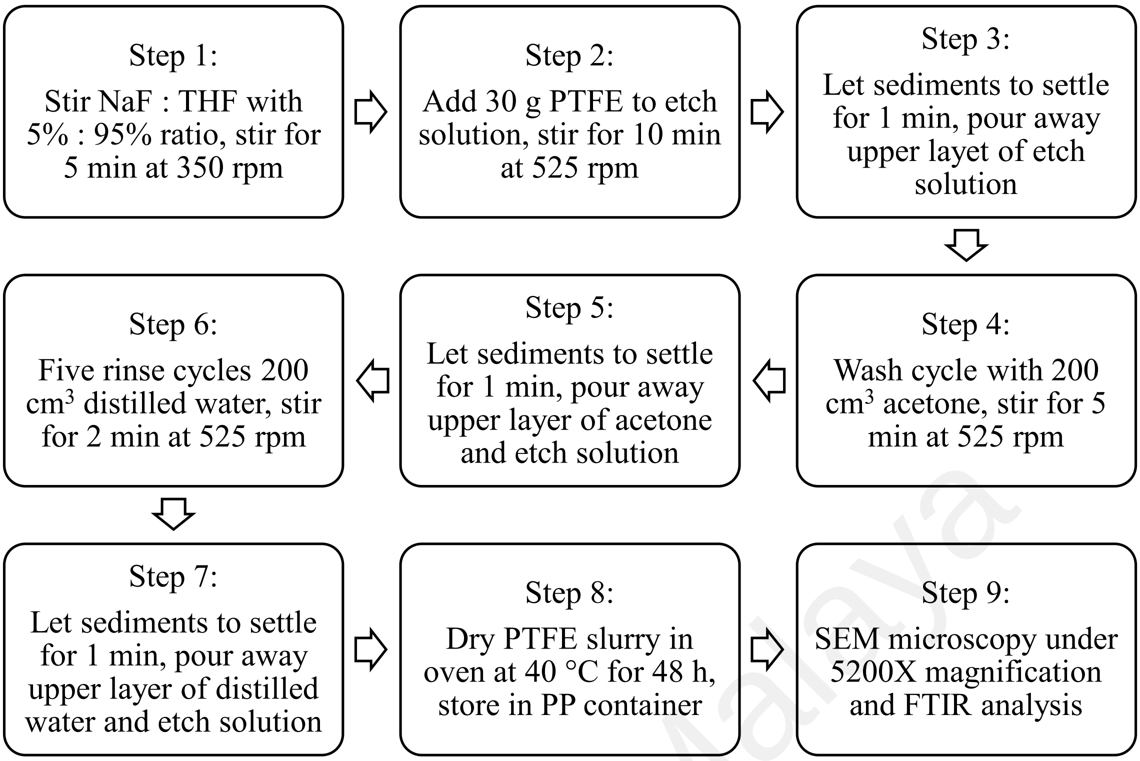

Figure 3.1: Flow chart for PTFE etching process and characterization

3.4 Fabrication of POM/GF/PTFE Composites using Injection Moulding

Injection moulding is a versatile processing technique, suitable for high production volume and low cost moulding of intricate plastic parts required in high volume. Virtually all thermoplastics, in pellet or powder form, can be converted into a variety of useful products using this method. As processing conditions may differ from one thermoplastic to another due to their inherent properties, it is important to characterize this process. The goal is to determine the process parameters that influence mechanical properties of POM composites. References were made against technical data sheets from resin manufacturers and injection moulding machine for the recommended process parameters. Preliminary test runs were performed by varying these parameters individually. Samples were inspected for formation without any voids, shrinkage, flashes, etc. The other consideration was adhesion of polymeric material upon removal of samples from the mould surface.

POM525GR and surface etched micro–PTFE with various weight fractions were compounded by melt blending using Brabender Mixer 50EHT 3Z (Brabender GmBH & Co KG, Kulturstraße, Duisburg, Germany). Processing parameters of the mixer were temperature 180 °C, blades rotational speed 60 rpm and 10 min mix time. The blend was then crushed to approximately 1–3 mm in length prior to injection moulding process using BOY XS machine (BOY Machines, Inc., Exton, PA, USA). The moulding comprised of three main processes, i.e. filling, plasticizing and holding. By using systematic experimentation design, the vital parameters for each process was identified and controlled. For filling process, injection pressure was 14 MPa with injection speed of 100 mm/s. For plasticizing process, pressure, screw rotational speed and barrel temperature controlled to 1 MPa, 170 rpm and 180 °C, respectively. Holding pressure of 12 MPa was maintained during the melt injection into the mould. Figure 3.2 shows step by step process involved in the fabrication of POM/GF/PTFE composite samples.

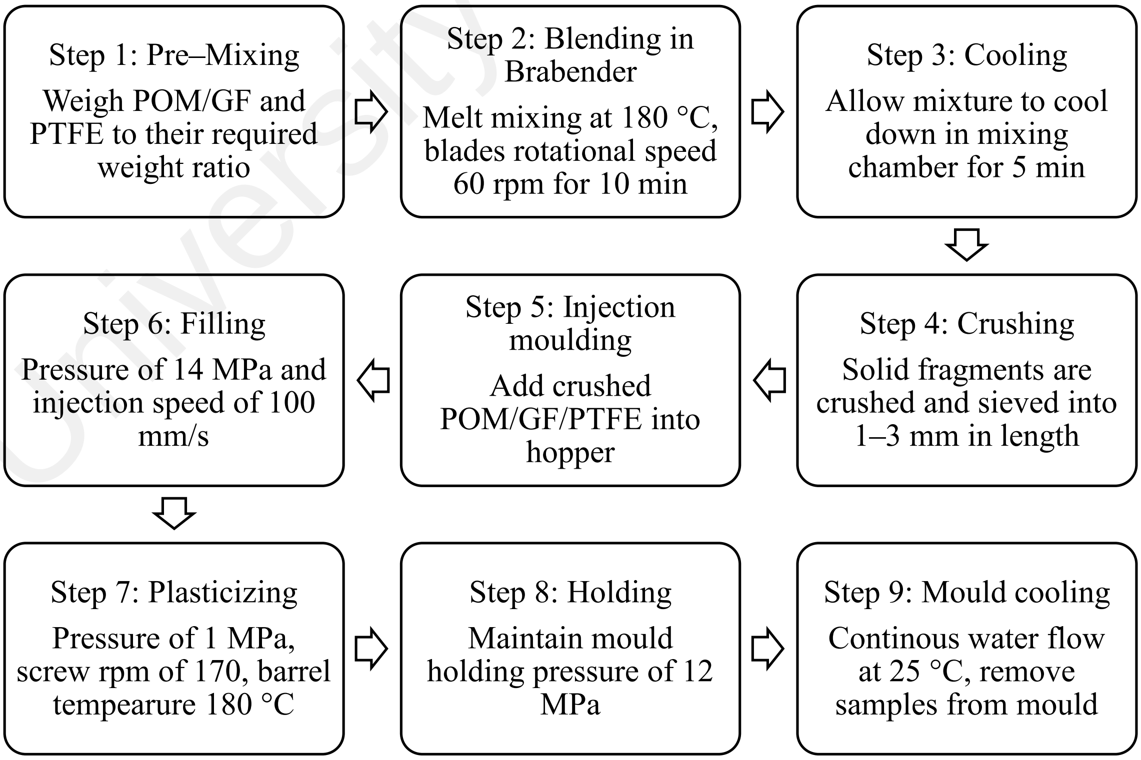

Figure 3.2: Flow chart for fabrication of POM/GF/PTFE composite samples

3.5 DOE of Injection Moulding Process Parameters

Prior to sample preparation, an important measure was to determine the working range of process parameters in order to obtain optimum mechanical properties for POM composites. Characterization, through fractional DOE, was carried using neat POM525GR to determine if the selected process parameters were appropriate. This step validated if mechanical properties were adversely affected by the designated injection moulding process parameters. Initially, the range of these parameters was obtained from material data sheets and subsequently carrying out preliminary experiments by varying one factor at a time. The samples produced via these experiments were inspected for voids, shrinkage, flashes and surface appearance.

Table 3.1 shows the selected key process input variables (KPIVs) whereas Table 3.2 shows the run order of characterization DOE using uncoded process parameters.

Table 3.1: List of KPIVs and corresponding high and low levels for injection moulding process

KPIV	Description	Low (–1)	High (+1)
A	Plasticizing pressure (MPa)	0.8	1.0
B	Screw speed (rpm)	80	170
C	Barrel temperature (°C)	175	185
D	Injection speed (mm/s)	100	150
E	Injection pressure (MPa)	12	18
F	Holding pressure (MPa)	9	15

Table 3.2: Uncoded design matrix for characterization DOE for injection moulding process

Run Order	Plasticizing Pressure (MPa)	Screw Speed (rpm)	Barrel Temperature (°C)	Injection Speed (mm/s)	Injection Pressure (MPa)	Holding Pressure (MPa)
1	0.8	80	185	100	18	15
2	0.8	80	175	100	12	9
3	1.0	80	185	100	12	15
4	0.8	170	185	150	12	15
5	1.0	170	185	100	18	9
6	0.8	80	185	150	18	9
7	0.8	170	175	150	18	9
8	1.0	170	175	150	12	9
9	1.0	170	175	100	12	15
10	1.0	80	185	150	12	9
11	0.8	80	175	150	12	15
12	0.8	170	185	100	12	9
13	1.0	80	175	100	18	9
14	1.0	170	185	150	18	15
15	1.0	80	175	150	18	15
16	0.8	170	175	100	18	15

Once the injection moulding process parameters were identified, initial experiments were conducted by varying the PTFE content and PTFE surface etching time. The effects of these parameters to mechanical properties of the POM composites, i.e. tensile strength and elasticity modulus were determined. PTFE contents of 0%, 10% and 20% and etch time for PTFE micro particles were 0 min, 10 min, 20 min and 30 min. Table 3.3 shows the variables used to produce samples for mechanical testing. Neat POM525GR was used as control sample and processed using the same mixing, crushing and injection moulding conditions as other samples.

Table 3.3: Configuration of initial experiment for POM composites prepared by varying PTFE content and etch time

SN	Sample	PTFE content (%)	PTFE etch time (min)
1	Neat POM525GR	0	0
2	POM–GF/PTFE10–ETCH0	10	0
3	POM–GF/PTFE20–ETCH0	20	0
4	POM–GF/PTFE10–ETCH10	10	10
5	POM–GF/PTFE10–ETCH20	10	20
6	POM–GF/PTFE10–ETCH30	10	30

The effects of these two variables are estimated based on the results of initial experiments. This type of experimentation approach is known as One–Variable–At–a–Time (OVAT). The first three composite samples were fabricated using non–etched PTFE by gradually increasing PTFE contents. The next three composite samples were produced by maintaining the PTFE content at 10% of weight ratio but with different PTFE etch times. Based on the tensile strength and elasticity modulus for these preliminary experiments, the range of PTFE content and PTFE etch time to be used for RSM was determined. Since RSM requires a combination of high and low factors and axial points, the values of these were adjusted. For example, the minimum PTFE content and PTFE etch time of an axial point cannot be negative.

3.6 Central Composite Design (CCD)

In order to obtain the optimum response of an experiment, the conventional two–level factorial design is insufficient. This is due to curvature for response is needed in the design. Therefore, augmenting the two–level design with additional points to obtain a polynomial is necessary. The added factors usually drawn as stars, along the x–axis results in CCD. It is possible to add the stars to the original two–level design if the range of selected factors falls within the optimum response. Figure 3.3 is a graphical representation of building CCD consisting of two factors. The axial distance to the stars is denoted by alpha (α), measured in terms of coded units, where +1 and –1 is the range of factors. Typically, α is taken as square root of the number of factors.

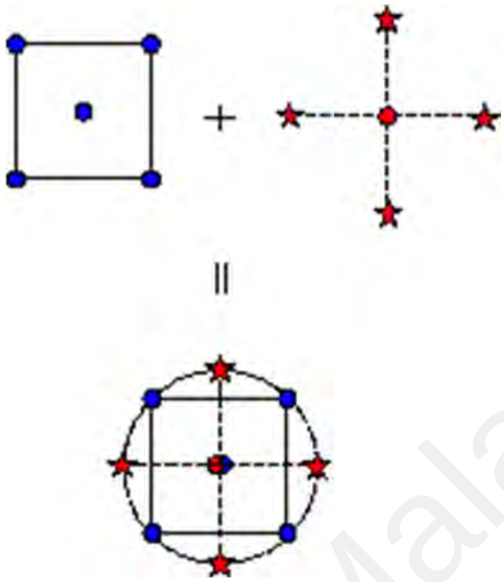

Figure 3.3: Build–up of central composite design for two factors

3.6.1 Statistical Model Development using RSM

RSM is a combination of both mathematical and statistical techniques. These techniques are useful for modelling and analysis of problems where a response of interest is influenced by several input variables with the objective of optimizing the response. This approach is commonly adopted by researchers in optimization studies for a parameter of interest (Ashenai Ghasemi, Ghasemi, Menbari, Ayaz, & Ashori, 2016; Azzahari, Yusuf, Selvanathan, & Yahya, 2016). RSM is able to quantify relationships of the response (Y) to the input variables (x_1, x_2, ... x_k). If these input variables are determinable, randomized on the experiment and with minimal error, the response (Y) can be expressed as;

$$Y = f(x_1, x_2, \dots, x_k) + \varepsilon \tag{3.1}$$

These input variables are transformed into coded values and are determined using the following equation;

$$x_i = (X_i - X_0)/(\left| X_i - X_0 \right|) \tag{3.2}$$

where x_i is coded value for *i–th* variable, X_i is uncoded value of the *i–th* variable and X_0 is the uncoded value of the *i–th* variable at center point. The regression analysis is performed to estimate the response function as a second order polynomial;

$$Y = \beta_0 + \sum_{i=1}^{k} \beta_i x_i + \sum_{i=0}^{k} \beta_{ii} {x_{ii}}^2 + \sum_{i=1}^{k-1} \sum_{i<j,j=2}^{k} \beta_{ij} x_i x_j + \varepsilon \tag{3.3}$$

where Y is the predicted response, β_0 constant and β_i, β_{ii} and β_{ij} are the linear, quadratic and interactions coefficients estimated from the regression design.

In this research, CCD was used to study the effects of PTFE content and PTFE etch time on mechanical properties of POM/GF/PTFE composites. Subsequently, the effects of these KPIVs towards responses or key process output variables (KPOVs) were used in optimization studies. Samples were tested for tensile strength, elasticity modulus, toughness and hardness as responses. This method suitably fitted a polynomial and optimized the effective input variables to obtain the desired responses. The correlation between these parameters were analyzed as well.

Statistical data analysis was performed to determine the relationship between the input variables to each of the responses. To model the response as a mathematical function where the independent input variables may include linear, interaction, quadratic and cubic terms, a regression design was used. The goal or desire is to obtain a model with good predictability of the responses with minimal error.

The CCD was built up from two level full factorial design with center and axial points coupled with one additional center point. These axial or augmented points were chosen as ±√2 since two factors were of interest. Thus, the experiment comprised of 13 runs consisting of 4 axial points, 4 high and low levels of factors and 5 central points. The values of each input variables were defined at low, mid and high points. Table 3.4 shows the selected KPIVs and their range.

Table 3.4: List of KPIVs and their corresponding levels for optimization mechanical properties for POM/GF/PTFE composites

KPIVs	Symbol	Axial (–√2)	Low (–1)	Mid (0)	High (+1)	Axial (+√2)
PTFE content (%)	A	1.7	4.0	9.5	15.0	17.3
PTFE etch time (min)	B	2.9	5.0	10.0	15.0	17.1

3.6.2 Statistical Analysis and Model Fitting

The statistical analysis comprising of regression and graphical analysis were performed using Design–Expert software (version 10.0.6, Stat–Ease, Inc., Minneapolis, USA). Based on the regression equation, optimum values of input variables were obtained. Analysis of variance (ANOVA) was used to further justify the adequacy of the models. The procedure calculated F–ratio, the ratio between regression mean square and the mean square error. The F–ratio, called as the variance ratio, is the variance ratio due to the effect of a factor and variance due to the error term. This ratio measured the significance of the model with respect to the variance of all terms included in error term. The desire is to obtain a model that is significant.

Testing for significance of individual model coefficients formed the basis for optimizing the model. This is achieved by adding or deleting coefficients through forward addition, backward elimination or stepwise elimination, addition or exchange. P–value or probability of risk to falsely rejecting a given hypothesis is determined. Generally, lowest order polynomial is chosen to adequately describe the system.

Lack–of–fit is a special diagnostic test for adequacy of a model. As replicate measurements are available, a test indicating the significance of the replicate error in comparison to the model dependent error can be performed. This test splits the residual or error sum of squares into two portions, one which is due to pure error based on the replicate measurements and the other due to lack–of–fit based on the model performance. The test statistic for lack–of–fit is the ratio between the lack–of–fit mean square and the pure error mean square. As stated previously, this F–test statistics can be used to determine as to whether the lack–of–fit error is significant. Insignificant lack–of–fit is desired as significant lack–of–fit indicates that there might be contributions in the input variables–response relationship that are not accounted for by the model.

In addition, verification is needed to determine whether the model actually describes the experimental data. Two basic components of a valid regression model are the deterministic portion and stochastic error. The deterministic portion is the predictor variables in the model. The expected value of response is a function of these predictor variables. Stochastic error is the difference between the actual and predicted values represented by residuals. The residuals must be unpredictable and centered on zero throughout the range of predicted values. Random errors produce residuals that are normally distributed. Therefore, the residuals are in symmetrical pattern and have a constant spread throughout the range. Normal probability plot of residuals tests the data set in the model if it fits a normal distribution. Once residual analysis validates no biased results, statistical measures for goodness of fit between experimental and predicted is performed.

Coefficient of determination, R^2, signifies the level of fit of the polynomial model with values between 0 and 1. R^2 is one of the measures for variability reduction of a response in statistical modelling. As more terms are added, the value of R^2 increases without consideration of the statistical significance of these additional terms. The goal is to obtain R^2 values close to 1. Adjusted R^2 (R^2_{adj}) takes into consideration only the terms that are statistically significant. A lower value of R^2_{adj} than R^2 indicates no necessity to add extra terms into the model.

Adequate precision is a measure of the signal to noise ratio. An adequate precision of more than 4.0 is desired, substantiating the model as capable to predict the response. Then, the model can be used to navigate the design space. Adequacy of the model is investigated by the examination of residuals. The residuals, which are the difference between the observed responses and the predicted responses are examined using the normal probability plots. For an adequate model, the points on the normal probability plots form a straight line. For a weak model, residuals versus the predicted response plots have no obvious patterns.

3.7 Optimization of Mechanical Properties using Desirability Method

Desirability method was utilized to determine the values of input variables, i.e. PTFE content and PTFE etch time for optimization of multiple responses, i.e. mechanical properties of POM/GF/PTFE composites simultaneously. The condition of each mechanical property (Y) is selected based on its importance by selecting as maximum, minimum or a target value of specification. Equation (3.4) obtained the overall desirability or D global index based on the combination of responses processed through a geometric mean.

$$D = (d_1(Y_1) \times d_2(Y_2) \times d_3(Y_3) \times \ldots \times d_n(Y_n))^{1/n} \tag{3.4}$$

The responses (Y_1, Y_2, Y_3, …, Y_n) are transformed such that $0 < d_i < 1$. The d value increases when the *i–th* response approaches the desired condition. Resulting from the geometric mean, value of D is evaluating levels of the combined responses with an index of $0 < D < 1$. It is maximized when all responses approach towards the desirable specification. Responses can be assigned with difference importance. All responses with their own importance are included into one desirability index. Multiplication causes an outcome to be low if any one response is unable to achieve its desirability.

The Design Expert software allows the input variables and responses to be changed to obtain the greatest overall desirability. These input variables are left to be within their experimental range and only responses are adjusted. This is where the subject matter expertise and engineering knowledge of the requirement for application becomes essential. The software also has an option to assign weightage in 1 to 10 scale and importance using 5–point scale. In this work, same weightage was assigned to all mechanical properties. Stiffness and hardness of the POM/GF/PTFE composites were assigned higher importance over strength and toughness considering their impact on tribological properties.

3.8 Characterization of POM/GF/PTFE Composites

3.8.1 Mechanical Properties

Injection moulded samples were tested for tensile strength, elasticity modulus and toughness using Instron 3369 universal tensile test machine (Instron, Norwood, MA, USA) according to ASTM D638. Type IV dumbbell–shaped specimens were prepared for tensile tests. Prior to testing, samples were conditioned in accordance to ASTM D618. The crosshead speed was fixed at 5 mm/min at room temperature with the distance between grips of 60 mm. The thickness and width of each sample was measured individually to obtain accurate cross–sectional area. Average value of six samples for each POM composite was used to determine its tensile strength, elasticity modulus and toughness.

Hardness testing was performed using Instron B2000 tester (Instron, Norwood, MA, USA) using HRR scale. Rectangular shaped injection moulded samples of approximately 63.5 (length) × 12.7 (width) × 3.0 (thickness) mm^3 were tested. Total of 4 fixed points along the length were taken. Similar to tensile testing, hardness data was taken as an average of six measured samples for each POM composite type.

3.8.2 Tribological Studies

Tribology tests were performed using Ducom Reciprocatory Friction and Wear Monitor (Ducom Instruments, TR–281–M8, Bangalore, India) according to Procedure A of ASTM G133–95, unlubricated wear testing. POM composite samples of 12.5 (length) × 12.5 (width) × 4.0 (thickness) mm^3 were placed on the stationary stage. The counterpart was an SST 440C (Grade 24) stainless steel ball of 4.7625 mm radius mounted to the reciprocating arm. Normal load of 25 N was applied using dead weights. The stroke length and oscillating frequency was controlled to 10 mm and 5 Hz respectively. Each sample was tested for 1000 sec resulting in sliding distance of 100 m. Table 3.5 shows the POM composites with varying PTFE content to determine coefficient of friction and wear loss measured directly on the Ducom tester. The data reported are mean values of three replicated tests.

Table 3.5: The composition of POM/GF/PTFE composites investigated

SN	Sample	PTFE Etch time (min)	PTFE weight (%)
1	Neat POM525GR	–	0
2	POM–GF–PT1.7	10	1.7
3	POM–GF–PT4.0	10	4.0
4	POM–GF–PT9.5	10	9.5
5	POM–GF–PT15.0	10	15.0
6	POM–GF–PT17.3	10	17.3

All contacting surfaces were cleaned using a damped cloth with isopropyl alcohol (IPA) to remove presence of any contamination. Tests were performed under ambient laboratory conditions with relative humidity (RH) of 50 ± 5% and temperature maintained 22 ± 2 °C. During reciprocating sliding motion, variations in the normal load occurs because of vibrations and inertia effects. The data acquisition system provided simultaneous and real time measurement of normal and friction forces at 5 Hz frequency. A new SST 440C ball was used for every test. Upon test completion, the POM composite samples were carefully removed from the test rig. Each sample was individually placed in a 70 ml capped polypropylene (PP) lab container to prevent any contact to the tested surface.

3.8.3 Morphology Analysis

SEM images provide information on the effects of etching to the surface of PTFE. The morphology of POM/GF/PTFE composites as a result of brittle fracture during tensile testing was also investigated. Central section of the dumbbells was selected for morphology analysis. Surface morphology of worn surfaces after tribology testing for POM composites was also inspected. At first, optical microscopy was performed using an electronic microscope (Keyence Corporation, VHX–500, Osaka, Japan). Further examination of these surfaces was conducted under Phenom ProX (Phenom–World B.V., Eindhoven, The Netherlands) desktop Field Emission Scanning Electron Microscope (FE–SEM) operated at 10 kV accelerating voltage.

Fiber–matrix mapping for presence of fluorine atoms at the interface region was carried out using Quanta FEG–450 (Thermo Fisher Scientific, Hillsboro, OR, USA) SEM. The geometry of the sample was a type IV dumbbell-shape prepared using injection molding. Gage length section of the dumbbell was milled out to a specimen of 3.0 (length) × 3.0 (width) × 10.0 mm (thickness) mm^3. The 9 mm^2 cross sectional surface area was ground using silicon carbide (Si–C) paper with a grain size from 600 to 1200 before applying gold sputtering. Samples were placed on a motorized stage located inside a vacuum chamber. The roomy chamber enabled navigation of samples in three axes for optimal view and analysis. The Quanta SEM system, equipped with electron backscatter diffraction (BSD) and energy dispersive x-ray spectroscopy (EDS), was operated at 15 kV. The AZtec analysis software package (Oxford Instruments Nano-Analysis, High Wycombe, UK) allowed elemental identification at specific points, every 0.5 µm intervals from the GF surface.

3.8.4 FTIR Spectroscopy

FTIR spectroscopy Fourier transform infra-red (FTIR) spectroscopy was performed utilizing the PerkinElmer Spectrum 400 FTIR spectrometer unit (PerkinElmer, Waltham, MA, USA) using the KBr pellet technique with the resolution of 4 cm^{-1} and 32 scans per recording. The functional groups of chemically etched PTFE micro-particles were compared against non-etched sample. POM/GF/PTFE composites were further characterized for presence of any new functional groups as a result of nucleophilic reaction.

3.8.5 Thermal Analysis

Thermal analysis is a series of techniques in which thermal properties of a polymer is monitored against time or temperature. The sample's temperature, in a specified atmosphere, is controlled. These techniques provide qualitative and quantitative information of a polymer. During transformation of a thermodynamic system from one phase to another, or known as phase transition, measurement of the transition temperature and its associated enthalpy provide vital information about the polymer and its constituents. Thermal characterization of the POM composites was carried out using a Perkin Elmer STA 6000 analyzer (Perkin Elmer, Waltham, MA, USA) according to ASTM E2550–11. STA 6000 combines the high flexibility of differential analysis feature with the proven capabilities of thermogravimetric measurement technology to provide very reliable information.

3.8.5.1 Differential Scanning Calorimetry (DSC)

DSC technique is used to measure thermal transitions such are the glass transition temperature (T_g) where the polymer changes from a hard, glassy to soft, rubbery state, the crystallization temperature (T_c), the melting temperature (T_m) and the decomposition temperature (T_d). These transition temperatures are indicative of the polymer. Composites consisting of more than one polymeric component will either exhibit transitions of each component or display intermediate transitions. DSC is capable of monitoring the endothermic or exothermic changes of a polymer as the temperature is gradually raised.

This is achieved by measuring the heat flowing in and out of the sample referenced to a standard. Phase transitions are recorded as a peak where the temperature is the thermal transition temperature and the area of the DSC peak is used to estimate the enthalpy of transition, ΔH. The mechanical properties of a polymer are affected by their crystallinity. Higher crystalline structure results in a polymer with stiff, strong and brittle characteristics. Degree of crystallinity (X_c) is defined as the following equation;

$$X_c = \frac{\Delta H_m}{\Delta H_m^0} \times 100\% \tag{3.5}$$

Where ΔH_m is the melt enthalpy of the net POM content in the sample and ΔH_m^0 is the theoretical enthalpy for 100% crystallizing POM. ΔH_m^0 for POM is 186 J/g (Siengchin, Karger-Kocsis, Psarras, & Thomann, 2008).

3.8.5.2 Thermogravimetric Analysis (TGA)

TGA monitors the weight loss instead of heat flow as in DSC technique. It is useful to determine the decomposition temperatures and mechanism of thermal decomposition.

Since different polymers used in composites may have different decomposition temperatures, TGA is also able to quantify the weight ratio of these components. Samples were heated from 30 °C to 800 °C at a heating rate of 10 °C/min.

DSC analysis were carried out using another sample to determine the melting and crystallization temperature and enthalpy. Samples were first heated from 30 °C to 210 °C at heating rate of 10 °C/min and then cooled at the same rate. Sample weight of ~5 mg was used under nitrogen atmosphere at 20 ml/min flow rate. The temperature and enthalpy calibration of the system was carried out prior to each run.

CHAPTER 4: RESULTS AND DISCUSSION

4.1 Analysis of Characterization DOE for Injection Moulding Process

Based on the process parameters identified in Table 3.1, a resolution IV screening DOE as described in Section 2.8.2, was applied to determine the vital process parameters for injection moulding. In these experiments, neat POM525GR in the form of pellets, as received from resin manufacturer, was used to prepare dumbbell shaped samples for tensile testing. Table 4.1 presents the design matrix and the mean and standard deviation for the responses, i.e. tensile strength and elasticity modulus. It can be noted that some of the process parameters for these experiments affected the mechanical properties. The standard deviations of less than 5% of the mean value of tensile strength and elasticity modulus indicate stable injection moulding process.

Table 4.1: Characterization DOE in uncoded levels with tensile strength and elasticity modulus as response

Run order	Plasticize pressure (MPa) A	Screw speed (rpm) B	Barrel temp (°C) C	Injection speed (mm/s) D	Injection pressure (MPa) E	Holding pressure (MPa) F	Tensile Strength (MPa) Y1	Elasticity modulus (MPa) Y2
1	0.8	80	185	100	18	15	121.5 ± 4.7	7707 ± 121
2	0.8	80	175	100	12	9	117.7 ± 3.5	8454 ± 163
3	1.0	80	185	100	12	15	128.5 ± 5.2	8462 ± 167
4	0.8	170	185	150	12	15	126.7 ± 5.1	8461 ± 396
5	1.0	170	185	100	18	9	133.0 ± 2.7	8606 ± 62
6	0.8	80	185	150	18	9	126.4 ± 5.2	8440 ± 74
7	0.8	170	175	150	18	9	126.2 ± 2.4	8350 ± 100
8	1.0	170	175	150	12	9	113.5 ± 2.1	8427 ± 56
9	1.0	170	175	100	12	15	122.0 ± 7.5	8563 ± 292
10	1.0	80	185	150	12	9	117.3 ± 1.0	8495 ± 76
11	0.8	80	175	150	12	15	117.3 ± 5.3	8426 ± 301
12	0.8	170	185	100	12	9	117.0 ± 2.3	8259 ± 169
13	1.0	80	175	100	18	9	128.9 ± 3.1	8647 ± 114
14	1.0	170	185	150	18	15	118.0 ± 3.5	7729 ± 80
15	1.0	80	175	150	18	15	123.0 ± 2.0	7987 ± 238
16	0.8	170	175	100	18	15	124.9 ± 2.6	8460 ± 209

Statistical analysis was performed to determine the process parameters or factors influencing injection moulding process. The effects of these factors were studied using half normal and pareto plots. The factors significantly contributing to the response fall out of the straight line whereas the ones fall in line represent the normal scatter. These trivial factors were used in ANOVA to estimate the error. The results were analyzed without the need to perform any transformation of the responses.

In order to verify whether the model accurately described the experimental data, a valid regression analysis consist of deterministic portion and stochastic error. The deterministic portion predicted the variables in the model whereas the stochastic error was analyzed by means of residuals. The relationship of the mechanical properties to the process parameters was established using a regression equation. Adequacy of the model was further verified using correlation coefficients and adequate precision that measured signal to noise ratio. The error portion was handled by plotting the residuals on a normal probability and residuals versus predicted level plots.

Investigation of interaction effects among the process parameters is important to determine the setting of these variables. Interactions occur if a factor does not generate the identical effect on the response at different levels of another factor. Interactions were graphically represented by grouping high and low levels of a factor in x–axis and effects of another factor plotted as two lines with y–axis as the response. Lastly, process parameters were determined by setting the goals of each response to the desired values.

In addition, the effects of process parameters for injection moulding was analyzed by comparing runs with high and low levels of response. Figure 4.1 displays the stress–strain curves of four runs where the responses showed significant deviation. For tensile strength, run 5 produced the highest strength of 133.0 MPa whereas run 8 yielded the lowest strength of 113.5 MPa. By comparing the process parameters between these two runs, the values of barrel temperature (C), injection speed (D) and injection pressure (E) were different whereas plasticizing pressure (A), screw speed (B) and holding pressure (F) were similar. Similarly, for elasticity modulus, run 13 showed stiffness of 8647 MPa while run 1 exhibited 7707 MPa influenced by plasticizing pressure (A), barrel temperature (C) and holding pressure (F). Other injection parameters, i.e. screw speed (B), injection speed (D) and injection pressure (E) were the same between the two runs.

In conclusion, the injection moulding parameters that influence tensile strength and elasticity modulus are different. Barrel temperature (C) affects both of these mechanical properties whereas screw speed (B) has not effect. This preliminary analysis considers the main effects only, i.e. influence of each process parameters independently, without taking into account the contribution of their interactions. Hence, a systematic data analysis by employing DOE methodology, elaborated in the next section, is necessary to determine the main and interaction effects of these process parameters to mechanical properties.

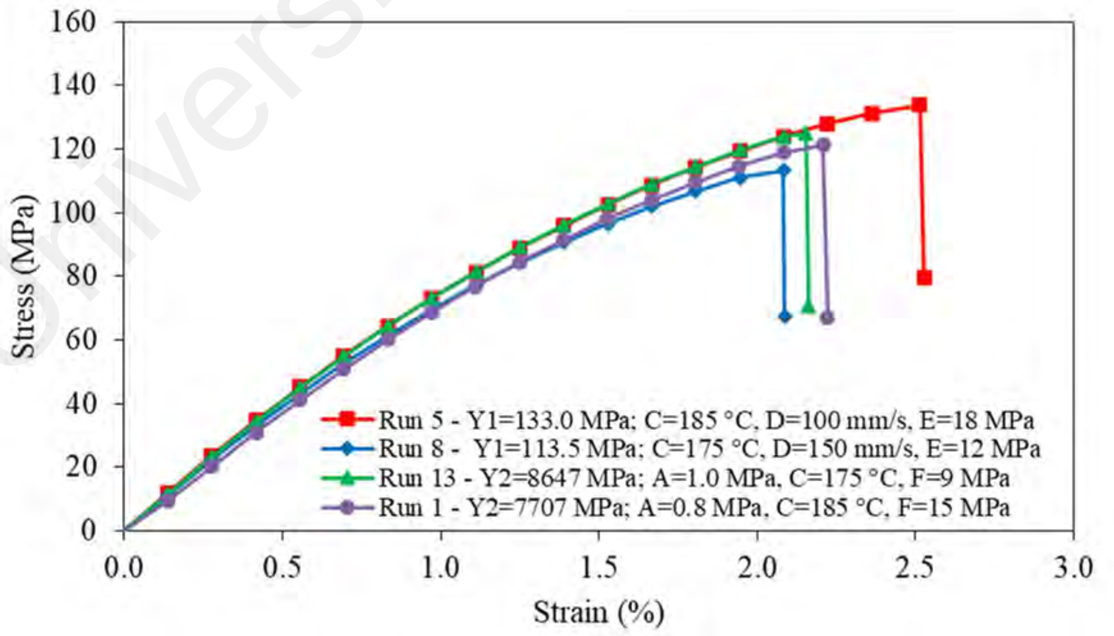

Figure 4.1: Stress vs. strain curves comparing the effects of injection moulding process parameters on POM525GR

4.1.1 ANOVA and Model Fitting for Tensile Strength

This section illustrates factorial analysis of the DOE results to obtain the relative effects of the six process variables towards the mechanical properties of the polymer. The half normal probability plot shown in Figure 4.2 revealed three large main effects, i.e. C, D and E out of six main factors as shown in Table 4.2. In addition, three interaction effects, AD, AB and ABF as shown in Table 4.3, were also distinctly dominant in affecting the tensile strength.

Table 4.2: Main factors for injection moulding that influenced tensile strength and elasticity modulus of POM525GR

Main factors	Description of main effects
A	Plasticizing pressure (MPa)
B	Screw speed (rpm)
C	Barrel temperature (°C)
D	Injection speed (mm/s)
E	Injection pressure (MPa)
F	Holding pressure (MPa)

Table 4.3: Interaction of factors for injection moulding that influenced tensile strength and elasticity modulus of POM525GR

Factor interactions	Description of interaction effects
AB	Plasticizing pressure and screw speed
AD	Plasticizing pressure and injection speed
AF	Plasticizing pressure and holding pressure
BD	Screw speed and injection speed
BF	Screw speed and holding pressure
ABF	Plasticizing pressure, screw speed and holding pressure

These effects fall off the normally distributed line of near zero effects and labelled. Since the interaction effects include terms A, B, F, AF and BF, these effects must be chosen to support the regression model's hierarchy. Any significant higher order term must be supported by parent terms to avoid classifying a factor as not significant when it contributes the model as an interaction. As such, these terms are also labelled to show their significance in modelling tensile strength.

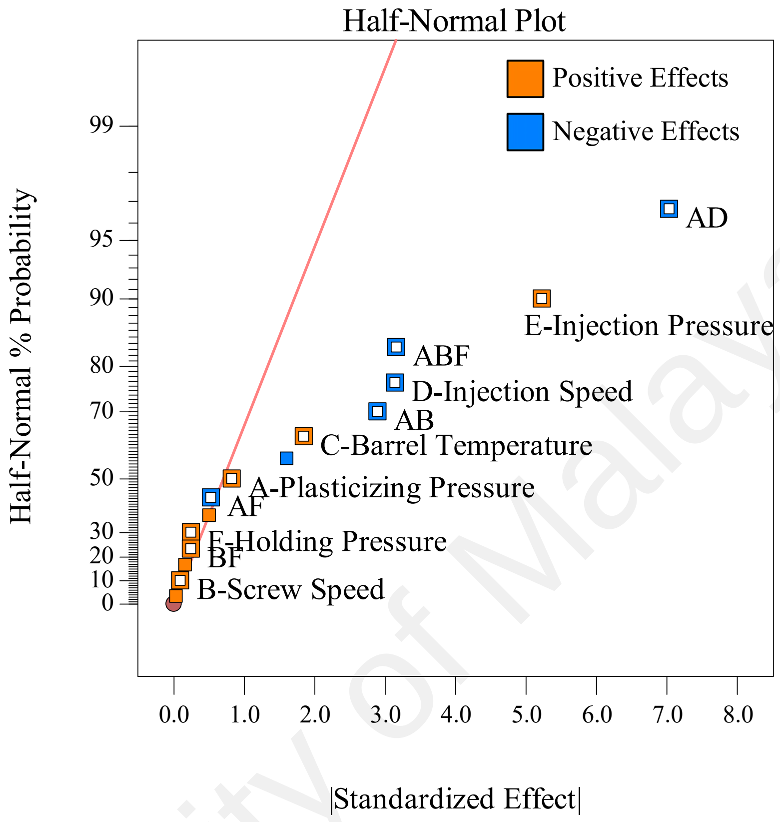

Figure 4.2: Half normal probability plot of effects for tensile strength

The Pareto chart in terms of the two–threshold t–values limits is shown in Figure 4.3. The t–value limit is calculated as the ratio numerical effect and its associated standard error. The conservative Bonferroni limit takes into account the number of estimated effects and dividing it into the desired probability of the risk value. All effects exceeding the t–value limits are important in predicting regression for the tensile strength. It validates the hypothesis that the main and interaction effects identified in Figure 4.2 are the few vital parameters as opposed to the others as being the trivial many in determining the tensile strength. As this is a Resolution IV fractional factorial DOE, no main effects are confounded with any other main effect or any other two factor interaction effects. However, two and three factor interactions may be confounded with each other. For example, CE is an alias of AB, EF is an alias of AD and ACD, BDE, CEF are aliases of ABF.

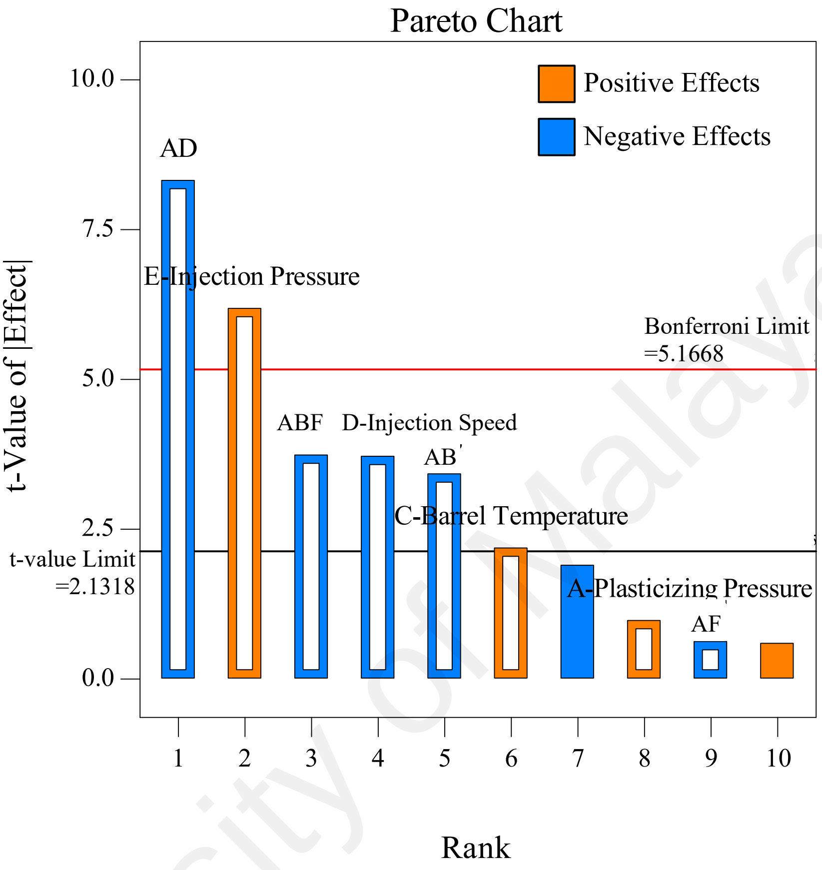

Figure 4.3: Pareto plot of effects for tensile strength

Next, based on the vital factors determined from the results, ANOVA analysis (Table 4.4) was performed by maintaining the model hierarchy and embedding the trivial factors in the error term. The F–value of 13.94 implies the model is significant. There is only a 1.07% chance that an F–value this large could occur due to noise. Values of "Prob > F" less than 0.10 indicate model terms are significant. Values greater than 0.10 indicate the model terms are not significant. The terms C, D, E, AB, AD and ABF are significant for tensile strength. The coefficient of determination, R^2 is one of the measures resulting in the reduction of response variability. R^2 of 0.9746 is very close to 1, in agreement that the model comprises of best fit data. The R^2_{adj} value of 0.9047 suggests the model is sufficient without needing to consider additional terms. An adequate precision measures the signal to noise ratio and value of greater than 4 is desirable. The adequate precision value of 11.784 indicates an adequate signal. This model can be used to navigate the design space.

Table 4.4: Results of ANOVA for tensile strength

Source	Sum of Squares	df	Mean Square	F	Prob. > F	Remarks
Model	438.7	11	39.88	13.94	0.0107	significant
A–Plasticizing Pressure	2.73	1	2.73	0.96	0.3836	
B–Screw Speed	0.035	1	0.035	0.012	0.9172	
C–Barrel Temperature	13.68	1	13.68	4.78	0.094	significant
D–Injection Speed	39.55	1	39.55	13.82	0.0205	significant
E–Injection Pressure	109.43	1	109.43	38.25	0.0035	significant
F–Holding Pressure	0.24	1	0.24	0.086	0.7845	
AB	33.54	1	33.54	11.72	0.0267	significant
AD	198.13	1	198.13	69.25	0.0011	significant
AF	1.12	1	1.12	0.39	0.565	
BF	0.24	1	0.24	0.084	0.786	
ABF	39.99	1	39.99	13.98	0.0201	significant
Residual	11.44	4	2.86			
Cor Total	450.15	15				
R^2, 0.9746; R^2_{adj}, 0.9047; Adequate Precision, 11.784						

The model above was used to predict the tensile strength of POM (Y1). It can be presented in terms of coded factors as in the following equation;

$$Y1 = 122.62 + 0.41*A + 0.05*B + 0.92*C - 1.57*D + 2.62*E + 0.12*F - 1.45*AB - 3.52*AD - 0.26*AF + 0.12*BF - 1.58*ABF \quad (4.1)$$

The residuals, i.e. deviation of actual values against the predicted values, analyzes the adequacy of the model by evaluating the data applied in the model. Random and normally distributed residuals indicate none of the predictive information is in the error. Normal probability plot and residuals versus predicted level are shown in Figure 4.4 and Figure 4.5 respectively. The residuals in prediction of response are minimal since they are very close to the diagonal line. Hence, the deterministic portion of the model is good at explaining the response that only the inherent randomness is leftover within the error portion (L. Liu, Wang, Zou, Yu, & Xie, 2017).

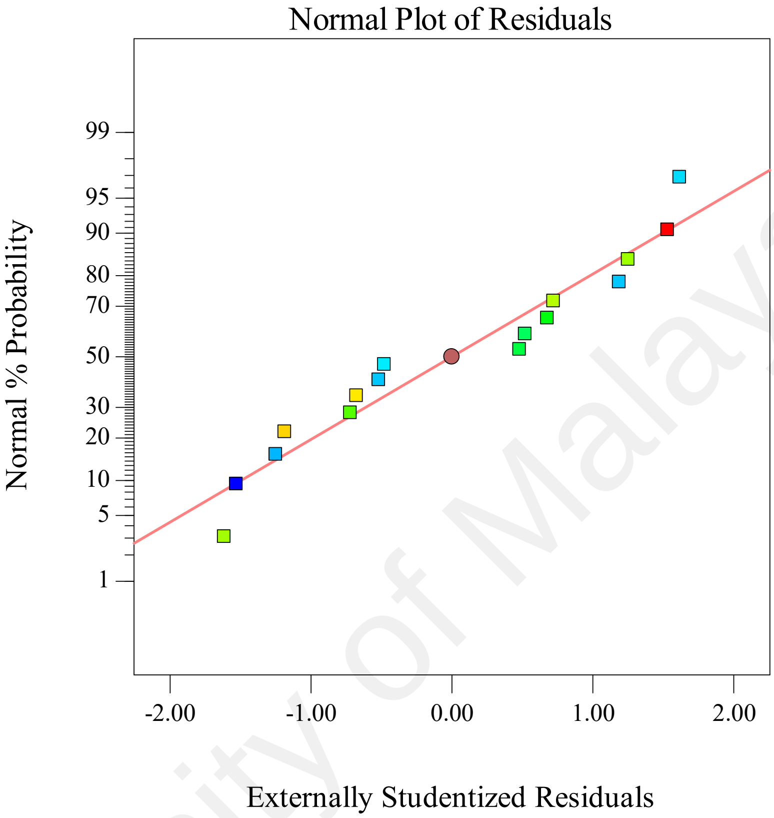

Figure 4.4: Normal plot of residuals for tensile strength

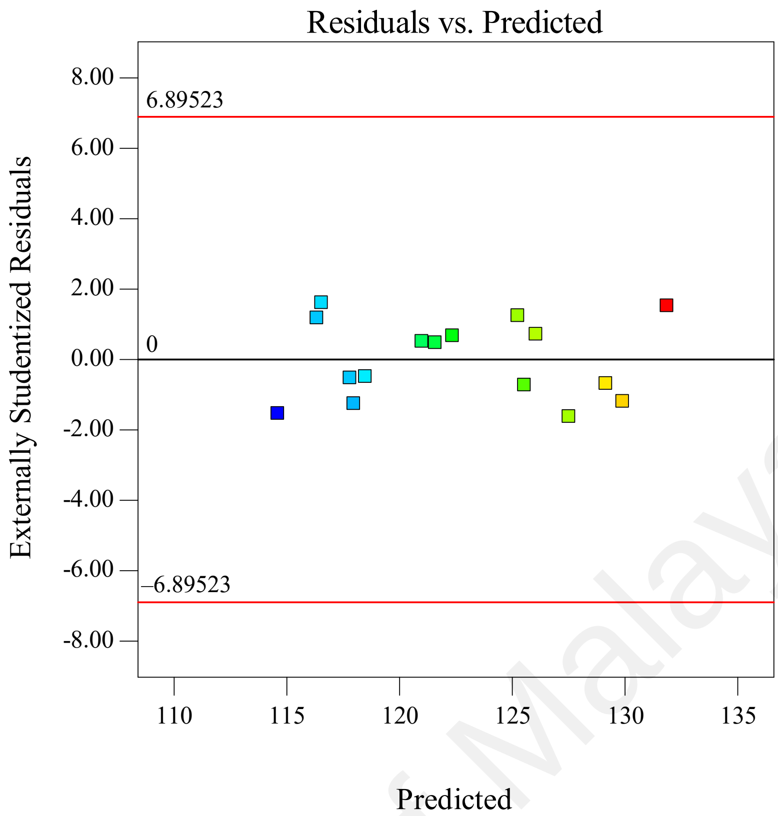

Figure 4.5: Residuals versus predicted tensile strength

Tensile strength is greatly affected by a combination main factors (C, D, E) and interaction effects (AB, AD, ABF). These observations can be illustrated by graphs of the effect changes versus the factor levels as shown in Figures 4.6(a)–(e). By analyzing the charts visually, higher barrel temperature (C), lower injection speed (D) and higher injection pressure (E) result in increased tensile strength without any interaction between them. When interaction exist between two factors, two lines appear on the plot. For example, Figure 4.6(d) revealed the effect of plasticizing pressure (A) is dependent on the level of screw speed (B). When screw speed is 80 rpm (low level), plasticizing pressure should be controlled to 1 MPa (high level) to achieve tensile strength of approximately 124 MPa. Similar strength can be also achieved by setting the screw speed and plasticizing pressure to 170 rpm (high level) and 0.8 MPa (low level) respectively.

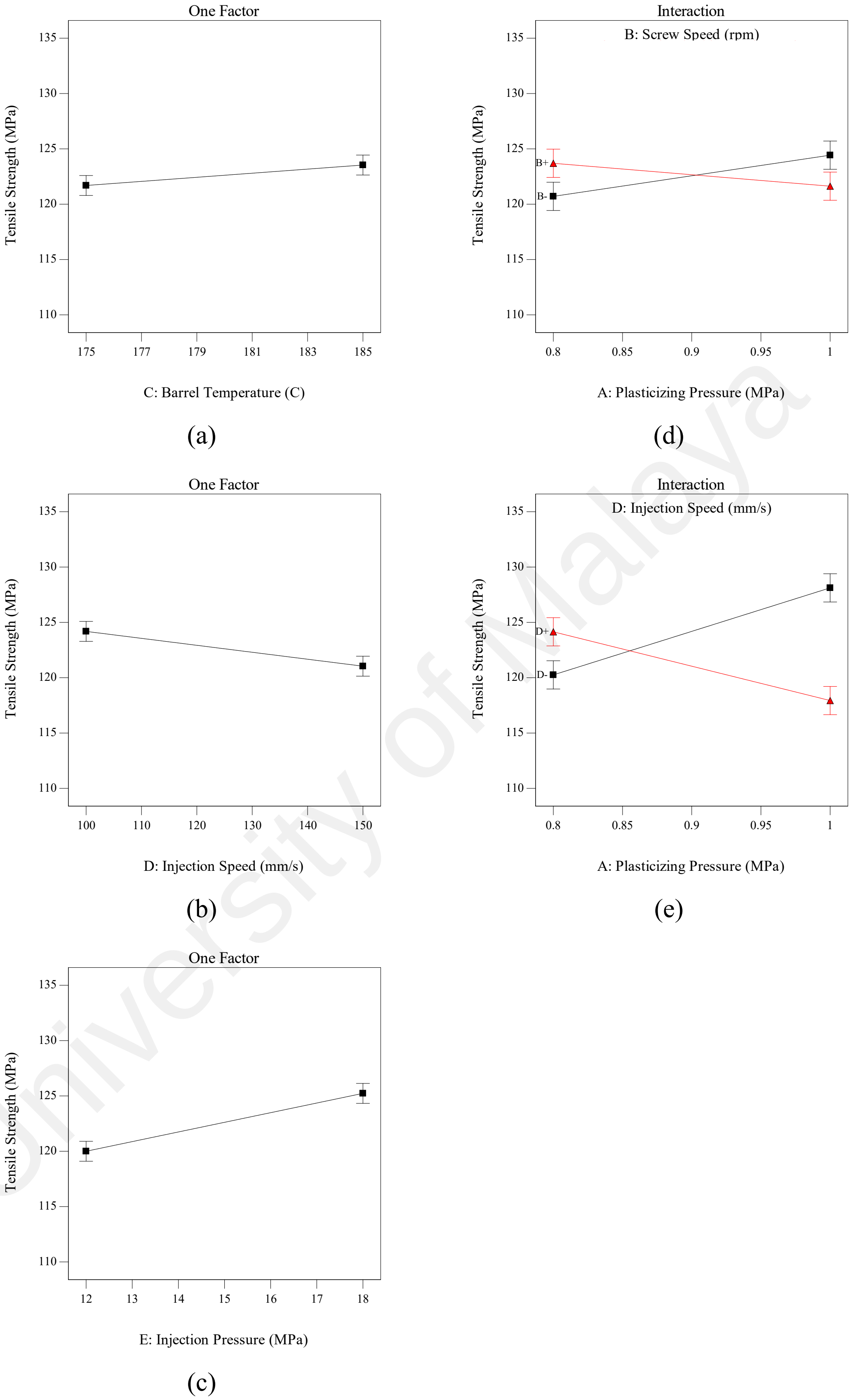

(a)

(d)

(b)

(e)

(c)

Figure 4.6: Main effects and interaction plots for tensile strength

The relationship of actual versus predicted tensile strength is shown in Figures 4.7. The values of R^2 of 0.9746 and R^2_{adj} of 0.9047 along with the residual analysis adequately fits the model to experimental data.

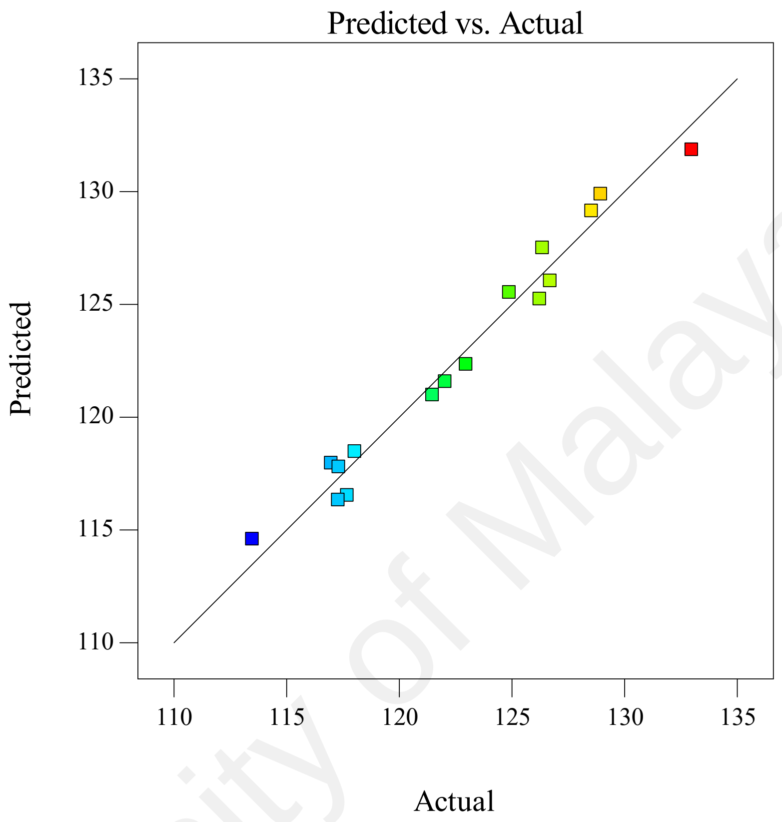

Figure 4.7: Predicted versus actual values of tensile strength

4.1.2 ANOVA Analysis and Model Fitting using Elasticity Modulus

The half normal probability plot shown in Figure 4.8 revealed three large main effects, i.e. barrel temperature (C), injection pressure (E) and holding pressure (F) out of six as shown in Table 4.2. In addition, five interaction effects, AD, AF, BD, BF and ABF as described in Table 4.3, may have slightly influenced elasticity modulus. These effects fall off the normally distributed line of near zero effects and labelled. Since the interaction effects include terms A, B, D, F, AF and BF, these effects must be chosen to support the regression model's hierarchy. Any significant higher order term must be supported by parent terms to avoid classifying a factor as not significant when it contributes the model as an interaction. As such, these terms are also labelled to show their significance in modelling elasticity modulus.

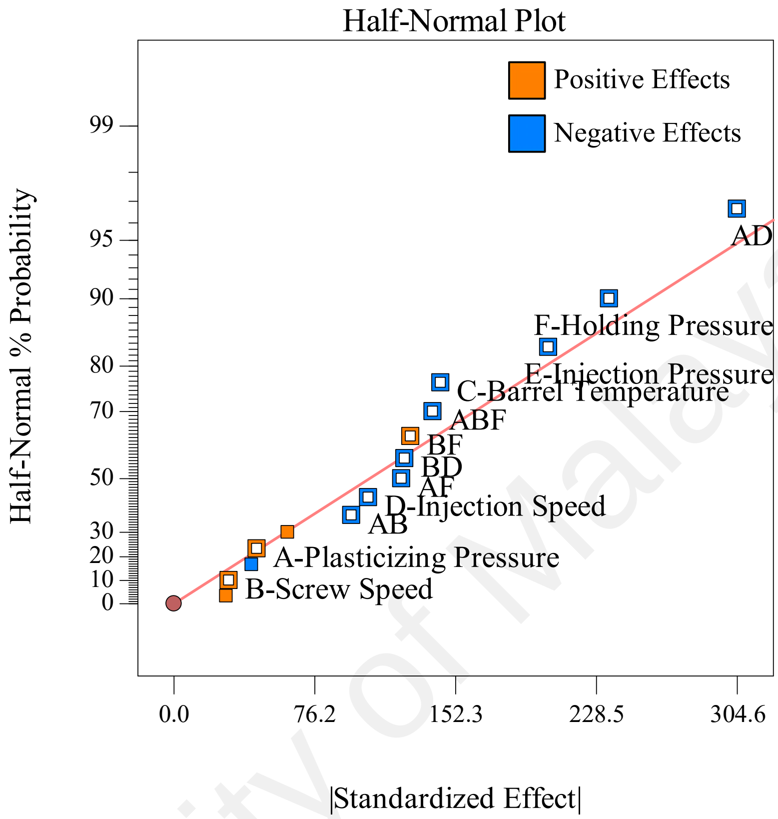

Figure 4.8: Half normal probability plot of effects for elasticity modulus

The Pareto chart in terms of the two–threshold t–values limits are shown in Figure 4.9. The t–value limit is calculated as the ratio numerical effect and its associated standard error. The conservative Bonferroni limit takes into account the number of estimated effects and dividing it into the desired probability of the risk value. All effects exceeding the t–value limits are important in predicting regression for the elasticity modulus. It validates the hypothesis that the main and interaction effects identified in Figure 4.8 are the few vital parameters as opposed to the others as being the trivial many in determining the tensile strength. As this is a Resolution IV fractional factorial DOE, no main effects are confounded with any other main effect or any other two factor interaction effects. However, two and three factor interactions may be confounded with each other. For example, CE is an alias of AB, EF is an alias of AD, DE is an alias of AF, CD is an alias of BF and ACD, BDE, CEF are aliases of ABF.

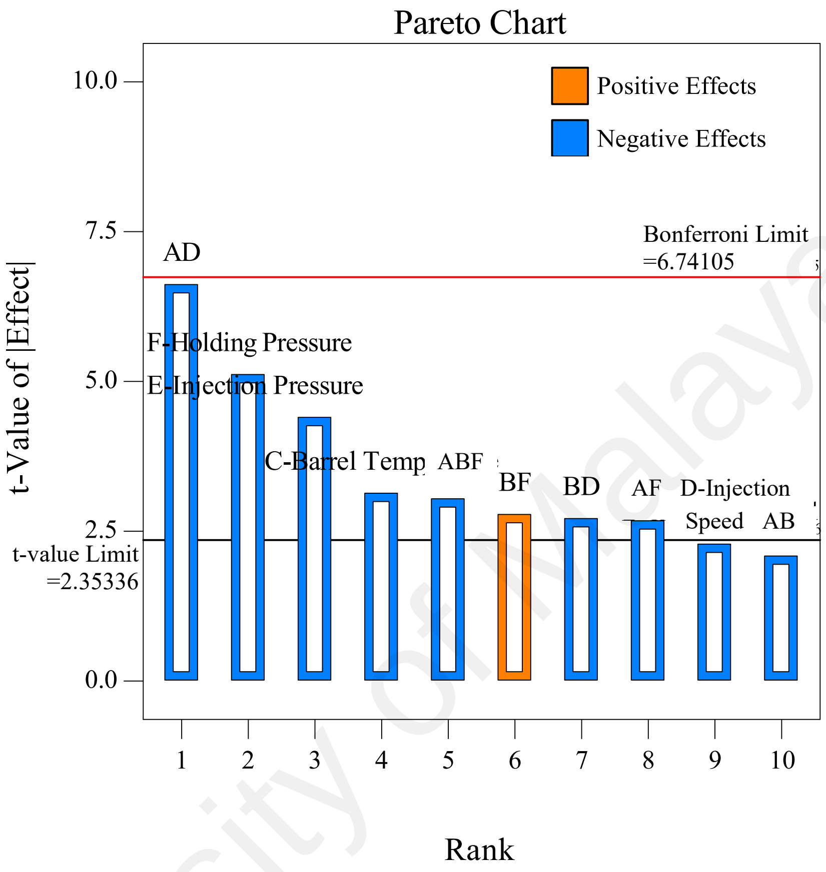

Figure 4.9: Pareto plot of effects for elasticity modulus

Next, based on the vital factors determined from the results, ANOVA analysis (Table 4.5) was performed by maintaining the model hierarchy and embedding the trivial factors in the error term. The F–value of 11.79 implies the model is significant. There is only a 3.30% chance that an F–value this large could occur due to noise. Values of "Prob > F" less than 0.10 indicate model terms are significant. Values greater than 0.10 indicate the model terms are not significant. The terms C, D, E, AB, AD and ABF are significant for tensile strength. The coefficient of determination, R^2 is one of the measures resulting in the reduction of response variability. R^2 of 0.9792 is very close to 1, in agreement that the model comprises of best fit data. The R^2_{adj} value of 0.8962 suggests the model is sufficient without needing to consider additional terms. An adequate precision measures the signal to noise ratio and value of greater than 4 is desirable. The adequate precision value of 11.795 indicates an adequate signal. This model can be used to navigate the design space.

Table 4.5: Results of ANOVA for elasticity modulus

Source	Sum of Squares	df	Mean Square	F	Prob. > F	Remarks
Model	1.20E+06	12	1.00E+05	11.79	0.033	significant
A–Plasticizing Pressure	8053.85	1	8053.85	0.95	0.4017	
B–Screw Speed	3536.89	1	3536.89	0.42	0.5644	
C–Barrel Temperature	83265.03	1	83265.03	9.82	0.0519	significant
D–Injection Speed	44240.81	1	44240.81	5.22	0.1065	
E–Injection Pressure	1.64E+05	1	1.64E+05	19.36	0.0218	significant
F–Holding Pressure	2.22E+05	1	2.22E+05	26.16	0.0145	significant
AB	36918.93	1	36918.93	4.35	0.1282	
AD	3.71E+05	1	3.71E+05	43.77	0.007	significant
AF	60633.25	1	60633.25	7.15	0.0754	significant
BD	62323.17	1	62323.17	7.35	0.0731	significant
BF	65551.9	1	65551.9	7.73	0.069	significant
ABF	78430.29	1	78430.29	9.25	0.0558	significant
Residual	25440.78	3	8480.26			
Cor Total	1.23E+06	15				
R^2, 0.9792; R^2_{adj}, 0.8962; Adequate Precision, 11.795						

The model above was used to predict the elasticity modulus of POM (Y2). It can be presented in terms of coded factors as in the following equation;

$$Y2 = 8341.9 + 22.4 * A + 14.9 * B - 72.1 * C - 52.6 * D - 101.3 * E - 117.7 * F - 48.0 * AB - 152.3 * AD - 61.6 * AF - 62.4 * BD + 64.0 * BF - 70.0 * ABF \qquad (4.2)$$

The residuals, i.e. deviation of actual values against the predicted values, analyzes the adequacy of the model by evaluating the data applied in the model. Random and normally distributed residuals indicate none of the predictive information is in the error. Normal probability plot and residuals versus predicted level are shown in Figure 4.10 and Figure 4.11 respectively. The residuals in prediction of response are minimal since they are very close to the diagonal line. Hence, the deterministic portion of the model is good at explaining the response that only the inherent randomness is leftover within the error portion (L. Liu et al., 2017).

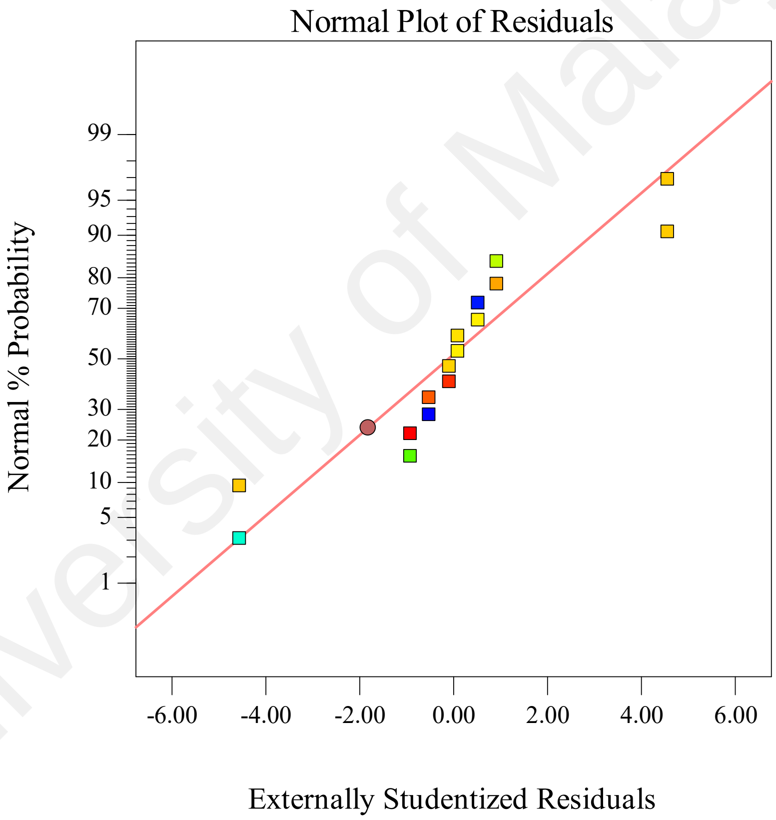

Figure 4.10: Normal plot of residuals for elasticity modulus

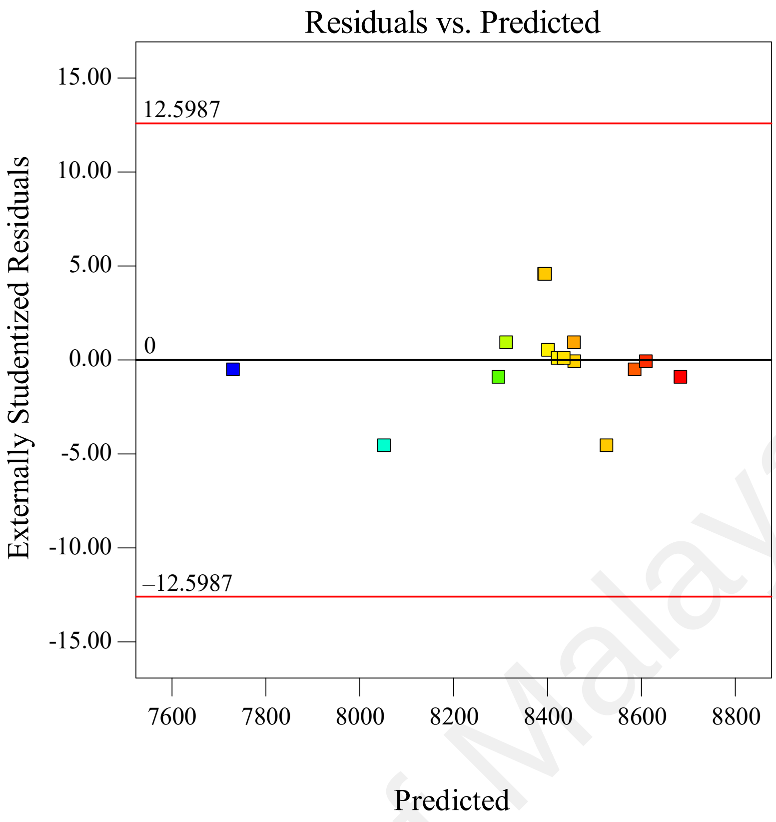

Figure 4.11: Residuals versus predicted elasticity modulus

Elasticity modulus is significantly affected by a combination main (C, E, F) and interaction effects (AD, AF, BD, BF, ABF). These observations can be illustrated by graphs of the effect changes versus the factor levels as shown in Figures 4.12(a)–(e). By visually reviewing the contribution of main effects, the barrel temperature (C), injection speed (D) and injection pressure (E) must be controlled to higher values to obtain higher elasticity modulus without considering there are no interaction between them. When interaction exist between two factors, two lines appear on the plot. For example, Figure 4.12(d) reveals the effect of plasticizing pressure (A) is dependent on the setting of injection speed (D). Improved stiffness can be achieved by setting the injection speed to 100 mm/s (low level) and plasticizing pressure to 1 MPa (high level). Alternatively, maintaining injection speed of 170 mm/s (high level) and plasticizing pressure of 0.8 MPa (low level) would also yield stiffness of approximately 8400 MPa.

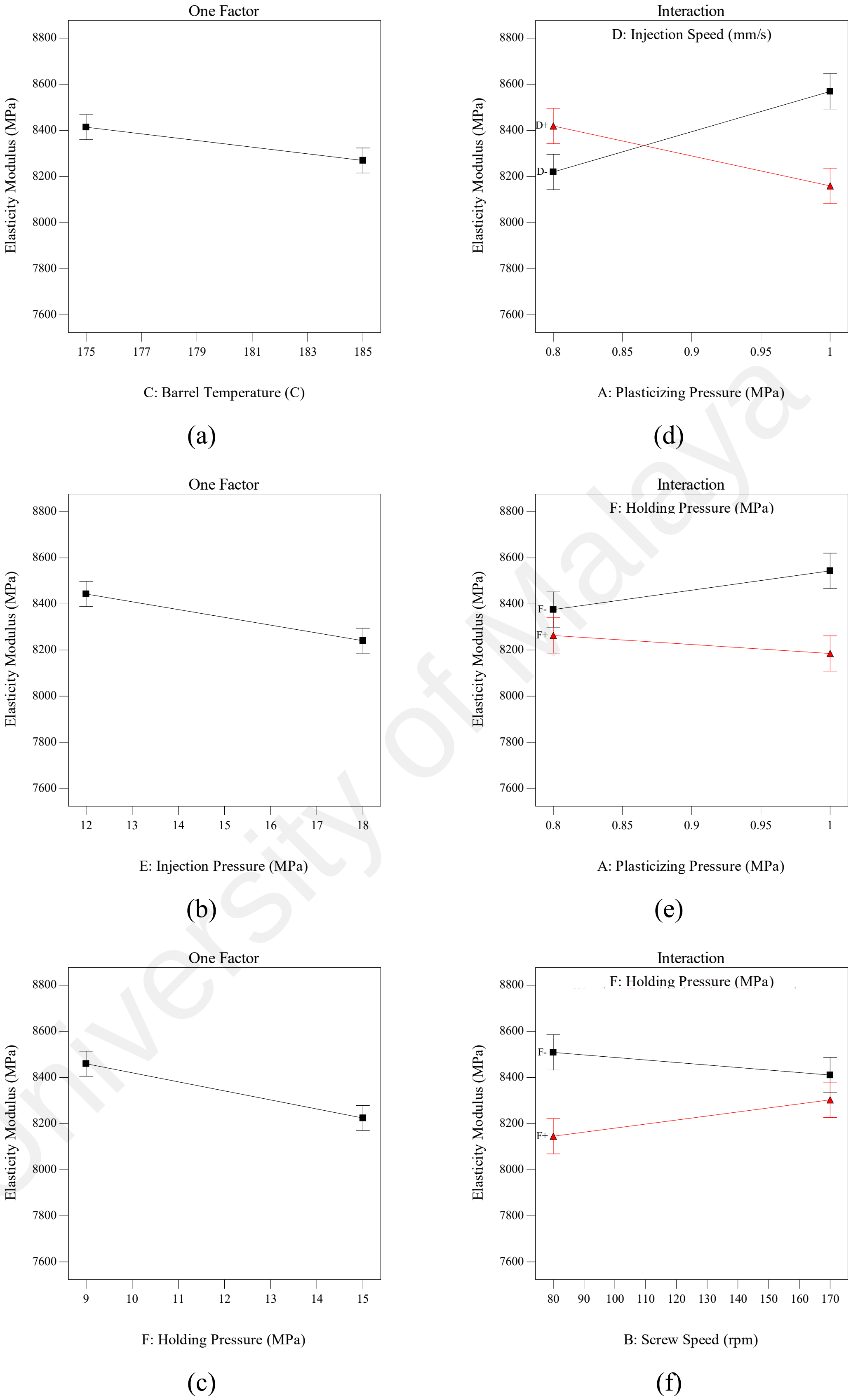

Figure 4.12: Main effects and interaction plots for elasticity modulus

The relationship of actual versus predicted tensile strength is shown in Figures 4.13. The values of R^2 of 0.9792 and R^2_{adj} of 0.8962 along with the residual analysis adequately fits the model to experimental data.

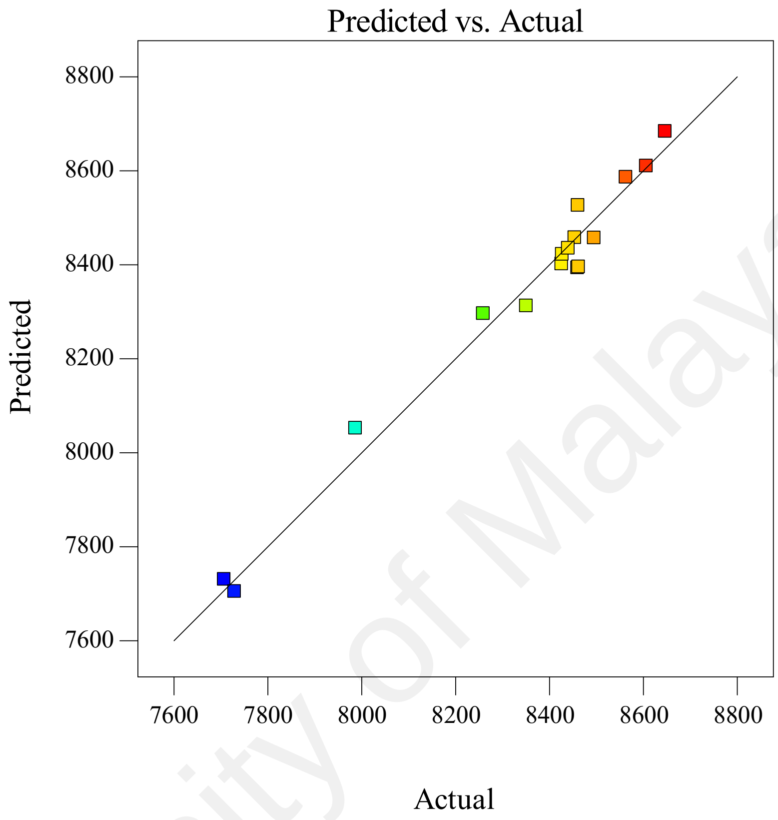

Figure 4.13: Predicted versus actual values of elasticity modulus

4.1.3 Optimization of Process Parameters for Injection Moulding Process

Desirability function was used to measure the overall success in optimizing tensile strength and elasticity modulus. It combines all the goals into one multiplicative function by allowing the process parameters and each of the mechanical properties to be adjusted within their experimental boundaries. The Design–Expert Software offers preferences that are minimum, maximum, target and in range for the factors and responses. Moreover, there is another preference to the above–mentioned one that is equal to for the independent variables. Initially, the process parameters were left to vary within their experimental range whereas highest tensile strength and elasticity modulus were desired. Based on these results, the setting for injection pressure and mould holding pressure were re–evaluated as the difference between these parameters should be relatively small. Higher holding pressure may affect mould life while significantly large difference between injection and holding pressure causes the polymer melt to flow out of the mould cavity. Hence, balancing these two parameters are important.

Table 4.6 shows the selected range of the process parameters and the corresponding tensile strength and elasticity modulus. By assigning equal weight and importance, all factors were left to vary within their experimental range. Maximum values for mechanical properties or responses were desired. Graphical representation of the factors and responses are shown in Figure 4.14 by using ramp plots. An overall desirability index of 95.9% was registered. The maximum values obtained for tensile strength and elastic modulus were 131.4 MPa and 8647 MPa respectively. As expected, these values are very similar to the highest experimental values, i.e. 133.0 MPa for tensile strength and 8647 MPa for elasticity modulus. To obtain these maximum responses, plasticizing pressure, screw speed, barrel temperature, injection speed, injection and holding pressure must be controlled to 1 MPa, 170 mm/s, 182 °C, 100 mm/s, 18 MPa and 9 MPa respectively.

Table 4.6: Initial specification of factors and the desired responses for injection moulding process parameters

Name	Specification	Unit	Lower Limit	Upper Limit	Weight	Importance
A: Plasticizing Pressure	is in range	MPa	0.8	1.0	1	3
B: Screw Speed	is in range	rpm	80	170	1	3
C: Barrel Temperature	is in range	°C	175	185	1	3
D: Injection Speed	is in range	mm/s	100	150	1	3
E: Injection Pressure	is in range	MPa	12	18	1	3
F: Holding Pressure	is in range	MPa	9	15	1	3
Y1: Tensile Strength	maximize	MPa	113.5	133.0	1	3
Y2: Elasticity Modulus	maximize	MPa	7707	8646	1	3

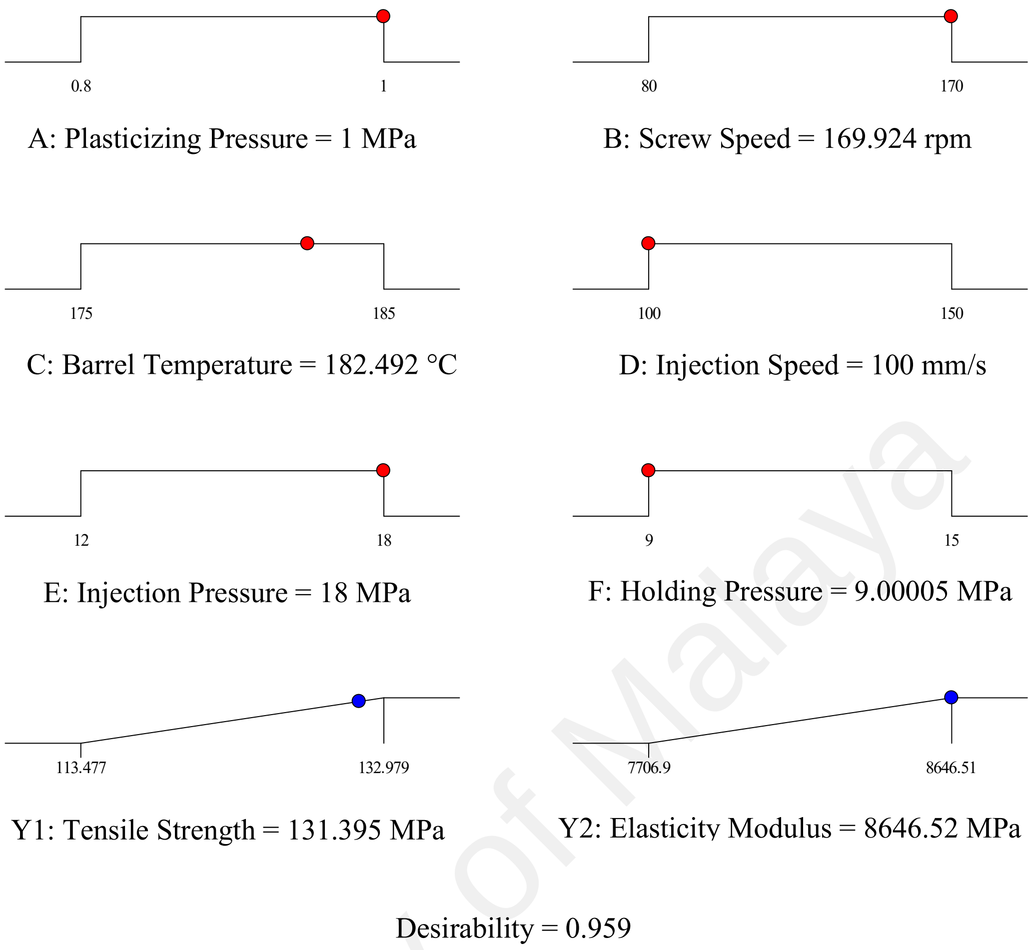

Figure 4.14: Ramp plots of initial numerical analysis for optimal process parameters for injection moulding process

It can be noted that the injection pressure of 18 MPa is the high level while the holding pressure of 9 MPa is the low level used in the DOE. The difference between these process parameters is 9 MPa. As it is preferred for the difference to be smaller, the numerical analysis was repeated by slightly increasing the holding pressure to 12 MPa and reducing the injection pressure to 14 MPa. The targeted values for other process parameters were maintained from the initial results. Ramp plots for the optimized process parameters and the corresponding tensile strength and elasticity modulus are presented in Figure 4.15.

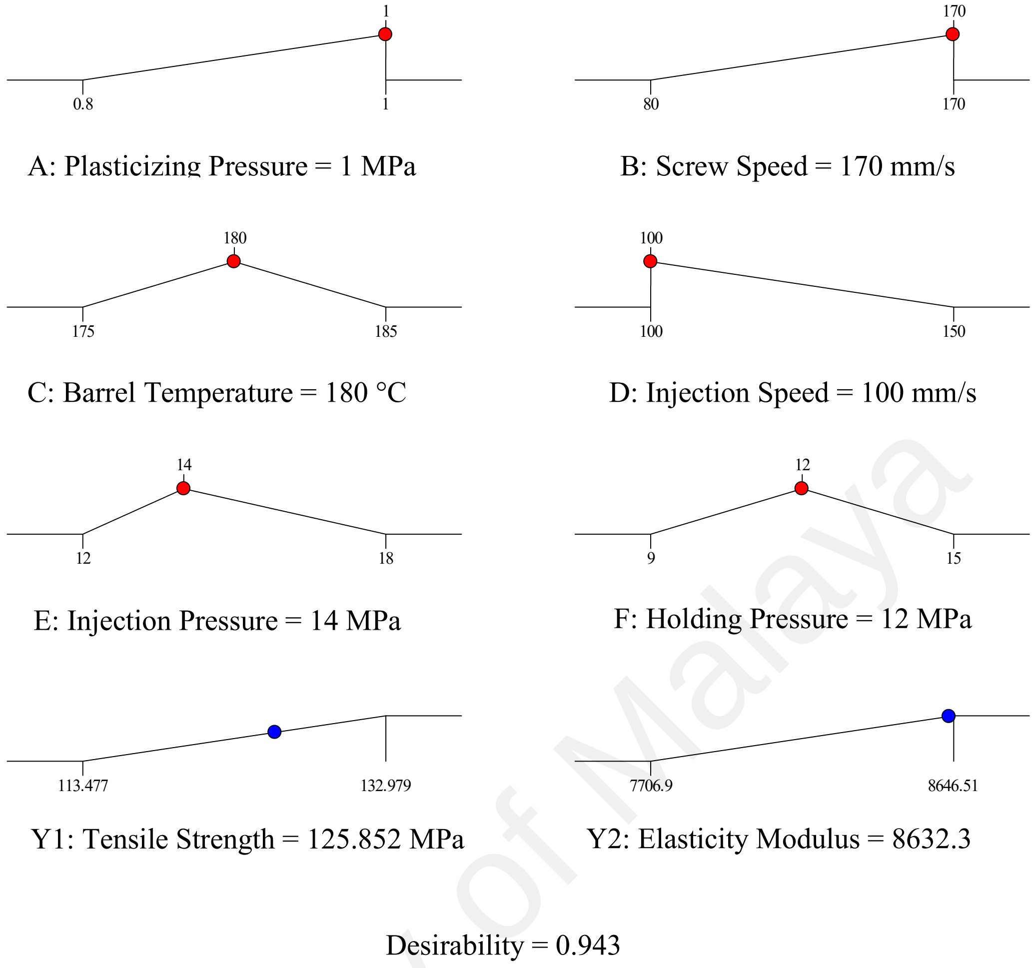

Figure 4.15: Ramp plots for final numerical analysis to determine process parameters

By imposing the targeted values for each of factors, tensile strength reduced by approximately 4% to 125.9 MPa whereas elasticity modulus remains unaffected at 8632 MPa with an overall desirability of 94.3%. Hence, the injection moulding process parameters as shown in Table 4.7 were selected.

Table 4.7: Final specification of factors and responses for optimal process parameters for injection moulding process

Name	Final specification	Unit	Lower Limit	Upper Limit	Weight	Importance
A: Plasticizing Pressure	is target = 1	MPa	0.8	1.0	1	3
B: Screw Speed	is target = 170	mm/s	80	170	1	3
C: Barrel Temperature	is target = 180	°C	175	185	1	3
D: Injection Speed	is target = 100	mm/s	100	150	1	3
E: Injection Pressure	is target = 14	MPa	12	18	1	3
F: Holding Pressure	is target = 12	MPa	9	15	1	3
Y1: Tensile Strength	maximize	MPa	113.5	133.0	1	3
Y2: Elasticity Modulus	maximize	MPa	7707	8647	1	3

4.2 Characterization of Mechanical Properties for POM/GF/PTFE composites

With the identification of optimal process parameters for injection moulding, POM/GF/PTFE composite samples were prepared by varying micro–PTFE etch time and weight percentage. This served as a preliminary study to determine effects of surface treated PTFE on mechanical properties of POM/GF/PTFE composites. Samples were prepared in accordance to Table 3.3. As control samples, the neat POM525GR was also intentionally processed through the Brabender mixer and crushed.

The tensile strength of different POM/GF/PTFE samples are presented in Figure 4.16 with each bar representing an average value of five samples. The results show that the tensile strength of composites consisting 10% non–etched PTFE micro particles reduced by 4% compared to neat POM control group. By increasing the PTFE weight percentage to 20%, the strength further decreased by approximately 10%. The negative reinforcing effect is caused by the change of interfacial bonding force between the matrix and fiber due to the presence of micro–PTFE (Sun, Yang, & Li, 2008a). Based on SEM microscopy of fractured samples shown in Figure 4.42, presence of more polymeric material adhered to the surface GF can be observed with increased PTFE content. In addition, PTFE has low tensile strength causing inability to undertake stress (Chiang et al., 1999).

On the other hand, stable tensile strength was found for composites with 10% micro–PTFE and etched for 10 min and 20 min. As the etch time was increased to 30 min, slight decrease in the composite's strength was noted. When the micro particles were subjected to longer etch time, larger particles disintegrated into smaller particles, causing higher concentration within the POM matrix. This is caused by increase of etching depth of the polymer surface as a result of sodium naphthalenide treatment. SEM images shown in Figure 4.41 revealed the surface of PTFE micro particles etched for 2.9 min was generally smooth and particles were circular in shape. With 10 min etching time, the particles' surface was rougher indicating the effects of etching whereas PTFE micro particles started disintegration at etch time of 17.1 min.

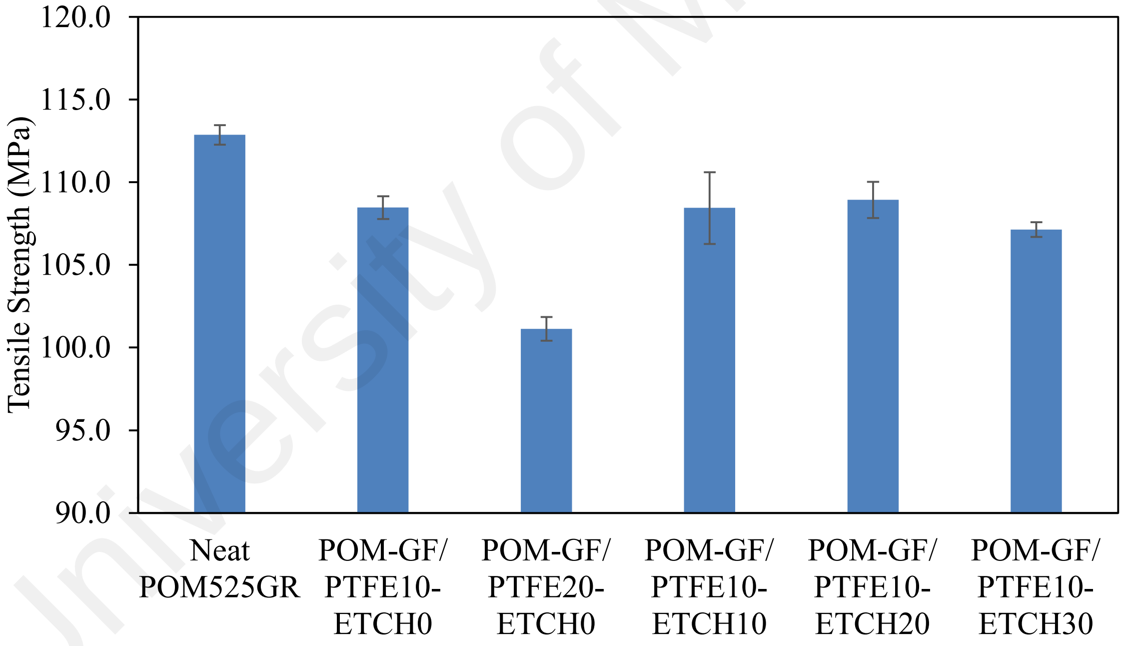

Figure 4.16: Comparison of tensile strength for POM/GF/PTFE composites

POM matrix in melt state was able to wet etched PTFE micro particles more effectively when compared to non–etched PTFE surface. This process starts with spreading of the melt POM over the micro–PTFE's surface and then followed with interfacial contact. Upon completion of this process, an interfacial zone is formed comprising of an interface and interphase. The wetting of PTFE by the melt POM reduces the total free energy of the composite. The extent of mechanical interaction determined the adhesion between POM matrix and the PTFE micro particles used as reinforcement.

When the PTFE was etched for 30 min, increased etching depth was obvious and the particles appeared to be disintegrated. Sodium naphthalenide can cause etching depth to extend 300 nm while X–ray would only result in 3–15nm depth. The excessive etching weakened the bond to the bulk of PTFE part. This is likely due to the existence of pores and cracks on the PTFE surface could have remained unfilled if the melt polymer was unable to penetrate into the surface imperfections prior to polymerization.

As shown in Figure 4.17, highest stiffness was achieved with neat POM525GR samples. By increasing non–etched PTFE content, the deformation resistance deteriorated as a result of agglomeration of PTFE micro particles. The poor miscibility between non–etched PTFE and POM further weakened the matrix and lowered the stiffness of the composite. In addition, low strength of PTFE was unable to undertake stress.

Similar to tensile strength, increased micro–PTFE etch time did not negatively impact its elasticity modulus. Improved miscibility between surface etched micro–PTFE, achieved by surface energy changes due to chemical etching, and POM matrix reduced the overall matrix strain at the vicinity of the fibers resulting in lesser deformation. The miscible POM and PTFE adhered to the surface of glass fibers as observed on SEM analysis of fractured samples shown in Figure 4.42. Homogenous dispersion of PTFE into viscous polymer melt may have also contributed to the composite’s stable stiffness.

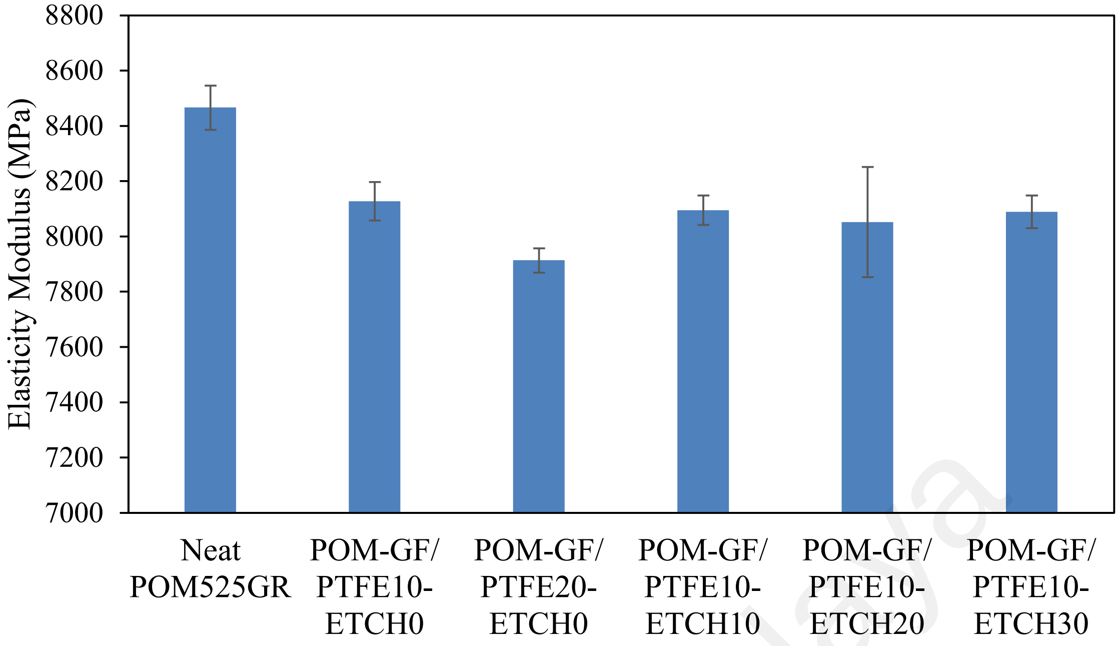

Figure 4.17: Comparison of elasticity modulus for POM/GF/PTFE composites

Addition of micro–filler is known to negatively impact the mechanical properties of polymer composites. PTFE, as a tribological property modifier, is known to have strong tendency to agglomerate making it difficult to be dispersed homogenously in viscous polymer melt. Adhesion between POM and surface etched micro–PTFE resulted in slightly decreased, but stable mechanical properties. These results warranted further investigations into reaping the benefits of tribological properties contributed by surface etched micro–PTFE without significantly compromising the mechanical properties of POM/GF/PTFE composite.

4.3 RSM Analysis of Mechanical Properties

The levels of factors and the effect of their interactions on mechanical properties were determined by CCD of RSM. The design matrix of experimental results by tests was planned according to a full factorial design. Thirteen experiments were performed with different combinations of factors and the central point was repeated five times. The observed responses along with design matrix are presented in Table 4.8. Without performing any transformation on the responses, the results were analyzed by ANOVA.

A regression equation provided the relationship of mechanical properties of the POM composites as a function of PTFE content and PTFE etch time. Test for significance of the regression model, test for significance on individual model coefficients and test for lack–of–fit is required. An ANOVA table is commonly used to summarize the tests performed.

Table 4.8: Central composite design in uncoded factors with tensile strength, elasticity modulus, toughness and hardness as responses

PTFE Content A	PTFE Etch Time B	Tensile strength (MPa) Y1	Elasticity modulus (MPa) Y2	Toughness (kJ/m^3) Y3	Hardness (HRR) Y4
1.7	10.0	106.8 ± 1.6	8377 ± 132	1636 ± 102	115.5 ± 0.6
4.0	5.0	111.9 ± 1.6	8287 ± 73	2020 ± 114	115.7 ± 0.3
4.0	15.0	108.9 ± 2.4	8301 ± 110	1836 ± 147	115.6 ± 0.3
9.5	10.0	107.5 ± 1.4	8046 ± 108	2013 ± 87	114.4 ± 0.4
9.5	10.0	108.6 ± 1.7	8087 ± 90	2021 ± 106	114.6 ± 0.7
9.5	17.1	107.7 ± 1.9	8069 ± 129	2090 ± 92	114.7 ± 0.6
9.5	10.0	107.2 ± 1.8	8057 ± 86	2014 ± 97	114.6 ± 0.3
9.5	10.0	108.1 ± 0.9	8067 ± 48	2025 ± 105	114.1 ± 0.3
9.5	2.9	108.2 ± 1.2	8048 ± 48	2149 ± 101	114.8 ± 0.3
9.5	10.0	108.0 ± 1.2	8118 ± 99	1909 ± 119	114.0 ± 0.6
15.0	5.0	105.1 ± 1.9	7884 ± 76	2032 ± 113	112.8 ± 0.3
15.0	15.0	102.0 ± 2.1	7803 ± 75	1879 ± 134	112.9 ± 0.3
17.3	10.0	101.7 ± 3.3	7867 ± 113	1805 ± 150	111.8 ± 0.2

The effects of PTFE content and PTFE etch time on the tensile properties of POM composites are displayed in Figure 4.18. With 10 min PTFE etch time, toughness, represented by the area under the stress vs. strain curves, steadily increased as PTFE content is increased from 1.7% to 17.3%. POM composites blended with PTFE etched for 2.9 min and 17.1 min show slightly better toughness than 10 min etched PTFE. Increase of toughness with higher PTFE content is at the cost of tensile strength and elasticity modulus. By comparing POM/GF/PTFE composites with 9.5% PTFE content at different PTFE etch time, no significant difference in strength and stiffness observed.

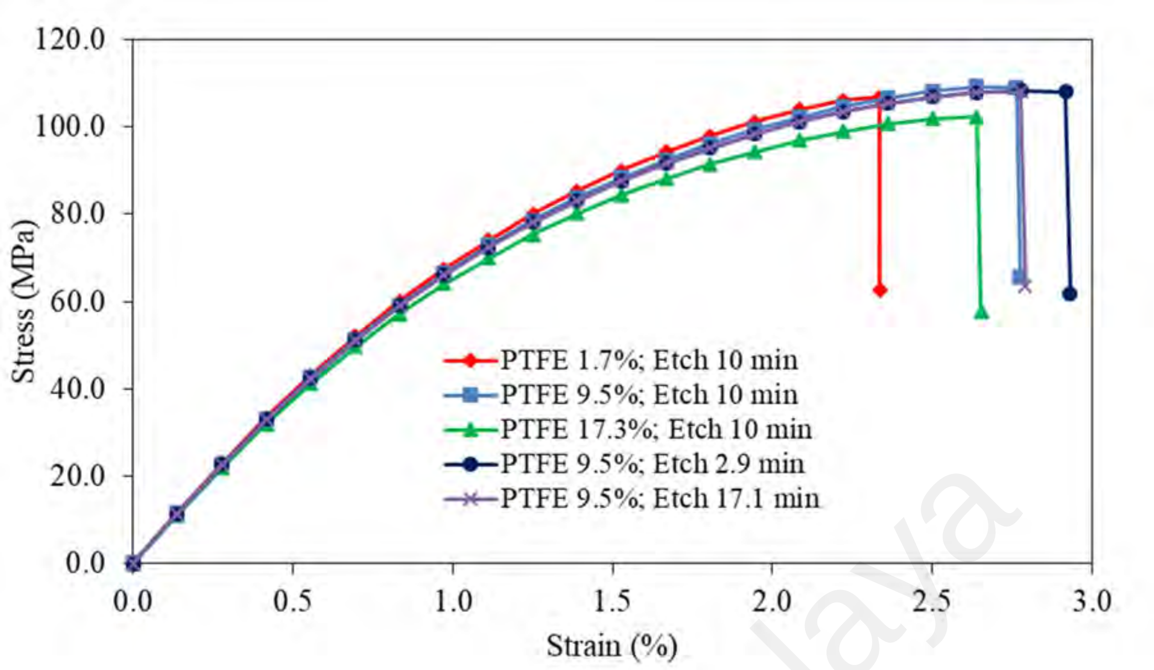

Figure 4.18: Stress vs. strain curves comparing effects of PTFE content and etch time on POM/GF/PTFE composites

4.3.1 ANOVA and Model Fitting for Tensile Strength of POM/GF/PTFE Composites

Table 4.9 shows the ANOVA table for response surface model for tensile strength. The F–value of 24.80 implied the model is significant. There is only a 0.14% chance that an F–value this large could occur due to noise. Values of “Prob > F” less than 0.05 indicate model terms are significant. Values greater than 0.10 indicate the model terms are not significant. The lack–of–fit can also be said to be insignificant. This was necessary as we want a model that fits. The terms A, A^2, A^2B, AB^2 were significant for the tensile strength of POM composites. The coefficient of determination, R^2 is one of the measures resulting in the reduction of response variability. R^2 of 0.9720 was very close to 1, in agreement that the model comprises of best fit data. The R^2_{adj} value of 0.9328 suggested the model was sufficient without needing to consider additional terms. An adequate precision measures the signal to noise ratio and value of greater than 4 is desirable. The adequate precision value of 17.698 indicated an adequate signal. This model was used to navigate the design space.

Table 4.9: Response surface model ANOVA for tensile strength of POM/GF/PTFE composites using CCD

Source	Sum of Squares	df	Mean Square	F	Prob. > F	Remarks
Model	88.44	7	12.63	24.80	0.0014	significant
A	13.06	1	13.06	25.62	0.0039	significant
B	0.15	1	0.15	0.30	0.6093	
AB	6.25E–04	1	6.25E–04	1.23E–03	0.9734	
A^2	17.31	1	17.31	33.98	0.0021	significant
B^2	0.46	1	0.46	0.90	0.3853	
A^2B	3.53	1	3.53	6.92	0.0465	significant
AB^2	5.29	1	5.29	10.38	0.0234	significant
Residual	2.55	5	0.51			
Lack of Fit	1.44	1	1.44	5.17	0.0853	not significant
Pure Error	1.11	4	0.28			
Cor Total	90.99	12				
R^2, 0.9720; R^2_{adj}, 0.9328; Adequate Precision, 17.698						

The model above was used to predict the tensile strength of POM composites (Y1) as a function of PTFE content (A) and PTFE etch time (B). It can be presented in terms of coded factors as in the following equation:

$$Y1 = 107.86 - 1.81A - 0.19B - 0.012AB - 1.58A^2 + 0.26B^2 - 1.33A^2B - 1.63AB^2 \qquad (4.3)$$

Normal probability plot for residuals, i.e. deviation of actual values against the predicted values, analyzed the adequacy of the model by evaluating the data applied in the model. Random and normally distributed residuals indicate none of the predictive information is in the error. The residuals in prediction of response were minimal since they were very close to the diagonal line. Hence, the deterministic portion of the model was good at explaining the response that only the inherent randomness was leftover within the error portion (L. Liu et al., 2017). The deterministic portion denoted by the relationship of actual versus predicted tensile strength is shown in Figure 4.19.

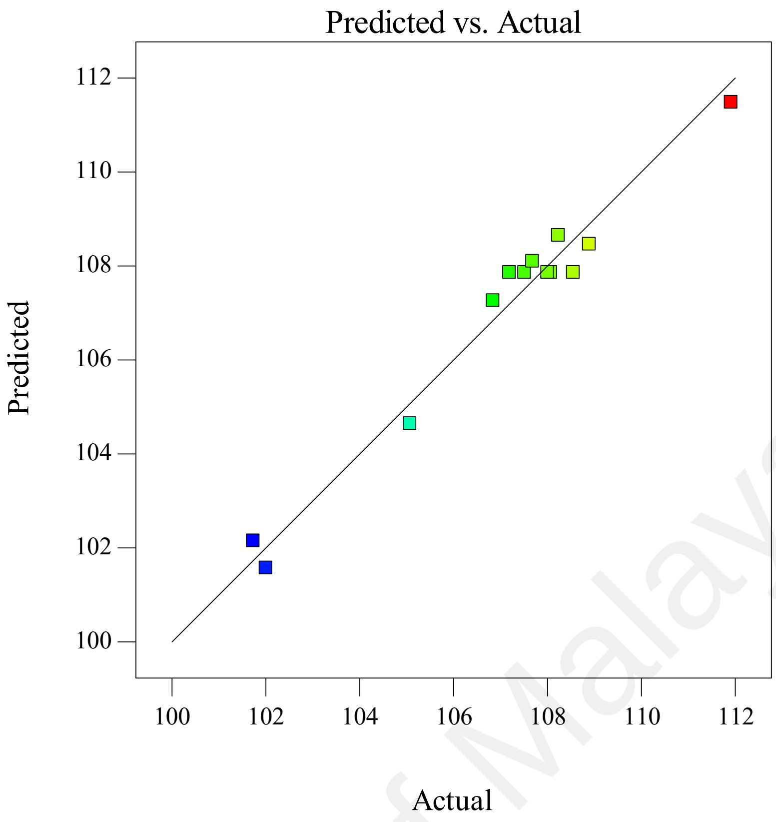

Figure 4.19: Deterministic portion for tensile strength of POM/GF/PTFE composites as predicted versus actual values

Normal probability plot for residuals in Figure 4.20 and the residuals versus predicted values of tensile strength in Figure 4.21 represented the stochastic error of the statistical model. The values of R^2 of 0.9720 and R^2_{adj} of 0.9328 along with the residual analysis adequately fitted the model to experimental data.

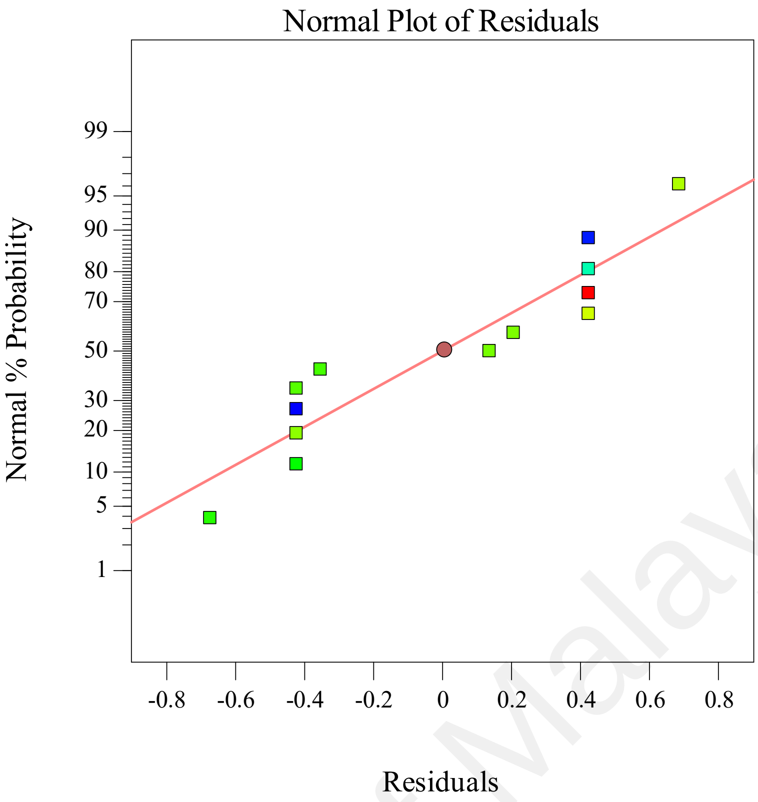

Figure 4.20: Stochastic error for tensile strength of POM/GF/PTFE composites as normal probability plot for residuals

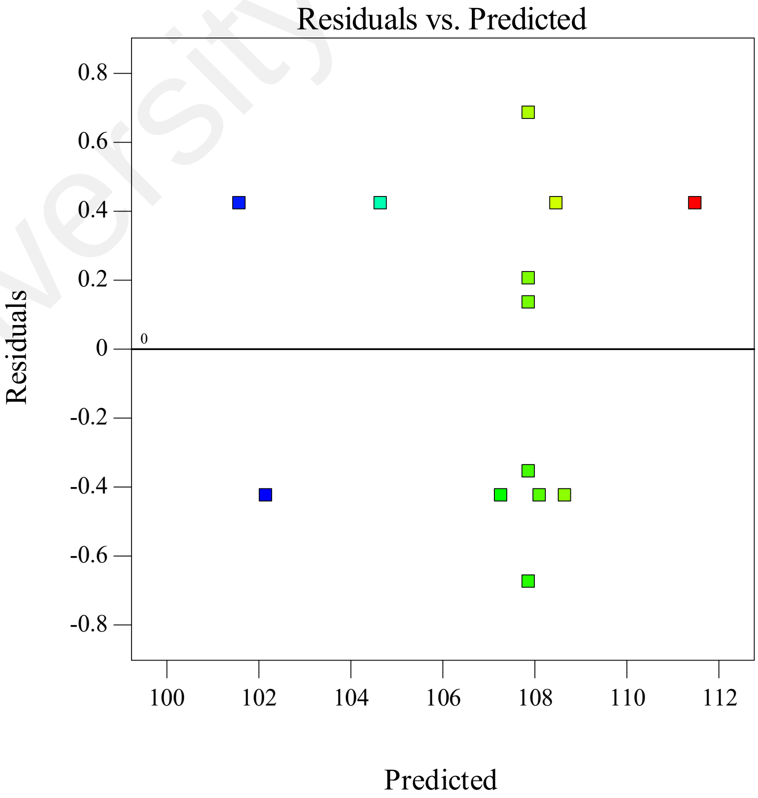

Figure 4.21: Stochastic error for tensile strength of POM/GF/PTFE composites as residuals versus predicted values

The interaction effects of PTFE content and PTFE etch time on the tensile strength were studied by plotting surface curves. The primary and secondary horizontal axes were the input variables whereas the vertical axis is the calculated response, i.e. the tensile strength. The 3D surface curves and 2D contour plots from the interactions of these variables were obtained. Figures 4.22 and 4.23 show the graphical representation of the tensile strength dependency on the PTFE content and PTFE etch time.

Generally, the POM composites exhibited continuous decline in tensile strength with increasing PTFE content. As expected, lowest strength is obtained at higher PTFE content with slight dependency of PTFE etch time. These observations indicated negative effects of particulate filler to the matrix. Since PTFE is amorphous, its softness leads to reduction of strength of the matrix. In addition, surface of PTFE particles insufficiently etched when exposed to low etch time as shown in Figure 4.41(a). The PTFE particles have low surface energy, resulting in poor wettability and inability to bond leading to weak interface with matrix and GF. By increasing PTFE content, these agglomerative PTFE form much bigger sized particles causing localized stress concentrations (C. Y. Huang et al., 2016). As shown in Figure 4.42(b), the adhesion polymeric material to GF, coupled with rather low compatibility with PTFE particles with POM is unable to undertake the stress during the tensile process. PTFE in the form of particles are known to cause agglomeration affecting the tensile strength and smaller particulates are able to reduce this effect (Sun et al., 2008a). Thus, tensile strength of studied composites decreases as the PTFE content increase. Disintegration of PTFE particles shown in Figure 4.41(c) and adhesion to GF observed in Figure 4.42(b) contributed to lower strength.

With PTFE content of 4.0% to 9.5%, tensile strength achieved a stable region of approximately 108 MPa, independent of PTFE etch time. At this region, the POM/PTFE appeared homogenous with slight adhesion to the surface of GF as shown in Figure 4.42(a). Surface of PTFE micro particles was influenced by etch time but its effect on tensile strength of POM/GF/PTFE composites was rather low. PTFE content of less than 9.5% was insufficient to overcome the GF’s reinforcement. Surface treatment of fluoropolymers changes chemical composition, increases surface energy, polarity, wettability and ability to bond (Ebnesajjad, 2015). This stable region is important so that other mechanical properties of POM/GF/PTFE composites can be optimized without compromising its strength.

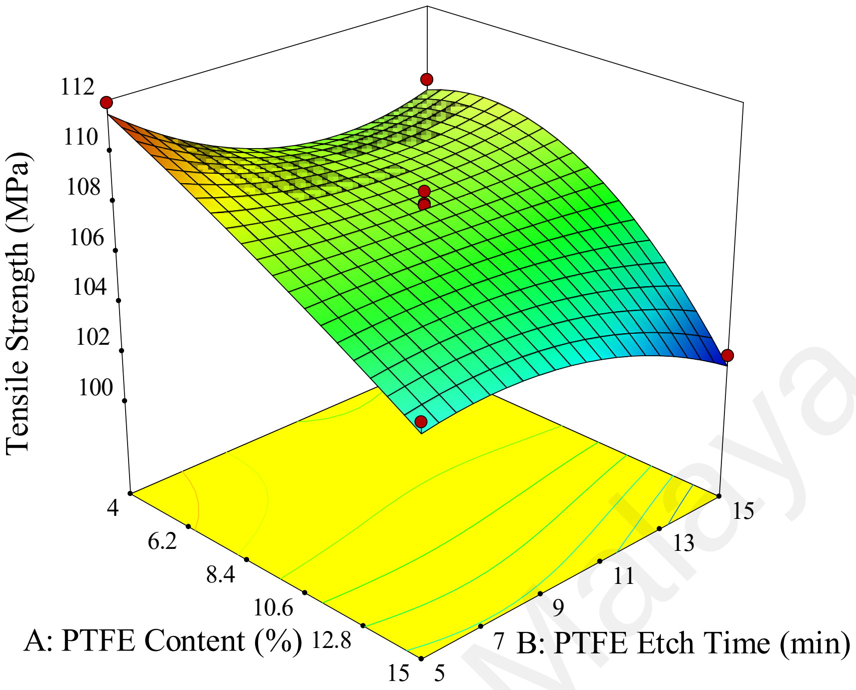

Figure 4.22: 3D response surface plot for the effects of PTFE content and PTFE etch time on tensile strength of POM/GF/PTFE composites

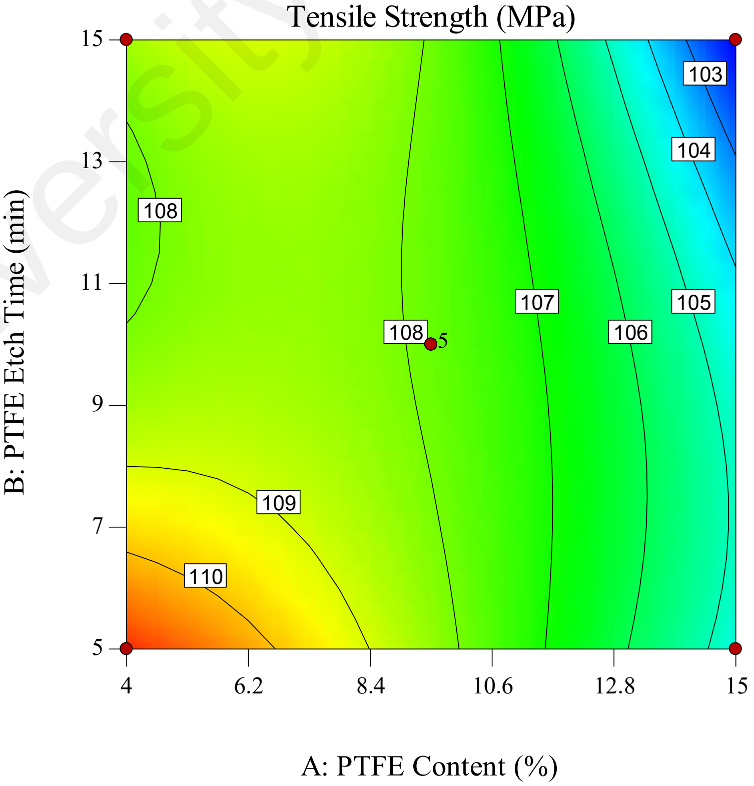

Figure 4.23: 2D contour plot for the effects of PTFE content and PTFE etch time on tensile strength of POM/GF/PTFE composites

4.3.2 ANOVA and Model Fitting for Elasticity Modulus of POM/GF/PTFE Composites

Table 4.10 shows the ANOVA table for response surface model for elasticity modulus. The F–value of 49.85 implies the model is significant. There is less than 0.0001% chance that an F–value this large could occur due to noise. Values of "Prob > F" less than 0.05 indicate model terms were significant. Values greater than 0.10 indicate the model terms were not significant. The lack–of–fit was also insignificant. Only the term A was significant for the elasticity modulus of POM composites. The coefficient of determination, R^2 of 0.9542 was very close to 1, in agreement that the model comprises of best fit data. The R^2_{adj} value of 0.9450 suggested the model was sufficient without needing to consider additional terms. Adequate precision measures the signal to noise ratio and value of greater than 4 is desirable. The adequate precision value of 30.038 indicated an adequate signal. This model was used to navigate the design space.

Table 4.10: Response surface model ANOVA for elasticity modulus of POM/GF/PTFE composites using CCD

Source	Sum of Squares	df	Mean Square	F	Prob. > F	Remarks
Model	3.353E+005	5	67068.87	49.85	< 0.0001	significant
A	3.288E+005	1	3.288E+005	244.38	< 0.0001	significant
B	164.62	1	164.62	0.12	0.7368	
AB	2244.00	1	2244.00	1.67	0.2376	
A^2	2299.33	1	2299.33	1.71	0.2324	
B^2	1306.86	1	1306.86	0.97	0.3572	
Residual	9418.45	7	1345.49			
Lack of Fit	6145.04	3	2048.35	2.50	0.1982	not significant
Pure Error	3273.41	4	818.35			
Cor Total	3.448E+005	12				
R^2, 0.9542; R^2_{adj}, 0.9450; Adequate Precision, 30.038						

A linear model was used to predict the elasticity modulus of POM composites (Y2) as a function of PTFE content (A) and PTFE etch time (B). It can be presented in terms of coded factors as in the following equation:

$$Y2 = 8077.55 - 202.73A - 4.54B \tag{4.4}$$

The deterministic portion presented the relationship of actual versus predicted elasticity modulus are shown in Figure 4.24 The normal probability plots for residuals and the residuals of the predicted elasticity modulus are shown in Figure 4.25 and Figure 4.26 respectively. Normal probability plot for residuals analyzed the adequacy of the model by evaluating the data applied in the model for elasticity modulus. Random and normally distributed residuals indicate none of the predictive information was in the error. The residuals in prediction of response were minimal since they were very close to the diagonal line. Hence, the deterministic portion of the model was good at explaining the elasticity modulus with only the inherent randomness was leftover within the error portion (L. Liu et al., 2017). The values of R^2 of 0.9542 and R^2_{adj} of 0.9450 along with the residual analysis adequately fitted the model to experimental data.

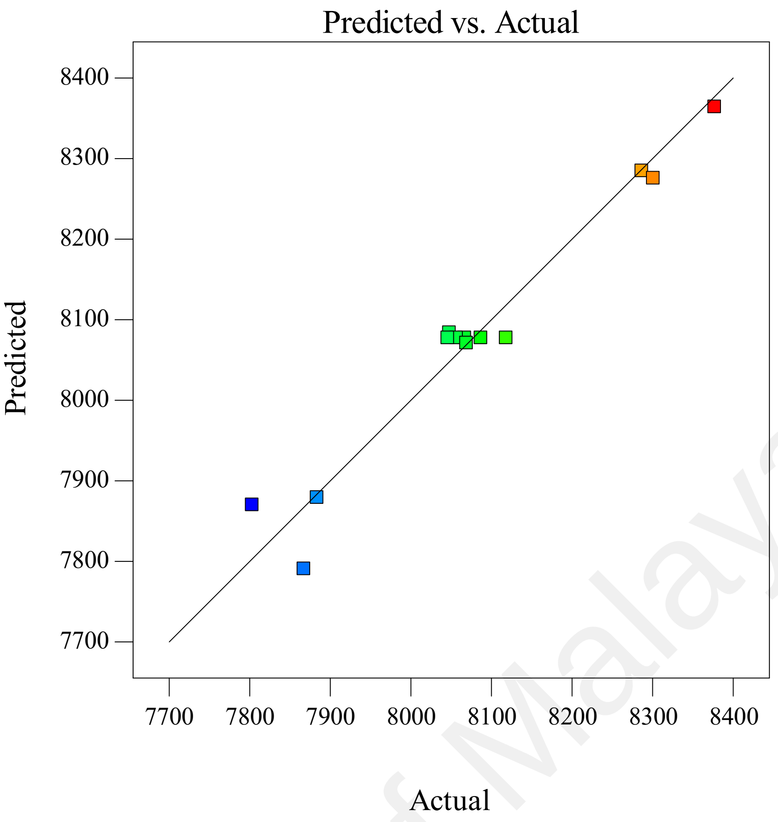

Figure 4.24: Deterministic portion for elasticity modulus of POM/GF/PTFE composites as predicted versus actual values

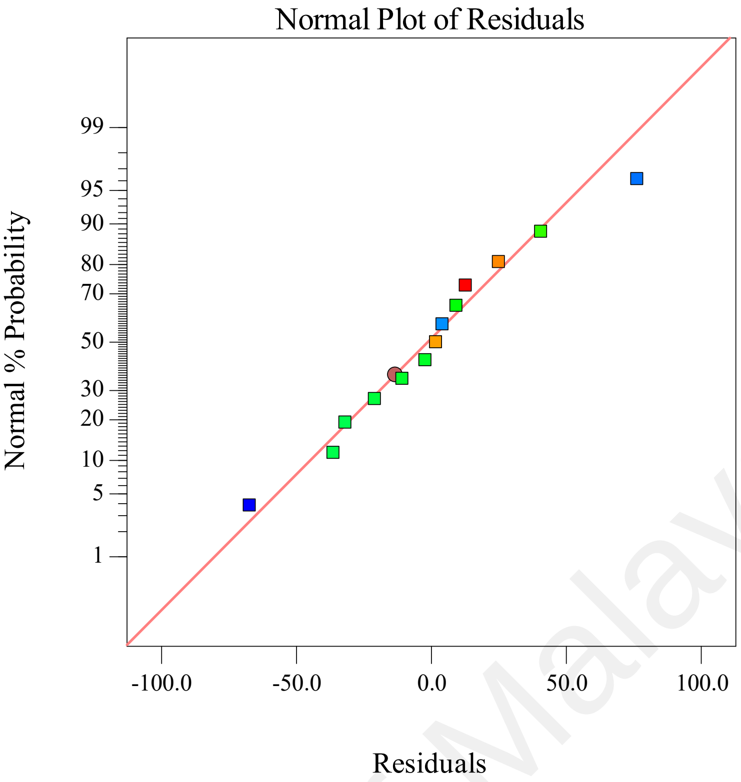

Figure 4.25: Stochastic error for elasticity modulus of POM/GF/PTFE composites as normal probability plot for residuals

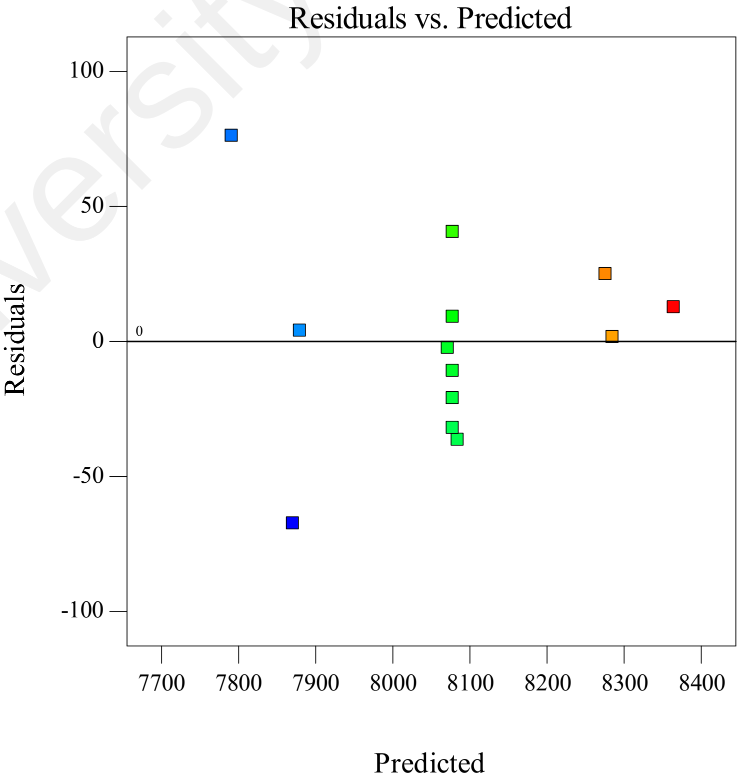

Figure 4.26: Stochastic error for elasticity modulus of POM/GF/PTFE composites as residuals versus predicted values

The interaction effects of PTFE content and PTFE etch time on the elasticity modulus were studied by plotting surface curves. The primary and secondary horizontal axes were the input variables whereas the vertical axis is the calculated response, i.e. the elasticity modulus. The 3D surface curves and 2D contour plots from the interactions of these variables were obtained. Figures 4.27 and 4.28 show the dependency of elasticity modulus on the PTFE content and etch time.

The elasticity modulus consistently decreased as the PTFE content was increased, independent of PTFE etch time. It is known that micro–fillers in the form of particulate cause a reduction in resistance to deformation. Nano or micro–sized particles have strong tendency to agglomerate because of their high surface activity (Ching, Goh, Luqman, & Kalyani, 2012; Udenni Gunathilake, Ching, Ching, Chuah, & Abdullah, 2017). Agglomeration takes places during melt blending to form much larger particles leading to stress concentration sites in composites (Sun et al., 2008a). In Figure 4.42(b), increasing PTFE content resulted in adhesion of POM/PTFE on the surface of GF. With changes to this interface, the reinforcement effects of GF within the composites was compromised. The deterioration in stiffness can be also caused by amorphous property and softness of PTFE. All of these negatively affected stress transfer to GF during tensile loading and reduce the resistance to deformation of the composites. Surface treated PTFE through chemical etching is known to enhance the compatibility with POM matrix when compared to non–treated PTFE (Chiang et al., 1999). Stiffness of POM composites was greatly influenced by GF due to its adhesion to POM, superior elasticity modulus strength and high composition within the composites (Suresha et al., 2014).

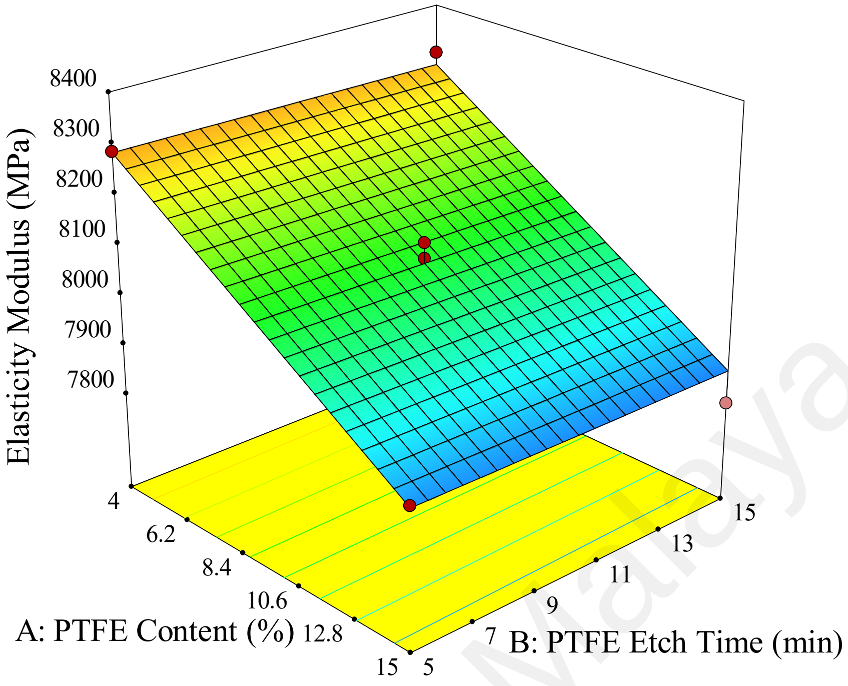

Figure 4.27: 3D response surface plot for the effects of PTFE content and PTFE etch time on elasticity modulus of POM/GF/PTFE composites

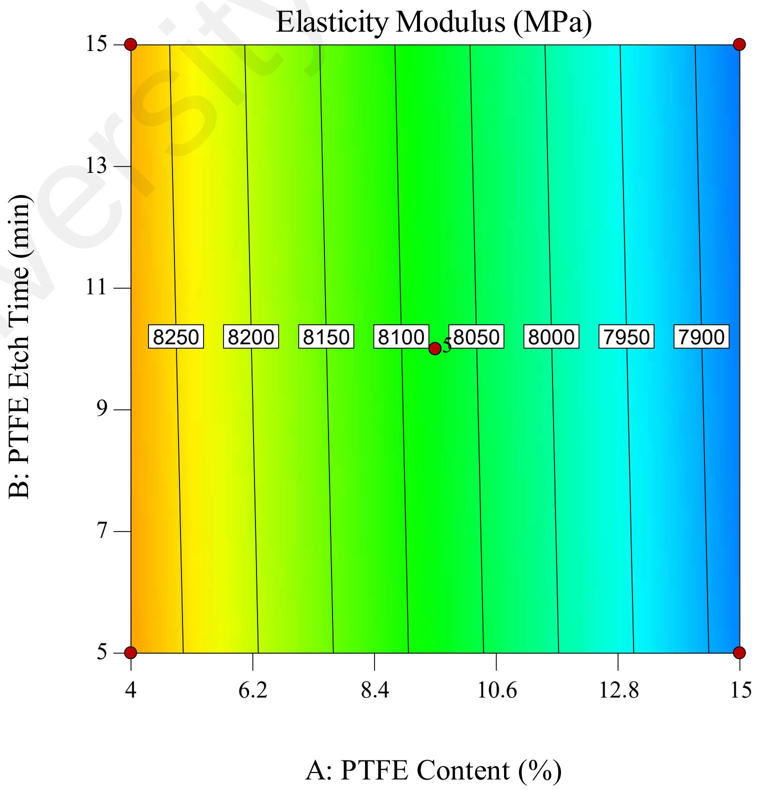

Figure 4.28: 2D contour plot for the effects of PTFE content and PTFE etch time on elasticity modulus of POM/GF/PTFE composites

4.3.3 ANOVA and Model Fitting for Toughness of POM/GF/PTFE Composites

Table 4.11 shows the ANOVA table for response surface model for elasticity modulus. The F–value of 12.59 implied the model is significant. There was only 0.22% chance that an F–value this large could occur due to noise. Values of "Prob > F" less than 0.05 indicated model terms were significant. Values greater than 0.10 indicated the model terms were not significant. The lack–of–fit was also insignificant. This model was desirable as the model that fits. The terms B, A^2 and B^2 were significant for the toughness of POM composites. The coefficient of determination, R^2 of 0.8988 was close to 1, in agreement that the model comprises of best fit data. The R^2_{adj} value of 0.8482 suggested the model was sufficient without needing to consider additional terms. An adequate precision measures the signal to noise ratio and value of greater than 4 is desirable. The adequate precision value of 15.760 indicated an adequate signal. This model was used to navigate the design space.

Table 4.11: Response surface model ANOVA for toughness of POM/GF/PTFE composites using CCD

Source	Sum of Squares	df	Mean Square	F	Prob. > F	Remarks
Model	2.055E+005	5	41102.41	12.59	0.0022	significant
A	10720.96	1	10720.96	3.28	0.1128	
B	22150.59	1	22150.59	6.79	0.0352	significant
AB	252.79	1	252.79	0.077	0.7888	
A^2	1.220E+005	1	1.220E+005	37.37	0.0005	significant
B^2	31322.35	1	31322.35	9.59	0.0174	significant
Residual	22851.58	7	3264.51			
Lack of Fit	13145.38	3	4381.79	1.81	0.2857	not significant
Pure Error	9706.20	4	2426.55			
Cor Total	2.284E+005	12				
R^2, 0.8988; R^2_{adj}, 0.8482; Adequate Precision, 15.760						

The model above was used to predict the toughness of POM composites (Y3) as a function of PTFE content (A) and PTFE etch time (B). It can be presented in terms of coded factors as in the following equation:

$$Y3 = 1996.21 + 36.61A - 52.62B - 132.43A^2 + 67.10B^2 \tag{4.5}$$

The deterministic portion presented as the relationship of actual versus predicted toughness is shown in Figure 4.29. The normal probability plots for residuals and the residuals of the predicted elasticity modulus are shown in Figure 4.30 and Figure 4.31 respectively. Normal probability plot for residuals analyzed the adequacy of the model by evaluating the data applied in the model for toughness. Random and normally distributed residuals indicated none of the predictive information was in the error. The residuals in prediction of response were minimal since they were very close to the diagonal line. Hence, the deterministic portion of the model was good at explaining the toughness with only the inherent randomness was leftover within the error portion (L. Liu et al., 2017). The values of R^2 of 0.8988 and R^2_{adj} of 0.8482 along with the residual analysis adequately fitted the model to experimental data.

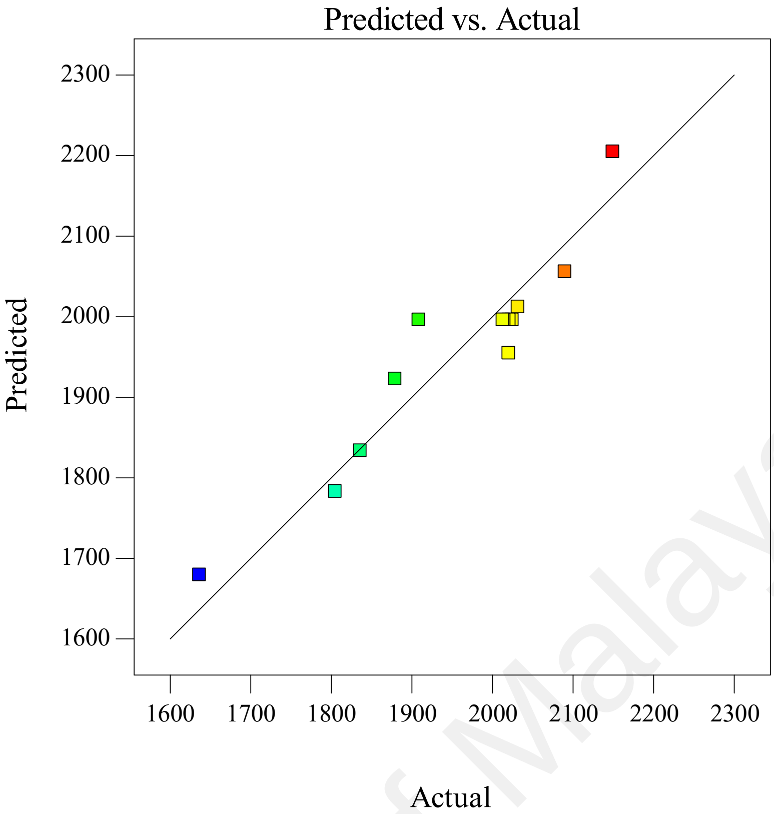

Figure 4.29: Deterministic portion for toughness of POM/GF/PTFE composites as predicted versus actual values

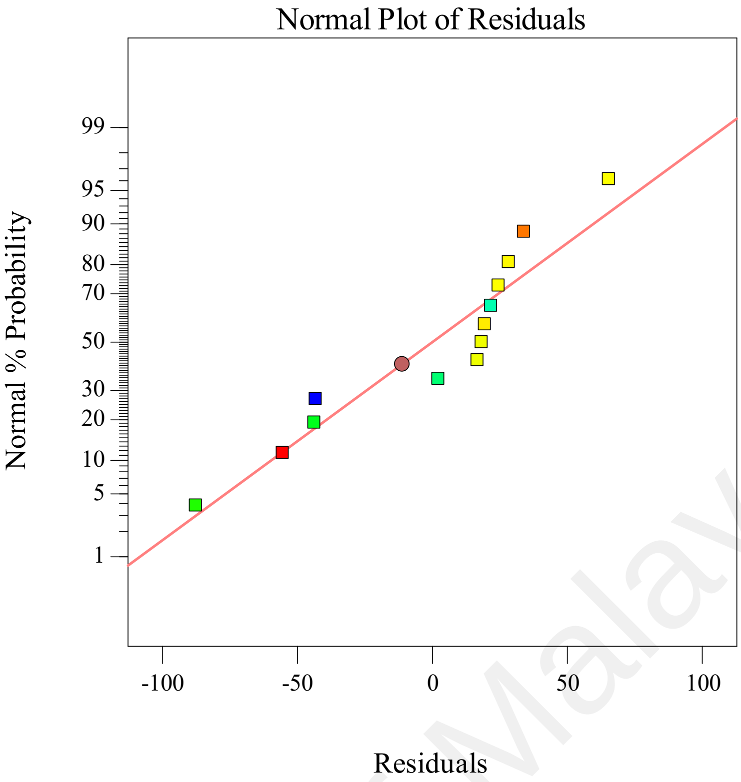

Figure 4.30: Stochastic error for toughness of POM/GF/PTFE composites as normal probability plot for residuals

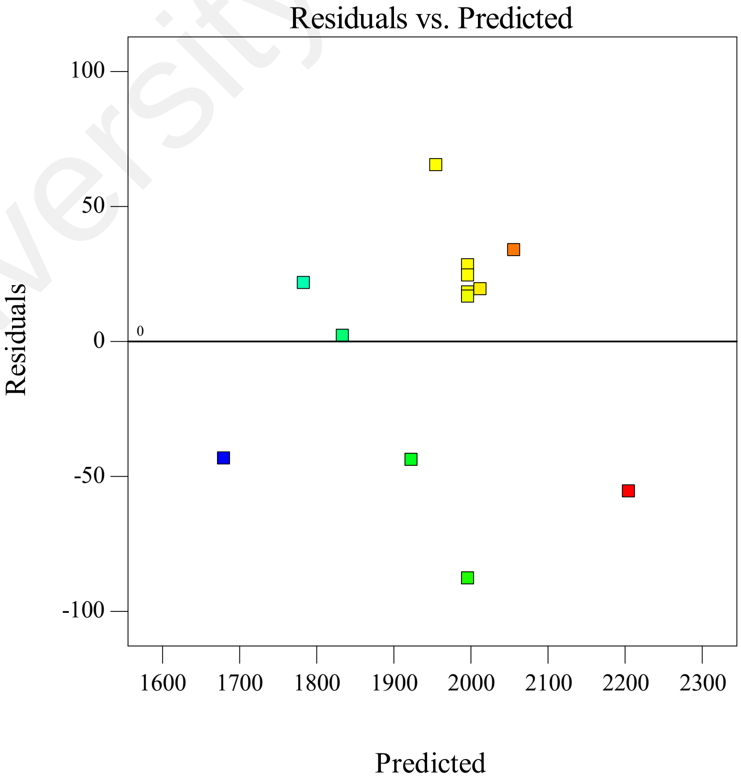

Figure 4.31: Stochastic error for toughness of POM/GF/PTFE composites as residuals versus predicted values

The interaction effects of PTFE content and PTFE etch time on toughness were studied by plotting surface curves. The primary and secondary horizontal axes were the input variables whereas the vertical axis is the toughness. The 3D surface curves and 2D contour plots from the interactions of these variables were obtained. Figures 4.32 and Figure 4.33 show the dependency of toughness on the PTFE content and PTFE etch time. The characteristics of toughness and elongation at break are known to be well correlated. As such, only toughness was considered for the study of mechanical properties of POM/GF/PTFE composite.

Generally, for any given PTFE etch time, toughness steadily increases with increasing PTFE content and highest when the PTFE content was approximately 10%. As the PTFE content was continuously increased, toughness started to deteriorate. At optimum PTFE content of 9.5%, toughness was highest, approximately 2150 kJ/m^3 with PTFE etch time of 5 min. With PTFE constant at 9.5%, toughness gradually decreases as PTFE etch time was increased, reached low of 2000 kJ/m^3 at PTFE etch time of 10 to 14 min before increasing slightly.

The improvement in toughness indicated that there is a synergistic toughening effect of the GF and PTFE on POM. Toughness for polymer composites is affected by the interfacial adhesion between matrix and fiber. Interaction between POM and GF was improved with the addition of PTFE particles, thus facilitating the mobility of macromolecular chains during tensile testing (Gao et al., 2011). However, improvement in toughness was at the expense of reduction in stiffness and hardness. For tensile strength, the stable region of 4% to 10% PTFE content and 8 to 15 min PTFE etch time, resulted in the composites strength not being compromised by toughness. Hence, composites with PTFE content of 9.5% was important because optimum toughness is achieved. Similar to characteristics of strength, this allowed other mechanical properties for the POM composite to be optimized without drastically affecting its toughness.

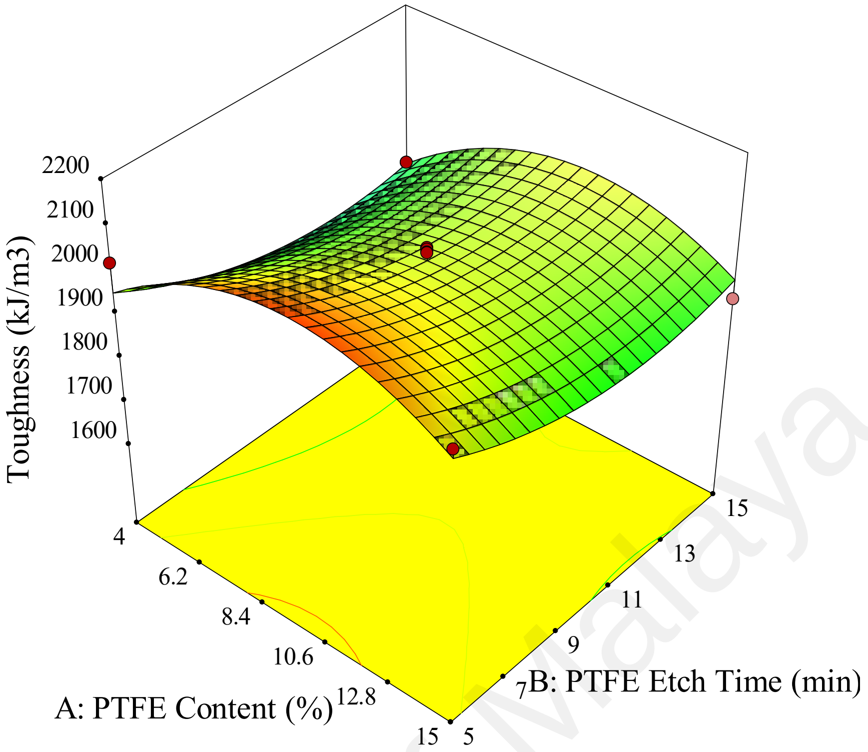

Figure 4.32: 3D response surface plot for the effects of PTFE content and PTFE etch time on toughness of POM/GF/PTFE composites

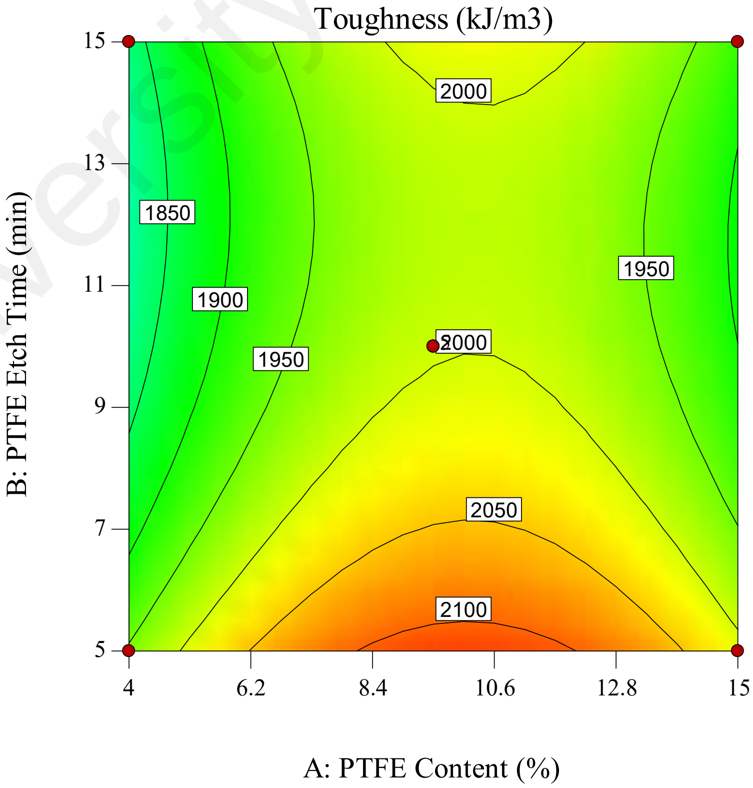

Figure 4.33: 2D contour plot for the effects of PTFE content and PTFE etch time on toughness of POM/GF/PTFE composites

4.3.4 ANOVA and Model Fitting for Hardness of POM/GF/PTFE Composites

Table 4.12 shows the ANOVA table for response surface model for hardness. The F–value of 68.50 implied that the model was significant. There was less than 0.01% chance that an F–value this large could occur due to noise. Values of "Prob > F" less than 0.05 indicate model terms were significant. Values greater than 0.10 indicated the model terms were not significant. The lack–of–fit was also insignificant. The terms A and A^2 were significant for the hardness of POM composites. The coefficient of determination, R^2 of 0.9800 was very close to 1, in agreement that the model comprised of best fit data. The R^2_{adj} value of 0.9657 suggested the model was sufficient without needing to consider additional terms. An adequate precision measures the signal to noise ratio and value of greater than 4 is desirable. The adequate precision value of 26.444 indicated an adequate signal. This model was used to navigate the design space.

Table 4.12: Response surface model ANOVA for hardness of POM/GF/PTFE composites using CCD

Source	Sum of Squares	df	Mean Square	F	Prob. > F	Remarks
Model	15.55	5	3.11	68.5	< 0.0001	significant
A	14.42	1	14.42	317.66	< 0.0001	significant
B	2.20E–03	1	2.20E–03	0.048	0.832	
AB	0.013	1	0.013	0.29	0.6074	
A^2	0.74	1	0.74	16.34	0.0049	significant
B^2	0.24	1	0.24	5.3	0.0549	significant
Residual	0.32	7	0.045			
Lack of Fit	0.016	3	5.42E–03	0.072	0.9719	not significant
Pure Error	0.3	4	0.075			
Cor Total	15.86	12				
R^2, 0.9800; R^2_{adj}, 0.9657; Adequate Precision, 26.444						

The model above was used to predict the hardness of POM composites (Y4) as a function of PTFE content (A) and PTFE etch time (B). It can be presented in terms of coded factors as in the following equation:

$$Y4 = 114.35 - 1.34A - 0.02B + 0.06AB - 0.33A^2 + 0.19B^2 \quad (4.6)$$

The deterministic portion presented as the relationship of actual versus predicted hardness is shown in Figure 4.34. The normal probability plots for residuals and the residuals of the predicted elasticity modulus are shown in Figures 4.35 and 4.36 respectively. Normal probability plot for residuals analyzed the adequacy of the model by evaluating the data applied in the model for hardness. Random and normally distributed residuals indicate none of the predictive information was in the error. The residuals in prediction of response were minimal since they were very close to the diagonal line. Hence, the deterministic portion of the model was good at explaining the hardness with only the inherent randomness was leftover within the error portion (L. Liu et al., 2017). The values of R^2 of 0.9800 and R^2_{adj} of 0.9657 along with the residual analysis adequately fitted the model to experimental data.

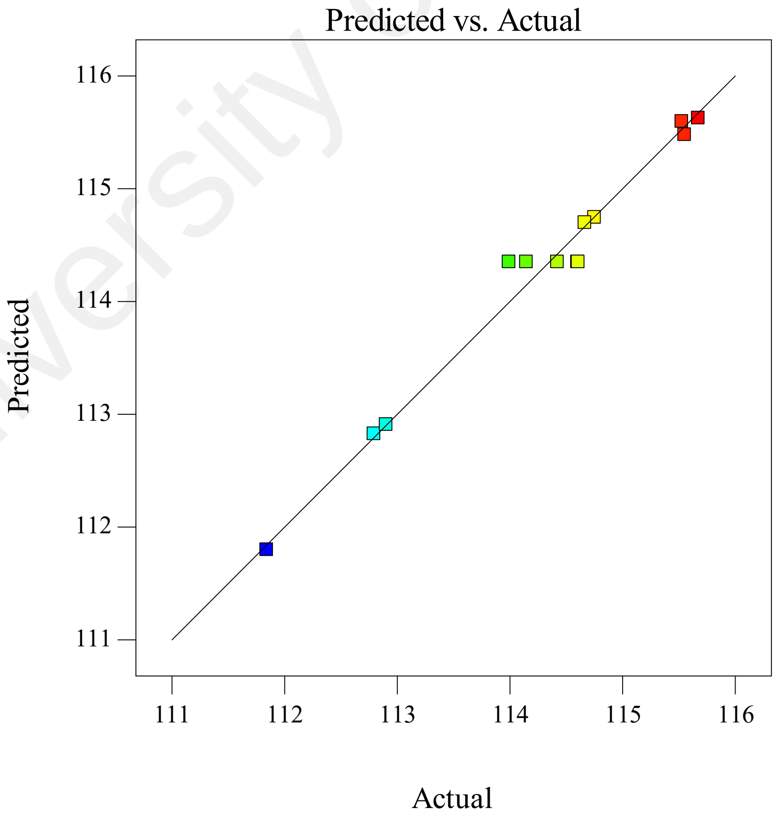

Figure 4.34: Deterministic portion for hardness of POM/GF/PTFE composites as predicted versus actual values

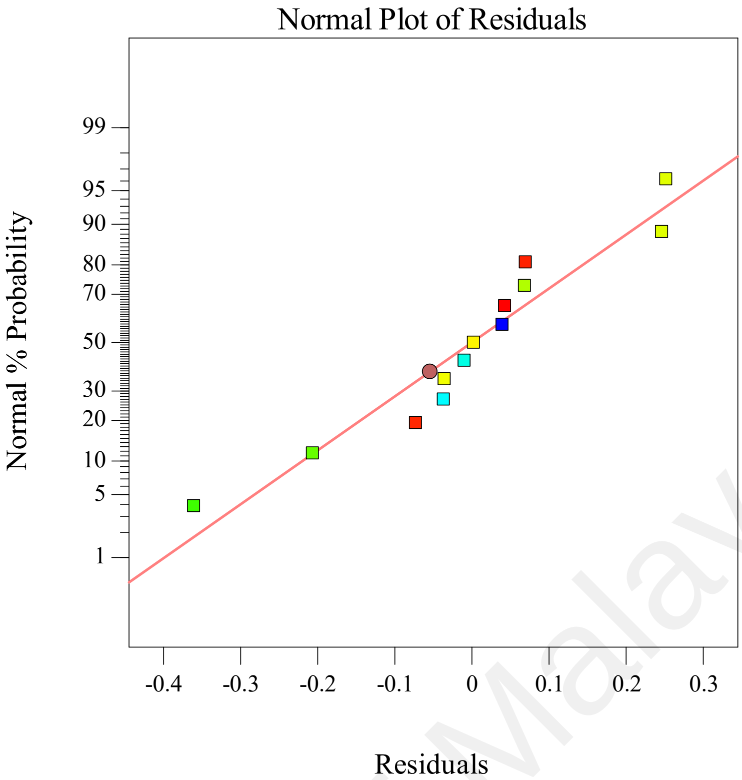

Figure 4.35: Stochastic error for hardness of POM/GF/PTFE composites as normal probability plot for residuals

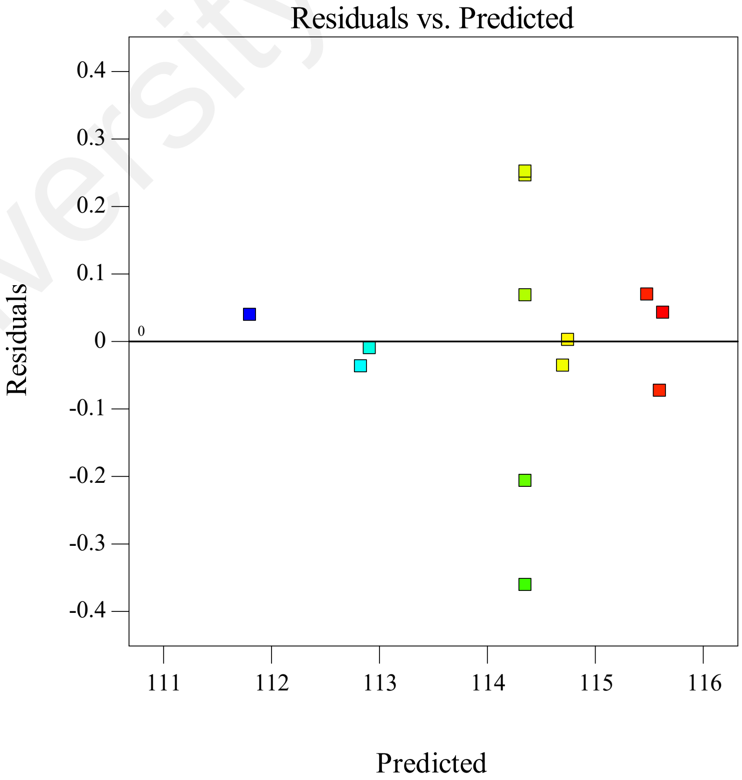

Figure 4.36: Stochastic error for hardness of POM/GF/PTFE composites as residuals versus predicted values

The interaction effects of PTFE content and PTFE etch time on the hardness were studied by plotting surface curves. The primary and secondary horizontal axes were the input variables whereas the vertical axis was the calculated response, i.e. the hardness. The 3D surface curves and 2D contour plots from the interactions of these variables were obtained. Figures 4.37 and 4.38 show the dependency of hardness on the PTFE content and PTFE etch time. Hardness decreased as PTFE content was increased, independent to PTFE etch time. SEM micrographs in Figure 4.19 shows PTFE embedded within POM matrix and surface of GF adhered with the polymeric material. These observations were similar to elasticity modulus where addition of PTFE filler as micro particles weakened the POM/GF/PTFE composites (Sun et al., 2008a).

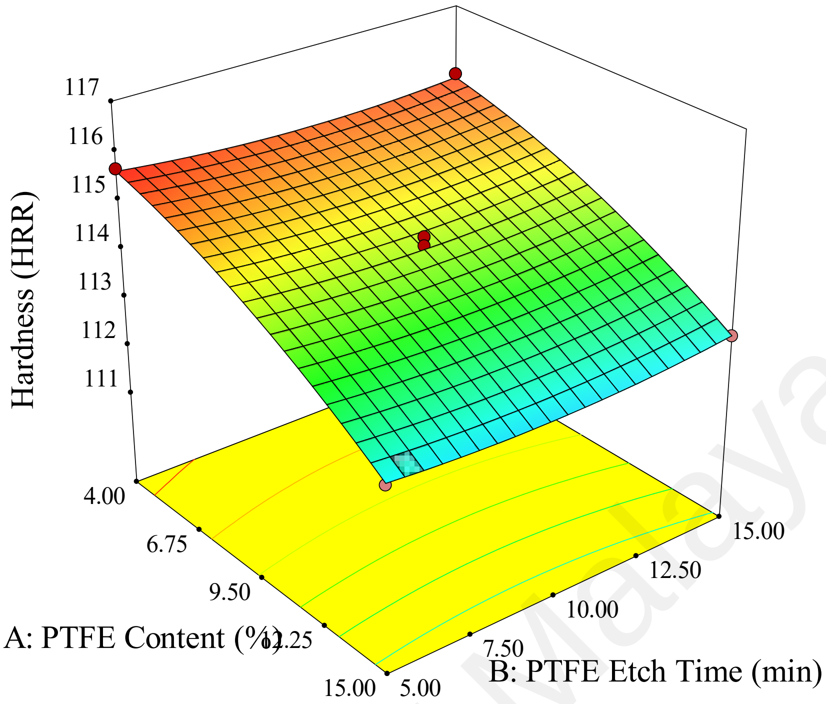

Figure 4.37: 3D response surface plot for the effects of PTFE content and PTFE etch time on hardness of POM/GF/PTFE composites

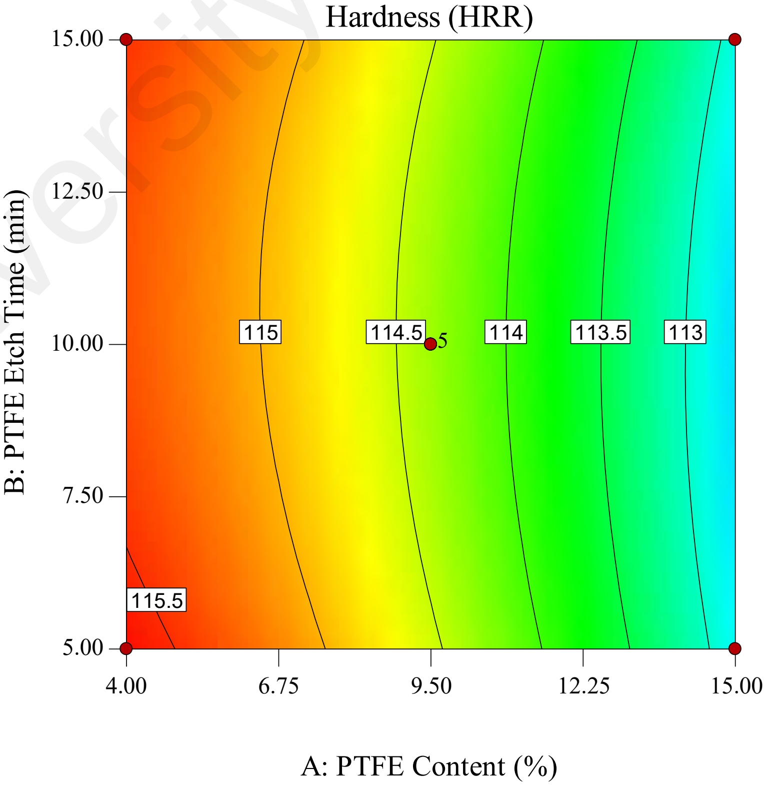

Figure 4.38: 2D contour plot for the effects of PTFE content and PTFE etch time on hardness of POM/GF/PTFE composites

4.3.5 Overall Desirability for Mechanical Properties for POM/GF/PTFE Composites

Analysis of RSM characterized each mechanical property with varying PTFE content and PTFE etch time. For the optimization study of the mechanical properties, the objectives were to simultaneously maximize POM composite's strength, stiffness, toughness and hardness. A useful approach for simultaneous optimization of multiple responses is to use desirability function. To optimize using overall desirability function, it was important to formulate the specification for each of the factors and responses as shown in Table 4.13. Specification for tensile strength and toughness were taken as above median of their respective range and of lower importance. For elasticity modulus, the specification was targeted at 8300 MPa with an importance index of 5. As for hardness, it was targeted at 115 HRR and with importance index of 5. These specifications were selected by referencing to the upper limit of experimental results.

Table 4.13: Specification for factors and responses with weightage and importance

Name	Goal	Lower Limit	Upper Limit	Lower Weight	Upper Weight	Importance	Desirability (d)
A: PTFE Content	In range	4	15	1	1	3	1
B: PTFE Etch Time	In range	5	15	1	1	3	1
Y1: Tensile Strength	Target = 108.0	101.7	111.9	1	1	3	0.8956
Y2: Elasticity Modulus	Target = 8300.0	7802.9	8377.0	1	1	5	0.7797
Y3: Toughness	Target = 2000.0	1636.3	2149.4	1	1	3	0.8274
Y4: Hardness	Target = 115.0	111.8	115.7	1	1	5	1

Figures 4.39 and 4.40 show the overall desirability function applied to multiple responses simultaneously, i.e., tensile strength, elasticity modulus, toughness and hardness. The optimum overall desirability (D) of 87.5% was achieved with PTFE content of 6.5% and PTFE etch time of 10 min. This optimal point of the system attained by geometric mean maximization calculated from the individual desirability (d) for each response shown in Table 4.11.

The obtained values for D and d were found to be close to the optimum condition of 1. This showed that the POM composites were well optimized. Thus, the mechanical properties of POM composites for this optimized condition agreed with the required specification. The tensile strength was 108.4 MPa, elasticity modulus is 8190.5 MPa, toughness is 1937.23 kJ/m^3 and hardness is 115.0 HRR.

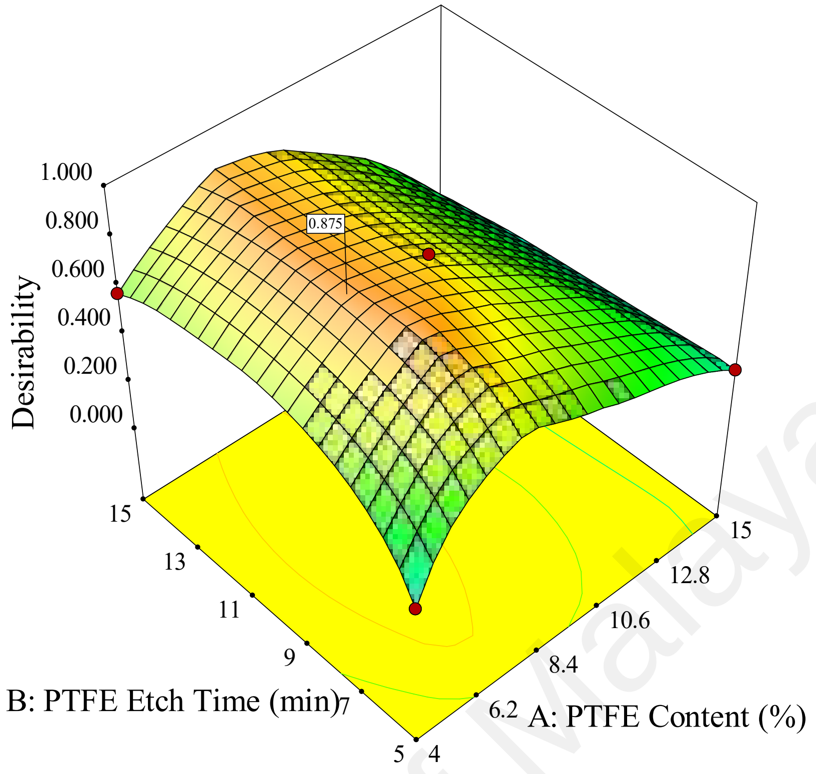

Figure 4.39: 3D response surface plot of desirability function applied to multiple responses

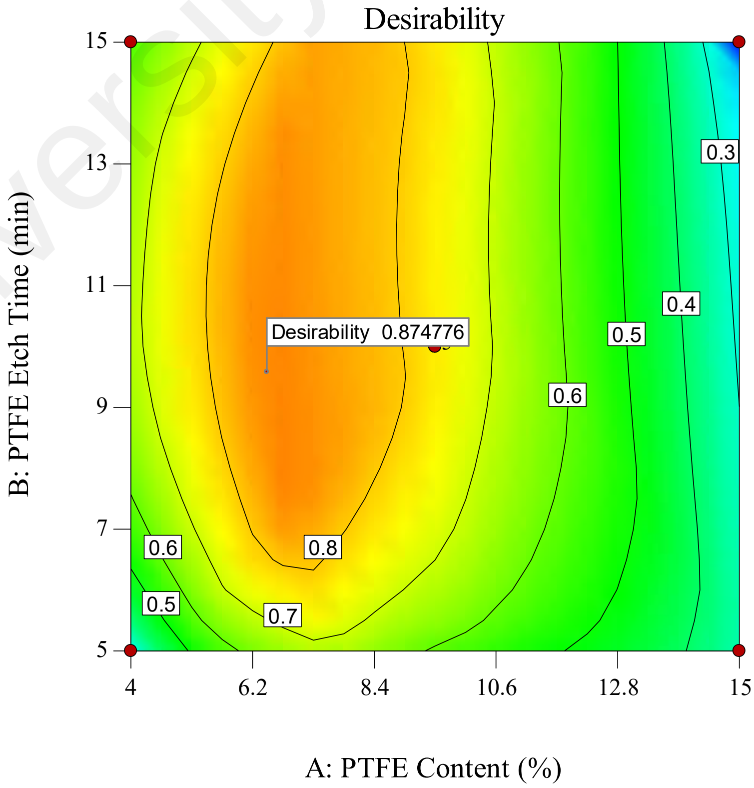

Figure 4.40: 2D contour plot of desirability function applied to multiple responses

4.4 Morphology Analysis using SEM

4.4.1 Surface Microscopy of Etched PTFE

The effects of chemical etching on the PTFE surface studied through SEM using 5200X magnification. The compatibility of POM and PTFE can be increased using this approach. Interfacial adhesion of polymeric material to fillers can provide more insights to mechanical properties for POM/GF/PTFE composites. The surface morphology of PTFE particles etched for 2.9 min, 10 min and 17.1 min shown in Figure 4.41. The surface of 2.9 min etched PTFE was generally smooth and particles appear spherical in shape. With 10 min etch time, the surface appeared to be rougher, indicating the effects of etching. When PTFE was etched for 17.1 min, etch depth increased with porous and cavities on the surface. In addition, PTFE micro particles showed signs of disintegration. The existence of these cavities remains unfilled if the melt polymer is unable to penetrate into these surface imperfections.

Investigations have shown etching depth on the PTFE surface is correlated to the sodium naphthalene etch time. Longer etch time yields highly porous etched layer. Adhesion mechanism to this porous surface is adhesive mechanical interlocking which may cause a bond failure by stripping of the etched layer away (Ebnesajjad, 2015). Hunke et al. (Hunke, Soin, Shah, Kramer, Pascual, et al., 2015; Hunke, Soin, Shah, Kramer, Witan, et al., 2015) reported functional groups in the etched layer were not completely removed even at temperatures more than 300 °C. This enabled use of treated PTFE particles as potential tribological fillers in high temperature engineering polymers.

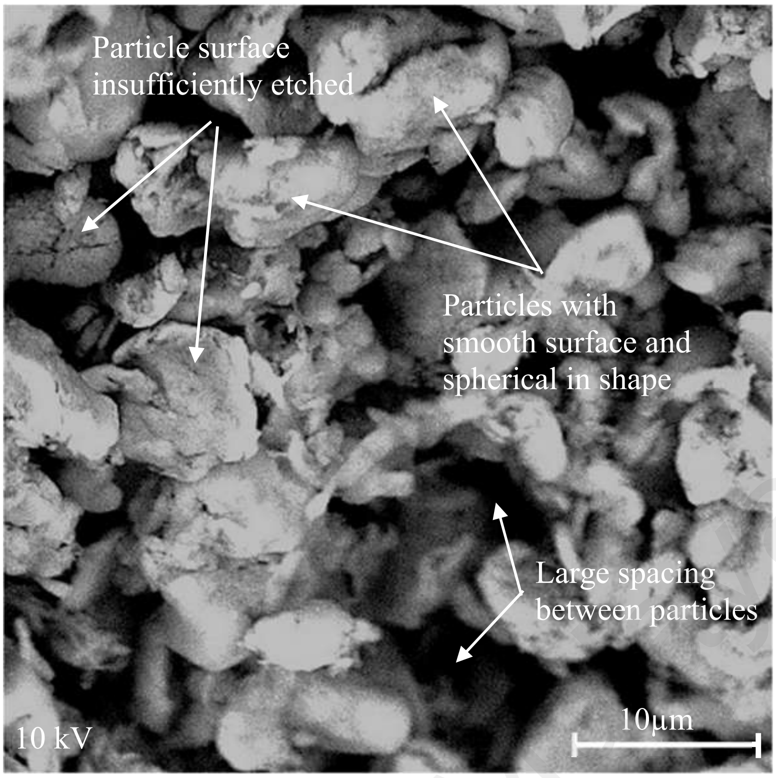
Particle surface insufficiently etched
Particles with smooth surface and spherical in shape
Large spacing between particles
10 kV
10µm

(a)

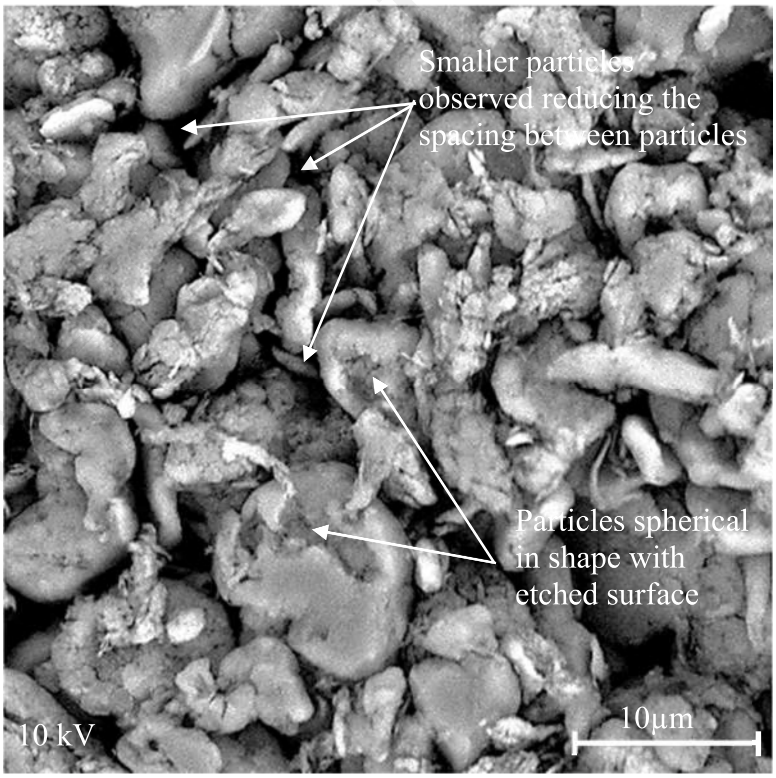
Smaller particles observed reducing the spacing between particles
Particles spherical in shape with etched surface
10 kV
10µm

(b)

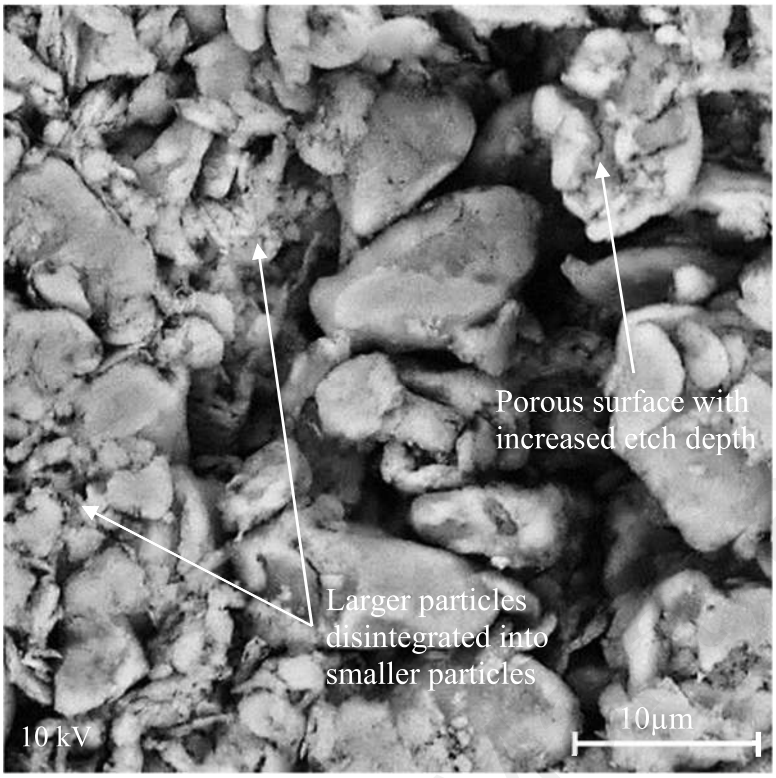

(c)

Figure 4.41: SEM micrographs of PTFE particles etched for (a) 2.9 min (b) 10 min (c) 17.1 min

4.4.2 Morphology of Fractured Surfaces

The fractured surfaces of POM/GF/PTFE composites after tensile testing were characterized through SEM using 1500X magnification. Surface morphology of composites blended with different PTFE content and PTFE etch time revealed information on PTFE interaction with POM and GF. SEM micrographs in Figure 4.42 showed the dispersion of PTFE within POM and adhesion of POM/PTFE to the surface of GF.

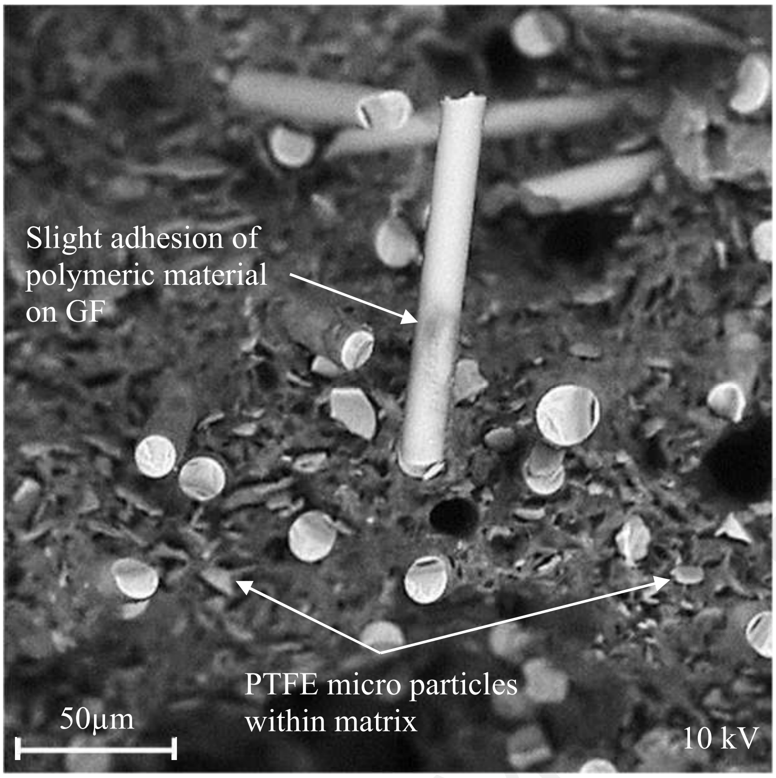
Slight adhesion of polymeric material on GF
PTFE micro particles within matrix
50µm
10 kV

(a)

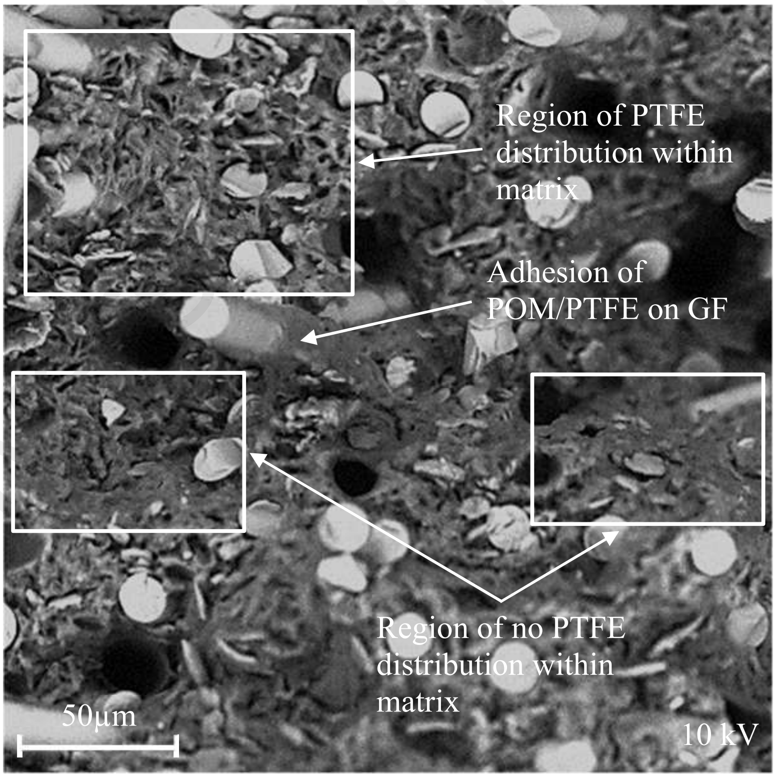
Region of PTFE distribution within matrix
Adhesion of POM/PTFE on GF
Region of no PTFE distribution within matrix
50µm
10 kV

(b)

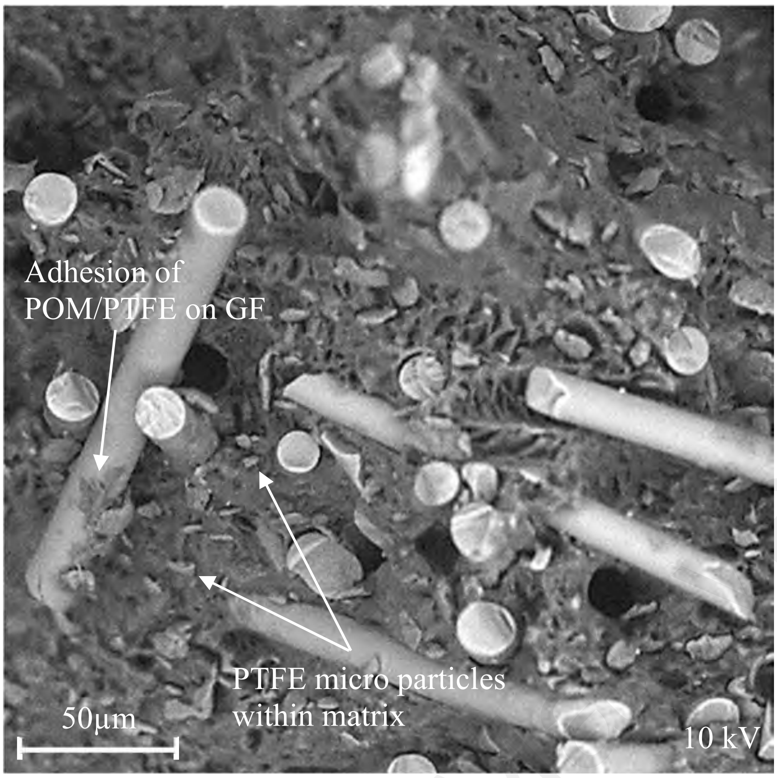

(c)

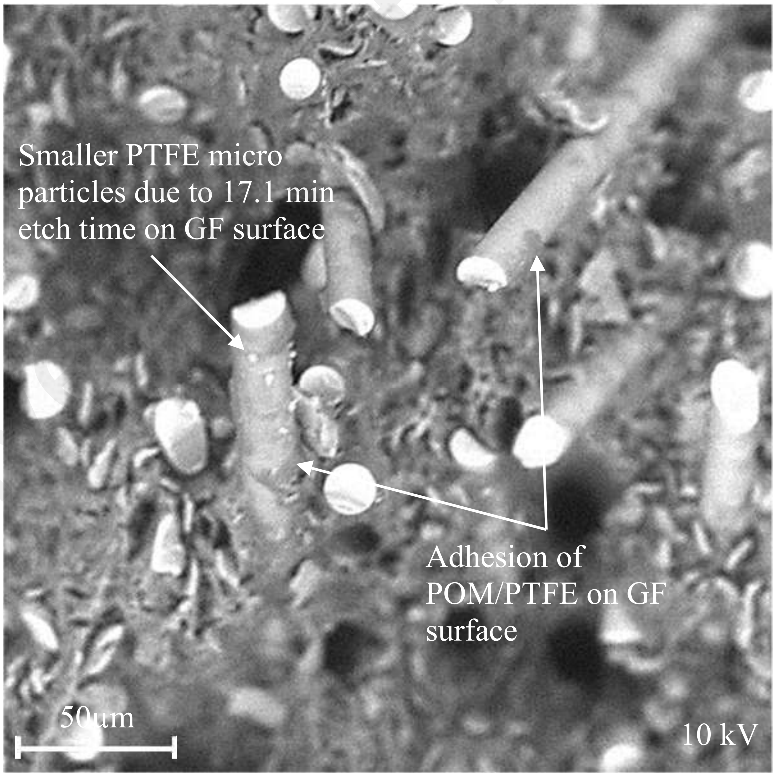

(d)

Figure 4.42: SEM micrographs of fractured surfaces for POM/GF/PTFE composites with (a) 4.0% PTFE etched for 10 min (b) 17.3% PTFE etched for 10 min (c) 9.5% PTFE etched for 2.9 min (d) 9.5% PTFE etched for 17.1 min

Figures 4.42(a) and 4.42(b) show the surface morphology of composites different PTFE contents etched for 10 min. PTFE particles were homogenously dispersed within the POM matrix with 4.0% PTFE content. POM matrix appeared smooth with slight adhesion of polymeric material to GF. Higher PTFE content of 17.3% caused the excessive particles non–homogenous dispersion within the POM matrix. Adhesion of POM/PTFE to GF surface could be observed.

Figures 4.42(c) and 4.42(d) compared the effects of 2.9 min and 17.1 min etch time with 9.5% PTFE content. Adhesion of polymeric material to the surface of GF were comparable. PTFE etched for 17.1 min showed slightly higher concentration of PTFE particles within the POM matrix, possibly as a result of disintegration caused by excessive etching (Figure 4.41(c)). The change of interfacial bonding force between the matrix and fiber weakened the composite causing reduction in both strength and stiffness. Presence of micro–fillers within the matrix is also known to negatively impact the mechanical properties (Sun et al., 2008a). Analysis of tensile properties in the subsequent sections quantitatively validated the morphology studies.

4.5 FTIR Spectroscopy

Morphology analysis of worn surfaces established that micro–PTFE amount and its ability to form a uniform transfer film determined the tribological characteristics. The abrasive GF was effectively coated by a PTFE rich layer. In order to clarify the effects of chemically etched micro–PTFE on tribological properties of POM/GF/PTFE composites, FTIR technique was employed.

4.5.1 Characterization of Surface Etched PTFE

Figure 4.43 shows the effects of chemical etching by comparing non–etched, 10.0 min etched and 17.1 min etched PTFE micro–particles studied using FTIR analysis. In the FTIR spectrograms, consistent absorption bands of 501 cm^{-1}, 554 cm^{-1}, 638 cm^{-1}, 1145

cm^{-1} and 1199 cm^{-1} in the C–F region were observed. The first three wave numbers correspond to CF_2 rocking, CF_2 bending and CF_2 wagging whereas 1145 cm^{-1} and 1199 cm^{-1} attributed to the CF_2 symmetric stretching vibration modes (C. Y. Huang & Tseng, 2000; Liang & Krimm, 1995). Absence of any new absorption bands within the wave number range indicated nucleophilic substitution of fluorine as a result of chemical etching did not occur.

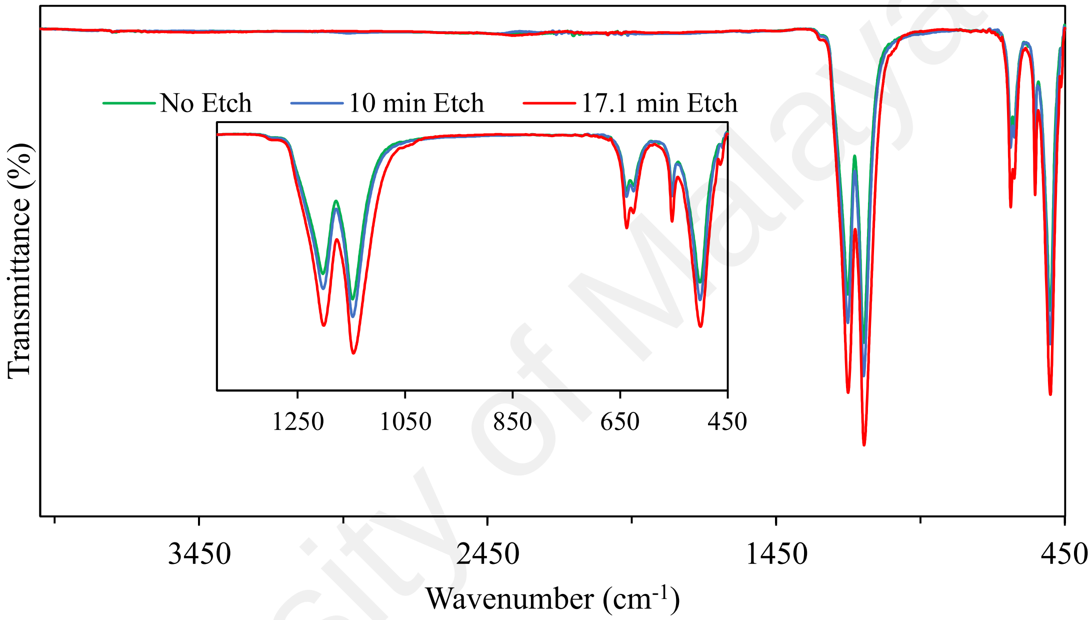

Figure 4.43: Fourier transform infra–red (FTIR) transmittance of PTFE micro particles non–etched, 10.0 min etched and 17.1 min etched

The prolongation of chemical etching led to the increase in the intensity of the absorption bands. The position of these absorption peaks did not shift. These consistent and active centers can be regarded as non–occurrence of PTFE surface oxidation because of chemical etching (Mihály et al., 2006). Surface morphology analysis using SEM revealed formation of rougher and more porous cavities as the etch time was increased. Disintegration of the micro particles were also noticeable (Kunnan Singh, Ching, Abdullah, et al., 2018). These physical changes slightly increased PTFE concentration resulting in the higher intensity of FTIR absorption peaks as a function of etch time. The porous and etched layer promoted mechanical interlocking as the melt blend filled these surface imperfections. Studies performed by Hunke et al. (Hunke, Soin, Shah, Kramer, Pascual, et al., 2015; Hunke, Soin, Shah, Kramer, Witan, et al., 2015) showed functional groups in the etched layer were not removed even at temperature exceeding 300 °C, enabling surface modified PTFE particles to be used as a tribological property modifier in high–temperature engineering plastics.

4.5.2 Characterization of POM/GF/PTFE Composites

In order to study the effects of blending micro–PTFE with POM/GF, FTIR analysis comparing POM/GF/PTFE composites blended with 0%, 9.5% and 17.3% micro–PTFE was performed (Figure 4.44). The spectrum for all three samples exhibited very intense integrated bands at 630 cm^{-1} (CH bending), 887 cm^{-1} (COC symmetric stretching), 1089 cm^{-1} (COC symmetric stretching) and 1236 cm^{-1} (CH_2 rocking). Other peaks, such as 1470 cm^{-1} (CH_2/CH_3 deformation) 2921 cm^{-1} (CH asymmetric stretching), 2978 cm^{-1} (CH_2 asymmetric stretching), attributed to the different vibration modes of groups in the POM chain (Le Roy et al., 2012). For composite samples blended with PTFE, the strong absorption band at 501 cm^{-1} (CF_2 rocking) is assigned to C–F group in PTFE. Absence of new functional groups indicates chemical reaction did not occur. The adhesion mechanism between the polymer melt to chemically etched micro–PTFE was mechanical interlocking, promoted by frictional component as a result of roughened surface.

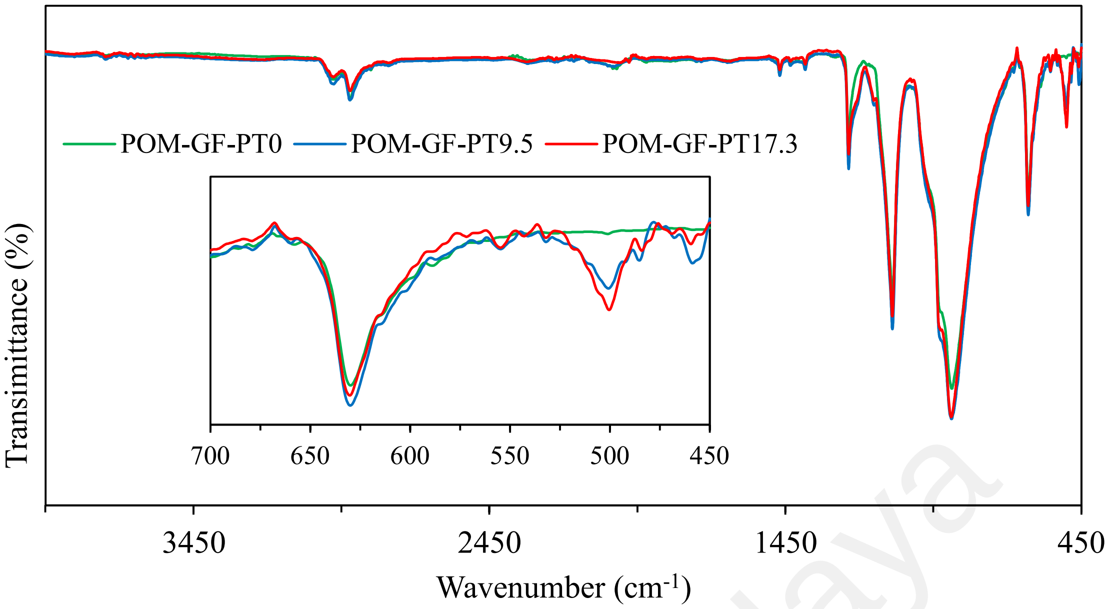

Figure 4.44: Fourier transform infra–red (FTIR) transmittance of POM/GF/PTFE composites blended with 0%, 9.5% and 17.3% PTFE micro particles

4.6 Thermal Properties of POM/GF/PTFE Composites

As observed in Table 4.8, weight fraction of PTFE in the POM/GF/PTFE composites directly influences its strength and stiffness. Morphology analysis (Figure 4.42) showed the non–homogenous distribution of micro–PTFE affected these mechanical properties. In addition, investigation of thermal properties was necessary to further discuss these observations. Thermal analysis was performed on three samples, i.e. POM composites blended with 0%, 9.5% and 15% micro–PTFE chemically etched for 10 min. Reference to Table 4.8, Figures 4.16 and 4.17, the tensile strength and elasticity modulus of these samples were taken as 120 MPa, 108 MPa, 102 MPa and 8500 MPa, 8050 MPa and 7800 MPa.

4.6.1 DSC Analysis

The characteristic of POM melt was investigated to evaluate the effects of micro–PTFE on the crystallinity of POM. The DSC heating and cooling curves are shown in Figures 4.45 and 4.46 whereas Table 4.14 reviews the T_m, T_c and ΔH_m. The values of ΔH_m were normalized to the amount of POM content in the composites.

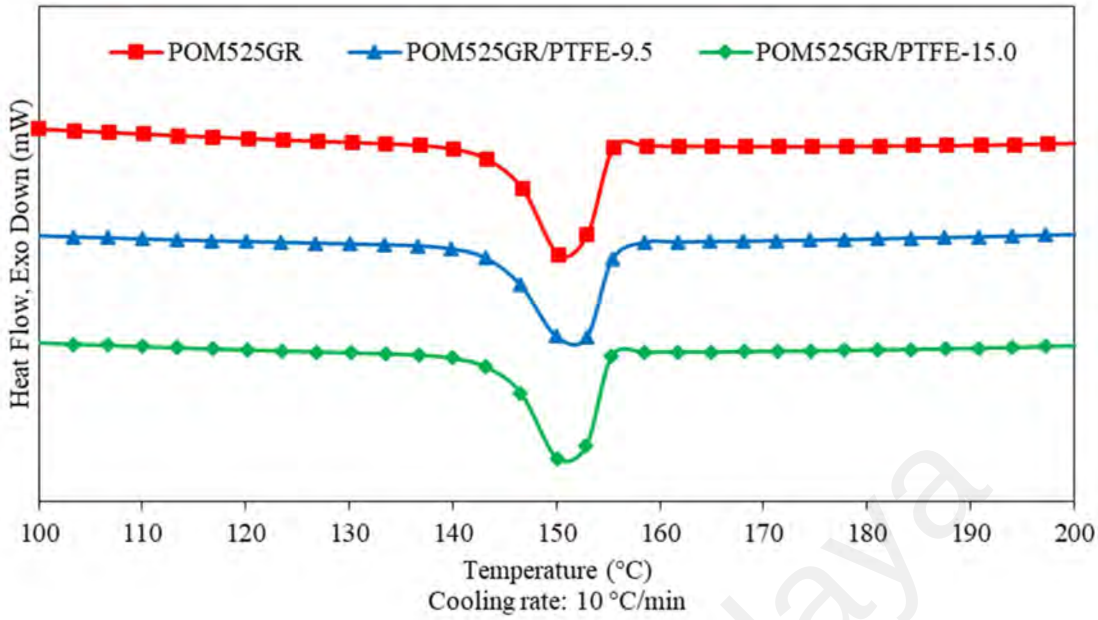

Figure 4.45: Crystallization thermograms of POM/GF/PTFE composites blended with 0%, 9.5% and 15.0% PTFE micro particles using DSC analysis

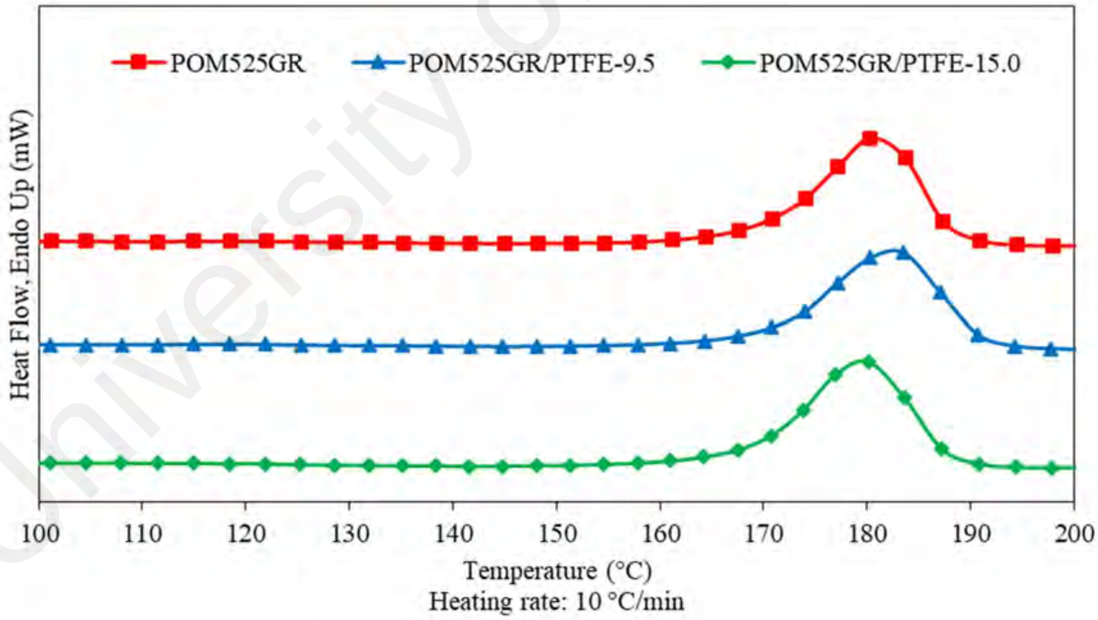

Figure 4.46: Melting thermograms of POM/GF/PTFE composites blended with 0%, 9.5% and 15.0% PTFE micro particles using DSC analysis

Table 4.14: DSC data of melting and crystallization temperature for POM/GF/PTFE composites blended with 0%, 9.5% and 15.0% PTFE micro particles

Sample	Melting temperature, T_m (°C)	Crystallization temperature, T_c (°C)	Enthalpy of melting, ΔH_m (J/g)	Degree of crystallinity, X_c (%)
POM525GR	180.6	151.6	83.4	44.8
POM525GR/ PTFE–9.5	182.9	151.6	74.8	40.2
POM525GR/ PTFE–15.0	179.5	151.7	66.1	35.5

Addition of micro–PTFE showed a peak melting temperature similar to that of neat POM. Examination of heat flows obtained from cooling and heating curves revealed the difference between the samples, especially the enthalpy of melting. The cooling heat flow showed a sharp endothermic signal starting at approximately 155 °C with the same crystallization temperature of 151.6 °C for all samples. The melting heat flow exhibited slightly broader exothermic peak starting at approximately 170 °C. Melting temperature for neat POM of 180.6 °C while for POM composites blended with 9.5% and 15.0% micro–PTFE, the composite melted at 182.9 °C and 179.5°C respectively. The broader melting peak may be arising from pre–melting of crystalline structure which occur at lower temperature that the melting point. Similar observations in the thermograms were reported by other researchers.

The POM525GR exhibited high crystallinity due to excellent structural regularity. DSC thermograms showed ΔH_m of 83.4 J/g and the corresponding crystallinity of 44.8%. With the addition of 9.5% micro–PTFE, the degree of crystallinity declined to 40.2%. Further reduction in crystallinity to 35.5% was observed as the micro–PTFE content was increased to 15.0%. It is deduced that the molecular structure of PTFE interfered in the crystallization of POM resulting in some crystals being disfigured. These results explain the deterioration of mechanical properties as observed in Table 4.8.

4.6.2 Thermal Stability

The thermal stabilities of the POM/GF/PTFE composites were studied by TGA with temperature range from room temperature to 800 °C. Figure 4.47 shows the thermogram of neat POM and its composites with 9.5% and 15.0% micro–PTFE and Table 4.15 summarized the initial 2% weight loss temperature and the rapid weight loss temperature. The latter can be defined as the decomposition temperature, T_d, where a material loses its weight rapidly during the degradation process (Gao et al., 2008). Water was effectively removed from the composites because of the negligible weight loss observed at temperature below than 100 °C.

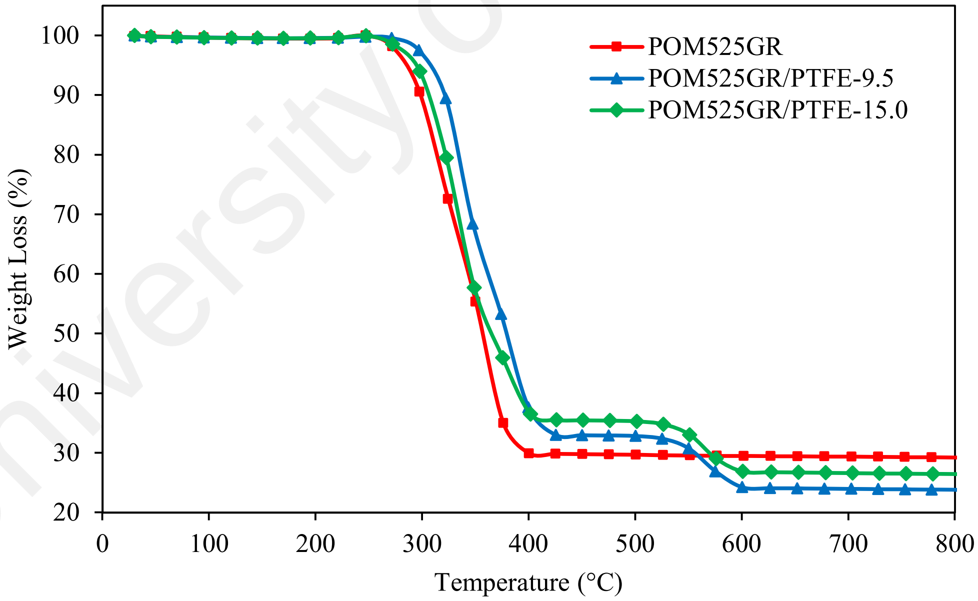

Figure 4.47: TGA of POM/GF/PTFE composites blended with 0%, 9.5% and 15.0% PTFE micro particles

Table 4.15: TGA data of 2% and rapid weight loss for POM/GF/PTFE composites blended with 0%, 9.5% and 15.0% PTFE micro particles

Sample	Temperature at 2 wt.% weight loss (°C)	Temperature at rapid weight loss, T_d (°C)	Char yield at 480 °C (wt.%)	Char yield at 800 °C (wt.%)
POM525GR	272.9	370.0	–	29.2
POM525GR/ PTFE–9.5	293.2	373.3	32.9	23.8
POM525GR/ PTFE–15.0	272.3	362.6	35.4	26.4

The thermal decomposition of neat POM/GF occurred through a one–step degradation. The initial decomposition with 2 wt.% weight loss and rapid weight loss temperatures of 272.9 °C and 370.0 °C respectively is indicative of good thermal stability. The char yield of 29.2% comprised of approximately 25% GF and the remaining weight of decomposed POM. The POM/GF/PTFE composites demonstrated a two–step degradation, where the first step corresponds to the decomposition of POM while the second step is related to the pyrolysis of PTFE and the GF remains, which consist of approximately 25% by wt.%. The addition of 9.5% micro–PTFE resulted in improvement of the decomposition temperatures due to its thermal stability. However, composites with 15.0% micro–PTFE caused slight reduction in the initial decomposition and rapid weight loss temperatures. This may be contributed by the impurities during processing or in the polymer itself.

At the end of first and second degradation steps, the char yield increased as the micro–PTFE content was increased. As expected, the higher char yield during the first step is contributed by the lower POM weight ratio in the composites. The char in the second step, comprising of GF, decomposed POM and PTFE, yielded at 23.8% and 26.4% for composites with 9.5% and 15.0% micro–PTFE, respectively. In general, the impact of blending of micro–PTFE has limited effects to thermal stability and will not restrict the use of POM composites with micro–PTFE in applications requiring high temperatures.

4.7 Tribological Behavior of POM/GF/PTFE Composites

The Ducom tester allowed instant accelerations and decelerations of the steel ball sliding on stationary POM composite samples. The dynamic coefficient of friction was computed as the ratio of friction and normal force measured simultaneously. The reciprocating test set up also permitted concurrent wear loss measurement.

4.7.1 Friction

Tribological properties were remarkably enhanced with the addition of micro–PTFE. The change of frictional coefficient as a function of time for different POM/GF/PTFE composites is shown in Figure 4.48. At the start of testing, a lower frictional coefficient was registered for composites with higher micro–PTFE content. As the test cycles progressed, the composites displayed either an increasing, stable, or slightly decreasing frictional coefficient depending on the amount of micro–PTFE.

Neat POM/GF demonstrated the highest coefficient of friction, that continuously increased throughout the test cycles due to the abrasive GF. A steadily increasing coefficient of friction was also observed for composites with 1.7% and 4.0% PTFE, but at a slower rate compared to neat POM/GF. For composite with 9.5% micro–PTFE, the frictional coefficient stabilized throughout the test. As the micro–PTFE content was further increased to 15.0% and 17.3%, slightly decreasing frictional behavior was observed.

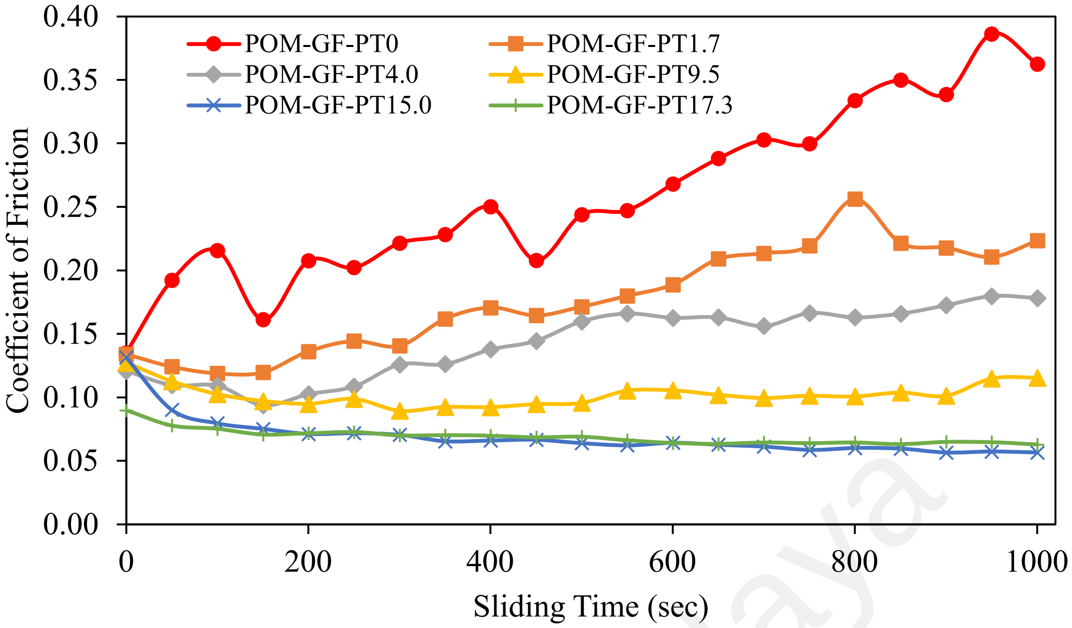

Figure 4.48: Characteristics of frictional coefficient as a function of sliding time for various POM/GF/PTFE composites

The effects of blending PTFE micro–particles in POM/GF matrix to enhance the tribological properties was obvious. As the weight fraction of micro–PTFE was increased, significant reduction of coefficient of friction and wear loss was observed, supporting the fact that PTFE is an efficient solid lubricant. It was also established that addition of PTFE created low friction film between the sliding partners, that reduced the adhesion (Mergler et al., 2004). For the case of neat POM/GF, POM–based transfer film could not form on the steel ball counter face during the sliding action due to the abrasiveness of GF.

4.7.2 Wear Loss

The test set up allowed simultaneous acquisition of wear loss and coefficient of friction over the test cycles. Considering the curved contacting surface of the steel ball, assumptions were made that the wear scars were flat and the depth of these scars were considered a measurement of wear loss. Figure 4.49 displays wear loss as a function of sliding time. The reported data were obtained based on three replicated tests. The cyclic behavior of wear loss profiles might be attributed to several factors, some of which include non–homogenous material properties of POM composites, variation of sample roughness during the reciprocating motion of the stainless–steel ball, and inherent system vibration (Benabdallah & Olender, 2006; Poulios et al., 2014).

Analogous to frictional behavior, the initial wear loss was higher for composites with lower PTFE content. A step increase of wear loss could be observed after 50 sec for POM composites with 0%, 1.7% and 4.0% micro–PTFE. The former two composites also displayed obvious cyclic wear loss pattern. POM composites blended with 9.5%, 15.0% and 17.3% micro–PTFE registered slightly decreasing wear loss trend. After 500 sec, rapid wear loss could be observed for composite with 9.5% micro–PTFE whereas gradual increase was noted for composite with 15.0% micro–PTFE. Further increase in the micro–PTFE content to 17.3% exhibited negligible wear loss throughout the test duration.

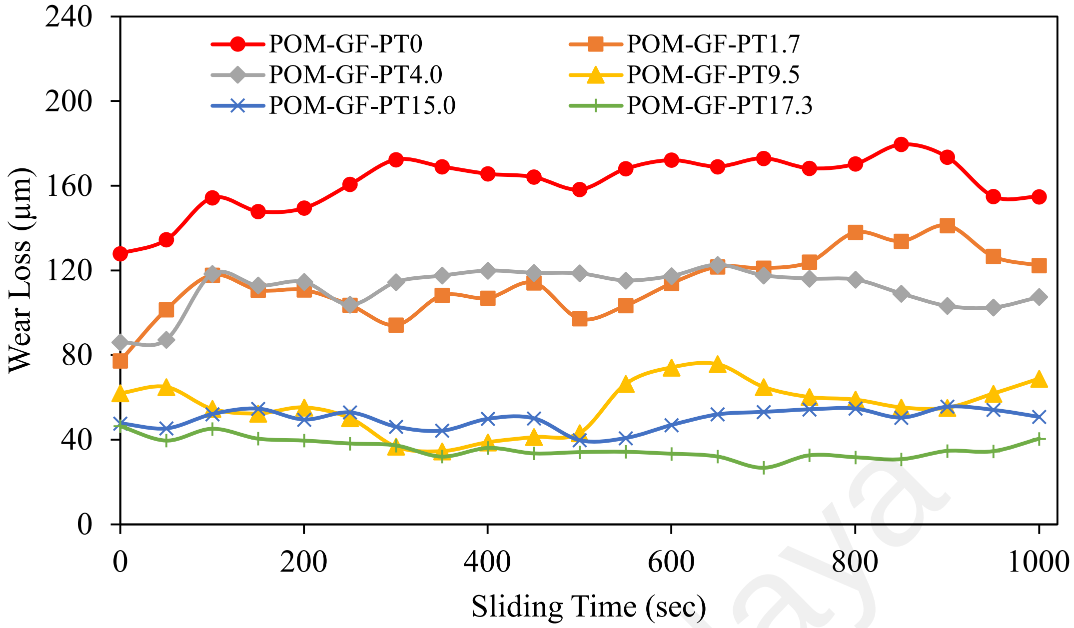

Figure 4.49: Characteristics of wear loss as a function of sliding time for various POM/GF/PTFE composites

Reduction of wear loss was clarified by the improved lubricating properties, attributable to the PTFE micro particles. Transfer film formed between the POM/GF/PTFE composites and steel ball during the reciprocating motion. As the PTFE content was increased, this transfer film repaired the worn surfaces resulting in either minimal or stable wear loss. This is witnessed by the SEM micrographs in Figures 4.51(d), 4.51(e) and 4.51(f) for the composites with 9.5%, 15.0% and 17.3% micro–PTFE respectively. Furthermore, chemical etching of micro–PTFE particles roughened the surface and possibly increased its surface energy. The PTFE rich wear debris effectively filled the scratches, forming an even and dense transfer film. This resulted in better interaction between the transfer film and counter surface, eventually reducing the coefficient of friction and wear loss (L. Zhang et al., 2017).

4.7.3 Optical microscopy of POM/GF/PTFE worn surfaces

Figure 4.50(a)–(f) illustrates the wear morphologies of neat POM/GF and POM/GF/PTFE composites with different composition of micro–PTFE. The PTFE micro particles influenced the morphology of worn surfaces significantly. As depicted in Figure 4.50(a), deep scratch grooves can be observed in the sliding direction due to abrasiveness of GF. In addition, surface cracks in normal direction to sliding because of adhesive wear was visible for the neat POM/GF. The composites containing lower micro–PTFE (Figures 4.50(b), 4.50(c) and 4.50(d)) exhibited obvious wear scars compared to composites with higher PTFE content (Figure 4.50(e)–(f)). Exposed GF on the worn surfaces was obvious for the neat POM/GF and composites with lower PTFE composition.

The formation of a PTFE–based transfer film is represented by the density of white regions on the worn surfaces. As presented in Figure 4.50(b)–(f), the spots of white areas were the flattened peaks whereas the dark regions are valleys that formed surface asperities. Shear in the contact between the steel ball and composite sample during sliding caused wear debris to fill up the valleys. This led to the formation of a patchy transfer film for POM composites blended with 1.7%, 4.0% and 9.5% and a more homogenous film for composites with higher micro–PTFE composition.

As the weight percentage of micro–PTFE was increased, the transfer film encapsulated GF surface along the sliding path. Formation of thicker transfer film resulted in wear loss reduction. The transfer film effectively concealed the valleys and encapsulated the GF, preventing asperities from further damaging the composite material. As noted in Figures 4.50(e) and 4.50(f), continuous and coherent transfer films were formed for composites blended with 15.0% and 17.3% micro–PTFE. These observations explain the lower coefficient of friction and wear loss during tribology testing.

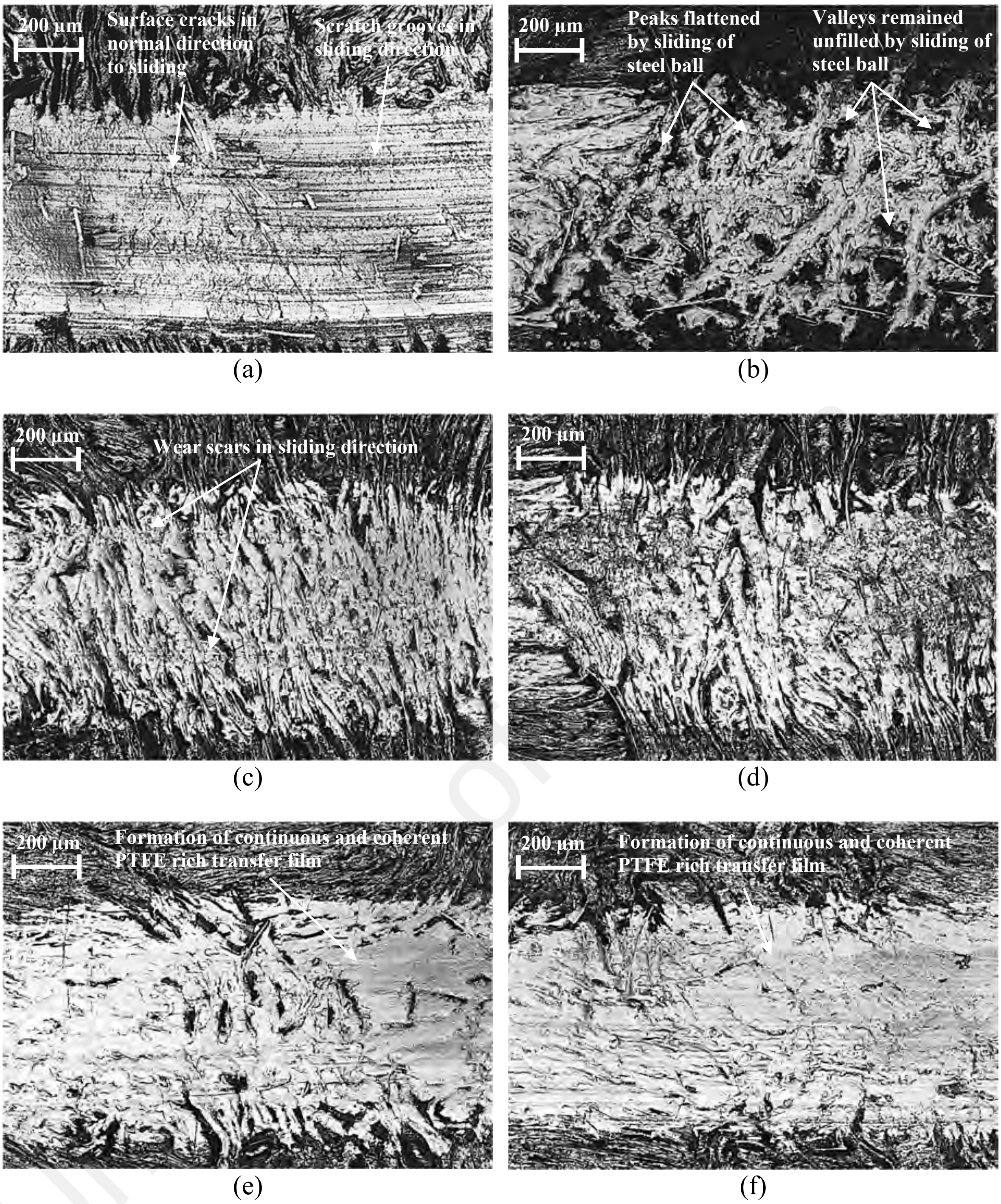

Figure 4.50: Optical micrographs of POM/GF/PTFE composites worn surfaces after tribology test: (a) Neat POM525GR; (b) POM–GF–PT1.7; (c) POM–GF–PT4.0; (d) POM–GF–PT9.5; (e) POM–GF–PT15.0; (f) POM–GF–PT17.3

Based on the optical micrographs of neat POM/GF, absence of PTFE in the composite and the abrasive GF prevented formation of a homogenous transfer film to facilitate steady lubricating conditions. Black areas surrounding the exposed GF might be caused by damaged polymeric carbon chain due to high pressure and temperature. These conditions caused sharp increase of frictional coefficient as the sliding cycles progressed.

Addition of micro–PTFE produced more wear debris that filled up surface asperities represented as the dark regions (Myshkin et al., 2015).

4.7.4 SEM microscopy of POM/GF/PTFE worn surfaces

Figure 4.51(a)–(f) shows the SEM images of worn surfaces for neat POM/GF and its composites. For the neat POM/GF (Figure 4.51(a)), continuous reciprocating rubbing of steel ball with high contact pressure caused the GF to be damaged. Fragments of GF, observed as white specks on the SEM micrographs, were generated. These fragments were not only present at the vicinity of GF, but also carried slightly further away from the GF. Similar to optical images, many scratch grooves were observed parallel to sliding direction. These scuff marks can be seen originating from the damaged GF. The surface temperature increased as a result of friction heat generated during the sliding motion, causing adhesive wear and plastic deformation. High shear stress destroyed the POM, forming surface cracks in the normal direction of sliding. Consequently, both coefficient of friction and wear loss continuously increased.

With the addition of micro–PTFE, stable rubbing conditions were facilitated through formation of a PTFE–based transfer film. As the micro–PTFE content was increased, the tribo–contact surfaces demonstrated capability to self–repair. The composite blended with 17.3% PTFE (Figure 4.51(f)) displayed the smoothest surface after test. The GF and its fragments were fully embedded in the matrix. For composites with lower PTFE content of 1.7% and 4.0% (Figure 4.51(b)–(c)), damage regions around the GF remain unrepaired. Formation of an effective transfer film was prevented at these regions due to the abrasiveness of GF and insufficient PTFE. The composites blended with 15.0% and 17.3% micro–PTFE (Figure 4.51(e)–(f)) exhibited a uniform PTFE rich layer, effective to endure the scrapping of hard GF and its fragments. The formation of a smooth surface exhibited low frictional coefficient and wear loss. As shown in Figures 4.48 and 4.49, the composites comprising of high PTFE content demonstrated self–repairing capability.

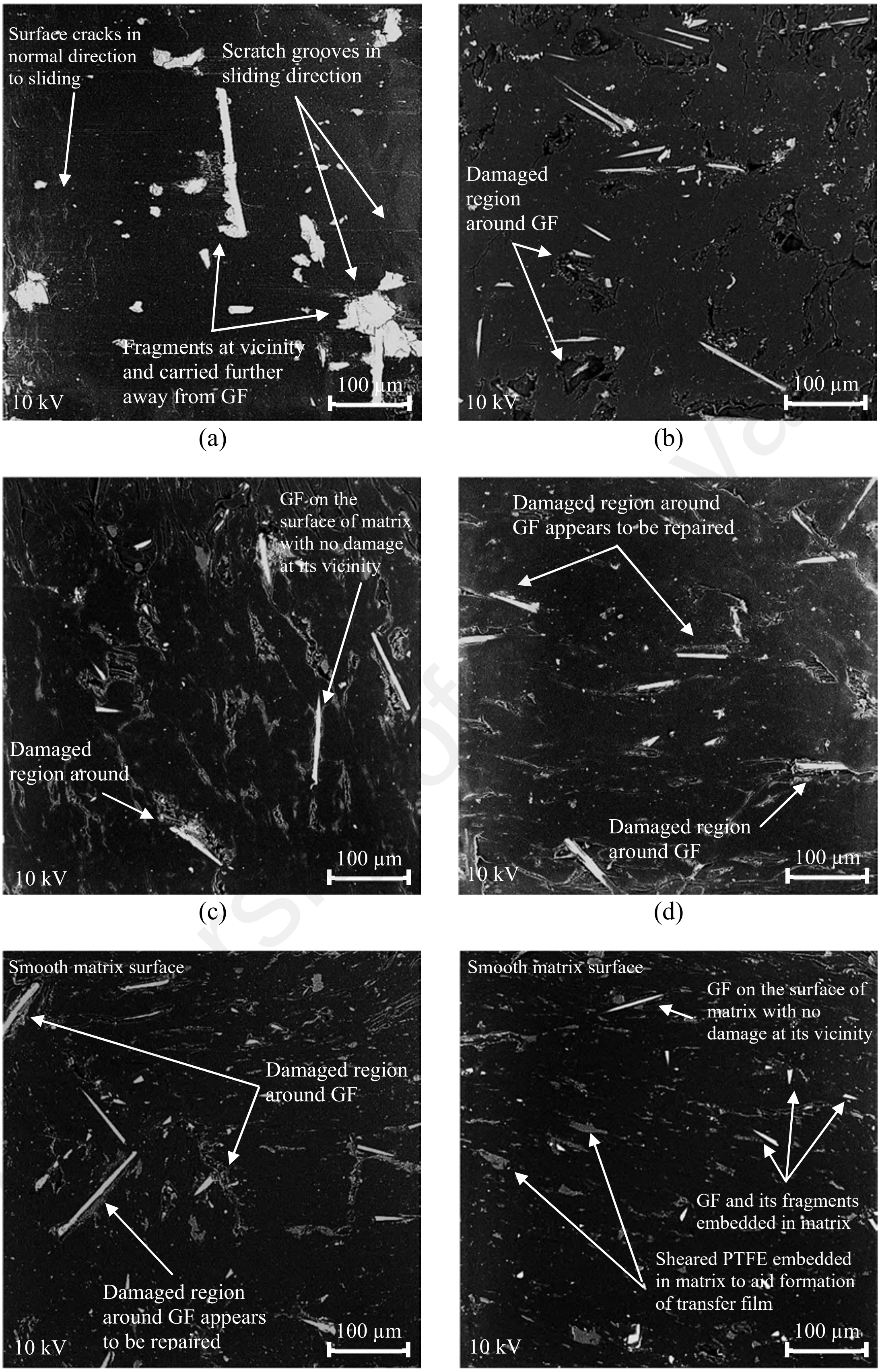

(a) (b)

(c) (d)

(e) (f)

Figure 4.51: SEM micrographs of POM/GF/PTFE composites worn surfaces after tribology test: (a) Neat POM525GR; (b) POM–GF–PT1.7; (c) POM–GF–PT4.0; (d) POM–GF–PT9.5; (e) POM–GF–PT15.0; (f) POM–GF–PT17.3

The composite with 9.5% micro–PTFE formed a relatively smooth surface (Figure 5d). The transfer film effectively coated some of the GF while not on others. The coefficient of friction and wear loss remained stable up to 500 sec into the test before increasing from its steady state condition. It is known that addition of PTFE reduces the strength and stiffness of these composites. Optimal mechanical properties were obtained by blending POM/GF with 6.5% PTFE by weight percentage (Kunnan Singh, Ching, Abdullah, et al., 2018). In applications where both mechanical and tribological properties are of equal importance, the PTFE amount can be a vital determination factor in order to satisfy the requirement.

PTFE easily shears to form transfer films due to its molecular structure, resulting in its superior self–lubricating properties. This is caused by the weaker van der Waals force between its molecular chains than the intramolecular bonds. SEM micrographs revealed self–repairing capability of the damaged surfaces because an even and tenacious transfer film was formed. The surface, comprising of POM and GF, was coated by this transfer film from direct counterface contact. The wear mechanism was both abrasive and adhesive, whereby, mainly abrasive for composites with none or lower PTFE content and primarily adhesive when the composites were blended with higher PTFE amount. Consequently, the characteristics of frictional coefficient and wear loss correlated well to the weight percentage of micro–PTFE.

4.8 Mapping of Fiber–Matrix Interface Region

The polished specimens containing 1.7%, 9.5% and 17.3% micro–PTFE were examined using SEM under 15,000× and elemental analysis using EDS. As shown in Figure 4.52 and Figure 4.53, mapping of the composite phases and interface evaluation were carried out on the basis of quantifying weight percentage of fluorine atoms at 0.5 μm intervals away from the GF surface. All composites displayed gradual increase of fluorine atom fraction further away from GF edge. Composites blended with higher amount of micro–PTFE revealed higher concentration of fluorine atoms. This greatly enhanced the tribological performance by enabling formation of PTFE based transfer film.

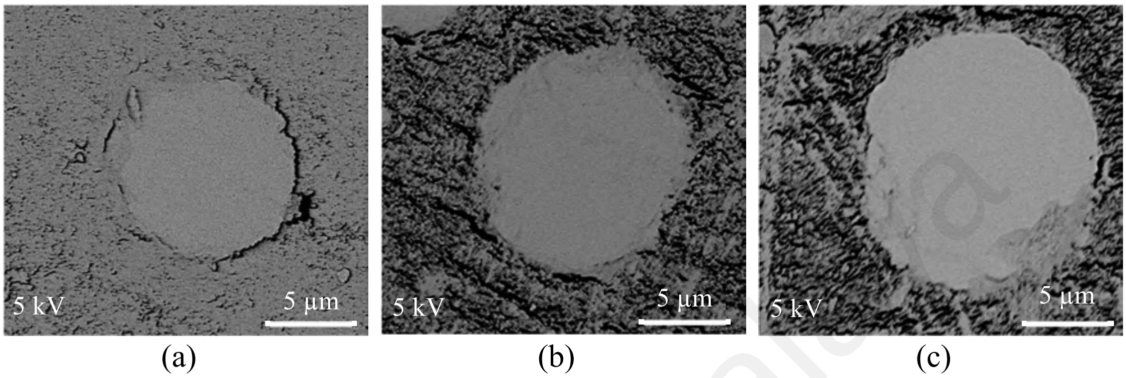

(a) (b) (c)

Figure 4.52: SEM micrographs of the interface and points for elemental analysis using EDS: (a) POM–GF–PT1.7; (b) POM–GF–PT9.5; (c) POM–GF–PT17.3

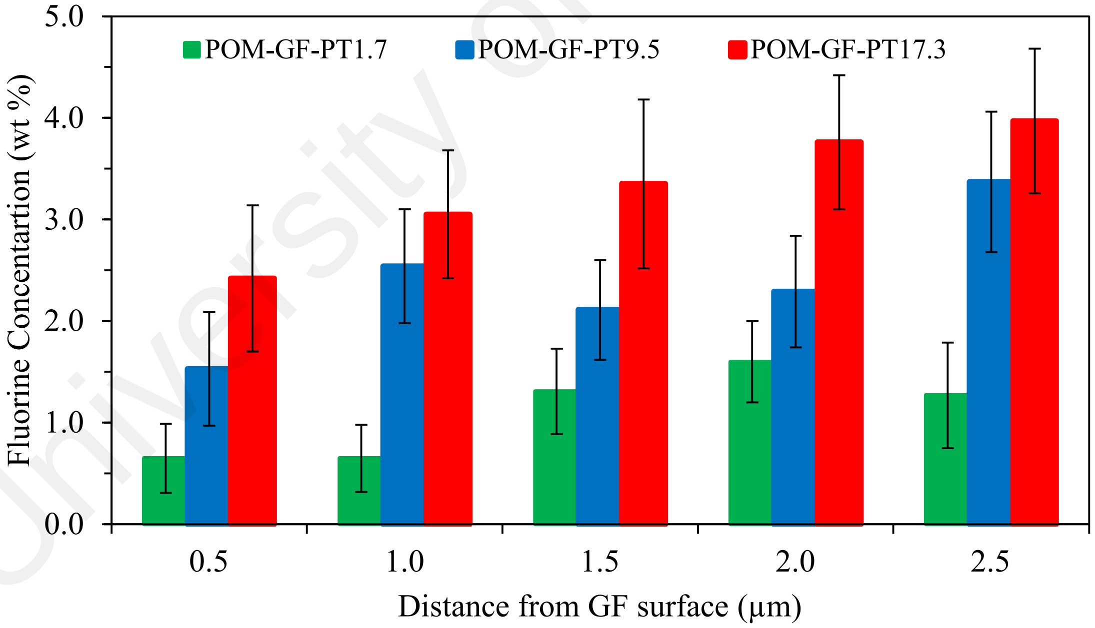

Figure 4.53: Weight percentage of fluorine atoms as a function of distance from GF surface

Fiber–matrix interface mapping using SEM–EDS method is unable to ascertain a sharp matrix–fiber interface nor determine interphase dimension. However, it is adequate to establish the presence of PTFE at the interface region of fiber–matrix, altering the tribological properties of POM/GF/PTFE composites. Several researchers (Graupner et al., 2014; Olmos et al., 2012; Schöneich et al., 2015) have studied the interphase thickness and identified a value of between 0.03 µm and 3 µm, dependent upon fiber fraction, type of matrix material and methods used. Experimental techniques of higher precision progressively decrease the interphase thickness.

CHAPTER 5: CONCLUSIONS AND FURTHER WORK

5.1 Conclusions

This study was performed to evaluate the effects of chemically etched PTFE micro particles on mechanical and tribological properties of POM/GF/PTFE composites. Samples were prepared using plastic injection moulding process. The process parameters that affect the tensile strength and elasticity modulus were identified and optimized via DOE methodology. The beneficial effect of blending PTFE micro particles to POM/GF matrix was the enhanced tribological performance without compromising its mechanical properties. The following conclusions can be drawn from this current work.

The injection moulding process parameters that affected tensile strength were barrel temperature, injection speed and injection pressure into the mould. In addition, interactions of plasticizing pressure–injection speed and plasticizing pressure–screw speed influenced tensile strength. This was evident from the ANOVA and model fitting analysis resulting in coefficient of determination, R^2 of 0.9746 and R^2_{adj} of 0.9047. Error analysis showed random and normally distributed residuals. This confirmed none of the predictive information were in the error.

For elasticity modulus, barrel temperature, injection pressure and holding pressure were dominant. In addition, interactions of plasticizing pressure–injection speed, plasticizing pressure–holding pressure, screw speed–injection speed and screw speed–holding pressure also influenced the stiffness. This was evident from the ANOVA and model fitting analysis resulting in coefficient of determination, R^2 of 0.9792 and R^2_{adj} of 0.8962. Random and normally distributed residuals confirmed none of the predictive information were in the error.

Desirability method was applied to determine the optimum specification of the injection moulding process parameters to obtain highest tensile strength and elasticity modulus. A desirability index, D of 94.3% was obtained by controlling the plasticizing pressure to 1 MPa, screw speed to 170 rpm, barrel temperature to 180 °C, injection speed to 100 mm/s, injection pressure to 14 MPa and holding pressure to 12 MPa. Based on these parameters, tensile strength of 125.9 MPa and elasticity modulus of 8632 MPa were achieved. Both of these mechanical properties were approximately 5% and 0.2% of the maximum value obtained from the DOE runs.

As PTFE is known to weaken polymer composite's strength and stiffness due to its low surface energy, chemical etching using sodium naphthalene salt dissolved in tetrahydrofuran was necessary to improve its compatibility to POM/GF matrix prior to blending. SEM micrographs showed good correlation between etch time to etched depth on the surface of PTFE particles. Etch time of 2.9 min revealed smooth surface morphology whereas highly porous and coarsely etched layer was observed with etch time of 17.3 min.

FTIR analysis comparing non-etched, 10 min and 17.3 min etched micro–PTFE displayed no formation of new absorption bands indicating nucleophilic replacement of fluorine in the PTFE chain did not occur. In addition, the effects of chemically etched micro–PTFE blended with POM/GF matrix were carried out using FTIR analysis. As expected, absence of new functional group indicated the bond between POM and PTFE was strictly mechanical interlocking as the melt filled surface imperfections of micro–PTFE.

The mechanical and tribological properties of POM/GF/PTFE composites were optimized by varying PTFE content and PTFE etch time. Therefore, PTFE content and PTFE etch time were important factors in determining mechanical properties of POM/GF/PTFE composites. RSM in conjunction with CCD was used to model the effects of these factors on the strength, stiffness, toughness and hardness of POM/GF/PTFE composites. Using experimental data and ANOVA, mathematical model was derived for each response. The normal probability test, significance test and correlation coefficients determined the significance of fit between the model and experimental data.

To optimize tensile strength, elasticity modulus, hardness and toughness simultaneously, each property was specified and desirability function was derived. The overall desirability or D global index for the mechanical properties of POM/GF/PTFE composite was 87.5% when PTFE content and PTFE etch time were 6.5% and 10 min respectively. The individual desirability index, d for tensile strength was 89.6%, elasticity modulus at 78.0%, toughness at 82.7% and hardness at 100%.

A contour plot for the overall desirability showed a wide region of 80% when the PTFE content ranged from 5.0% to 8.0% and PTFE etch time ranged 8 min to 13 min. This stable region is important to determine the range of PTFE content and PTFE etch time that would affect the mechanical properties of POM/GF/PTFE composite when optimizing tribological properties.

Morphology study of fractured surfaces during tensile testing revealed the effects PTFE content and PTFE etch time to matrix and GF. The polymeric material adhesion to GF affected the interfacial bond. As a result, strength, stiffness and hardness were compromised but toughness improved. The altered GF surface can be an enabler for applications requiring polymer composites with superior strength and tribological properties.

DSC analysis showed degree of crystallinity for neat POM/GF and its composites with 9.5 wt.% and 15.0 wt.% micro–PTFE were 44.8%, 40.2% and 35.5% respectively. These values correlated to tensile strength of 120 MPa for neat POM/GF, 108 MPa for POM/GF/PTFE composite blended with 9.5 wt.% micro–PTFE and 102 MPa for

POM/GF/PTFE composite blended with 9.5 wt.% micro–PTFE. TGA analysis revealed the impact of blending PTFE micro particles had negligible effects on the thermal stability of POM/GF/PTFE composites. Hence, this will not restrict the use of POM/GF/PTFE composites in applications requiring higher temperatures.

Friction and wear behavior of POM composites filled with GF and PTFE micro particles were comprehensively investigated. In particular, the mechanism of PTFE to effectively enhance tribological properties through transfer film formation. In the absence of PTFE, stress induced during reciprocating motion fractured the GF, inducing damage to the POM surface. Based on SEM micrographs of worn surfaces, the abrasive GF prevented formation of POM–based transfer film. Addition of PTFE greatly enhanced the tribological properties through formation of PTFE–based transfer film that was capable of enduring the scraping of GF. The worn surfaces, as a result of abrasive and adhesive wear, were self–repaired as the PTFE content was increased.

Fiber–matrix mapping technique using FESEM–EDS was neither able to ascertain a sharp interface nor determine the interphase dimension. However, this technique adequately established the presence of PTFE at the interface region of fiber–matrix. This higher concentration of fluorine atoms for composites blended with higher micro–PTFE weight fraction confirmed the behavior of tribological properties. The concentration of PTFE, detected as fractions of fluorine atoms, at the fiber–matrix interface region, gradually increased from to the GF surface.

In conclusion, the objectives of this research were achieved. Addition of PTFE micro particles enhanced the tribological performance of POM/GF/PTFE composite without compromising its mechanical properties. At the same time, it was found that the use of micro–sized particles was a good choice as higher concentrations could be added to the matrix to obtain the required tribological properties without significantly impacting the composite's strength and stiffness.

5.2 Further Work

Below are some suggestions for further work to be done:

1. The use of plasma treatment or electron beam irradiation for PTFE micro particles' surface modification to enhance its free surface energy. Low pressure 2.45 GHz microwave plasma using hydrogen and ammonia as process gases is able to impart functional polar groups on PTFE surface. Another process to modify surface properties of PTFE is by pure hydrogen sulfide gaseous plasma sustained by a radio frequency discharge. These techniques successfully impart new functional groups to increase interaction between PTFE and matrix.
2. Measure effectiveness of chemical etching using X–ray photoelectron spectroscopy (XPS) or electron spectroscopy for surface analysis (ESCA). The disappearance of fluorine peaks and detection of oxygen or other peaks provide quantifiable measurements for the etching efficiency.
3. Interphase mapping using a more sophisticated method such as nano–imaging technique. The key feature of the specimen is a unidirectional GF orientation in the measurement section. The surface preparation requires grinding using silicon carbide (Si–C) with a grain size of 600 to 1200 followed by polishing using alumina nano or micro particles. Nano scratch can be performed using a high precision nano–indenter such as Hysitron TI 900 TriboIndenter.

REFERENCES

Akil, H. M., Omar, M. F., Mazuki, A. A. M., Safiee, S., Ishak, Z. A. M., & Abu Bakar, A. (2011). Kenaf fiber reinforced composites: A review. *Materials & Design, 32*(8-9), 4107-4121.

Anderson, M. J., & Whitcomb, P. J. (2015). *DOE Simplified: Practical Tools for Effective Experimentation.* New York, USA: CRC Press.

Arao, Y., Yumitori, S., Suzuki, H., Tanaka, T., Tanaka, K., & Katayama, T. (2013). Mechanical properties of injection-molded carbon fiber/polypropylene composites hybridized with nanofillers. *Composites Part A: Applied Science and Manufacturing, 55*, 19-26.

Archodoulaki, V. M., Lüftl, S., & Seidler, S. (2004). Thermal degradation behaviour of poly(oxymethylene): 1. Degradation and stabilizer consumption. *Polymer Degradation and Stability, 86*(1), 75-83.

Archodoulaki, V. M., Luftl S., Koch T., Seidler S. (2007). Property changes in polyoxymethylene (POM) resulting from processing, ageing and recycling. *Polymer Degradation and Stability, 92*, 2181-2189.

Ashenai Ghasemi, F., Ghasemi, I., Menbari, S., Ayaz, M., & Ashori, A. (2016). Optimization of mechanical properties of polypropylene/talc/graphene composites using response surface methodology. *Polymer Testing, 53*, 283-292.

Azzahari, A., Yusuf, S., Selvanathan, V., & Yahya, R. (2016). Artificial Neural Network and Response Surface Methodology Modeling in Ionic Conductivity Predictions of Phthaloylchitosan-Based Gel Polymer Electrolyte. *Polymers, 8*(2), 22.

Bahadur, S. (2000). The development of transfer layers and their role in polymer tribology. *Wear, 245*, 8.

Bai, S., & Wang, Q. (2012). Effect of injection speed on phase morphology, crystallization behavior, and mechanical properties of polyoxymethylene/poly(ethylene oxide) crystalline/crystalline blend in injection processing. *Polymer Engineering & Science, 52*(9), 1938-1944.

Benabdallah, H. (2003). Friction and wear of blended polyoxymethylene sliding against coated steel plates. *Wear, 254*(12), 1239-1246.

Benabdallah, H., & Olender, D. (2006). Finite element simulation of the wear of polyoxymethylene in pin-on-disc configuration. *Wear, 261*(11-12), 1213-1224.

Biswas, A. K., Cherif, C., Hund, R.-D., Shayed, M. A., & Hossain, M. (2014). Influence of Coatings on Tensile Properties of Glass Fiber. *Materials Science, 20*(1), 50-54.

Bledzki, A. K., Mamun, A. A., & Feldmann, M. (2012). Polyoxymethylene composites with natural and cellulose fibres: Toughness and heat deflection temperature. *Composites Science and Technology, 72*(15), 1870-1874.

Bose, S., Khare, R. A., & Moldenaers, P. (2010). Assessing the strengths and weaknesses of various types of pre-treatments of carbon nanotubes on the properties of polymer/carbon nanotubes composites: A critical review. *Polymer, 51*(5), 975-993.

Box, G. E. P., & Wilson, K. B. (1951). On the Experimental Attainment of Optimum Conditions. In S. Kotz & N. L. Johnson (Eds.), *Breakthroughs in Statistics, Volume II (Methodology and Distribution)* (1st ed., Vol. II). New York, NY: Springer, New York, NY.

Brostow, W., Deborde, J. L., Jaklewicz, M., & Olszynski, P. (2003). Tribology with emphasis on polymers: Friction, scratch resistance and wear. *Journal of Materials Education, 24*(4-6), 119-132.

Brostow, W., Kovačević, V., Vrsaljko, D., & Whitworth, J. (2010). Tribology of polymers and polymer-based composites. *Journal of Materials Education, 32*(5-6), 273-290.

Brostow, W., Lobland, H. E., Hnatchuk, N., & Perez, J. M. (2017). Improvement of Scratch and Wear Resistance of Polymers by Fillers Including Nanofillers. *Nanomaterials (Basel), 7*(3), 66.

Cai, P., Li, Z., Wang, T., & Wang, Q. (2015). Effect of aspect ratios of aramid fiber on mechanical and tribological behaviors of friction materials. *Tribology International, 92*, 109-116.

Cech, V., Palesch, E., & Lukes, J. (2013). The glass fiber-polymer matrix interface/interphase characterized by nanoscale imaging techniques. *Composites Science and Technology, 83*, 5.

Cerclé, C., & Favis, B. D. (2012). Generalizing interfacial modification in polymer blends. *Polymer, 53*(20), 4338-4343.

Chen, J., Cao, Y., & Li, H. (2006). Investigation of the friction and wear behaviors of polyoxymethylene/linear low-density polyethylene/ethylene-acrylic-acid blends. *Wear, 260*(11-12), 1342-1348.

Chen, Z., Zhou, T., Hui, J., Li, L., Li, Y., Zhang, A., & Yuan, T. (2012). Tracing the crystallization process of polyoxymethylene/poly(ethylene oxide) crystalline/crystalline blends by two-dimensional infrared correlation spectroscopy. *Vibrational Spectroscopy, 62*, 299-309.

Chiang, W. Y., & Huang, C. Y. (1999). *Compounding and compatibilization of high-performance polymer alloys and blends* (1st ed.). New York: Marcel Drekker, Inc.

Chiang, W. Y., & Luor, J. J. (1991). The properties of polymer-coated glass fiber reinforced copolymer-type polyacetal composite. *Tatung Journal, 21*(123).

Ching, Y. C., Goh, K. Y., Luqman, C. A., & Kalyani, N. (2012). Effect of nanosilica and titania on thermal stability of polypropylene/oil palm empty fruit fibre composite. *Journal of Biobased Materials and Bioenergy, 6*(6), 6.

Cho, M. H., & Park, S. (2011). Micro CNC surface texturing on polyoxymethylene (POM) and its tribological performance in lubricated sliding. *Tribology International, 44*(7-8), 859-867.

Clark, S. (2014). Plastic Additives Market by Functions (Property Modifiers, Property Stabilizers, Property Extenders, Processing Aids), Product Types (Plasticizers, Flame Retardants, Impact Modifiers, Antioxidants, Antimicrobials, UV Stabilizers) and Applications (Plasticizers, Flame Retardants, Impact Modifiers, Antioxidants, Antimicrobials, UV Stabilizers) - Global Opportunity Analysis and Industry Forecast, 2012 - 2020

Dan-Mallam, Y., Abdul Majid, M. S., & Abdullah, M. Z. (2015). Interfacial Shear Stress in Kenaf/Polyethylene Terephthalate Fiber Reinforced Polyoxymethylene Composite. *Applied Mechanics and Materials, 786*, 74-78.

Dan-mallam, Y., Abdullah, M. Z., & Yusoff, P. S. M. M. (2019). Mechanical Properties of Short and Continuous Kenaf/Pet Fibre Reinforced Polyoxymethylene Composite. *Advanced Composites Letters, 24*(4), 096369351502400.

De Baets, P., Glavatskih, S., Ost, W., & Sukumaran, J. (2014). *Polymer tribology: Challenges and Opportunities*. Paper presented at the 1st International Conference on Polymer Tribology, Bled, Slovenia.

De Santis, F., Gnerre, C., Nobile, M. R., & Lamberti, G. (2017). The rheological and crystallization behavior of polyoxymethylene. *Polymer Testing, 57*, 203-208.

Drelich, J., & Miller, J. D. (1995). A critical review of wetting and adhesion phenomena in the preparation of polymer-mineral composites. *Minerals and Metallurgical Processing, 12*(4), 8.

Dziadur, W. C. (2001). The effect of some elastomers on the structure and mechanical properties of polyoxymethylene. *Materials Characterization, 46*, 5.

Ebewele, R. O. (2000). *Polymer Science and Technology.* New York, USA: CRC Press.

Ebnesajjad, S. (2015). *Fluoroplastics Volume 1: Non-Melt Processible Fluoropolymers - The Definitive User's Guide and Data Book* Vol. 1. New York, USA: Elsevier.

Ebnesajjad, S., & Morgan, R. A. (2012). *Fluoropolymer Additives.* New York, USA: Elsevier.

Espinach, F. X., Granda, L. A., Tarrés, Q., Duran, J., Fullana-i-Palmer, P., & Mutjé, P. (2017). Mechanical and micromechanical tensile strength of eucalyptus bleached fibers reinforced polyoxymethylene composites. *Composites Part B: Engineering, 116*, 333-339.

Forintos, N., & Czigany, T. (2019). Multifunctional application of carbon fiber reinforced polymer composites: Electrical properties of the reinforcing carbon fibers – A short review. *Composites Part B: Engineering, 162*, 331-343.

Franklin, S. E., & de Kraker, A. (2003). Investigation of counterface surface topography effects on the wear and transfer behaviour of a POM–20% PTFE composite. *Wear, 255*(1-6), 766-773.

Fried, J. R. (2014). *Polymer Science & Technology* (Third ed.). Massachusetts, USA: Prentice Hall.

Fu, Y. F., Hu, K., Li, J., Sun, Z. H. Y., Zhang, F. Q., & Chen, D. M. (2012). Influence of nano-SiO_2 and carbon fibers on the mechanical properties of POM composites. *Mekhanika Kompozitnykh Materialov, 47*(6), 931-936.

Gadioli, R., Morais, J. A., Waldman, W. R., & De Paoli, M.-A. (2014). The role of lignin in polypropylene composites with semi-bleached cellulose fibers: Mechanical properties and its activity as antioxidant. *Polymer Degradation and Stability, 108*, 23-34.

Gao, Y., Sun, S., He, Y., Wang, X. D., & Wu, D. Z. (2011). Effect of poly(ethylene oxide) on tribological performance and impact fracture behavior of polyoxymethylene/polytetrafluoroethylene fiber composites. *Composites Part B: Engineering, 42*(7), 1945-1955.

Giannekas, N., Zhang, Y., & Tosello, G. (2018). Investigation on Product and Process Fingerprints for Integrated Quality Assurance in Injection Molding of Microstructured Biochips. *Journal of Manufacturing and Materials Processing, 2*(4), 79.

Graupner, N., Rößler, J., Ziegmann, G., & Müssig, J. (2014). Fibre/matrix adhesion of cellulose fibres in PLA, PP and MAPP: A critical review of pull-out test, microbond test and single fibre fragmentation test results. *Composites Part A: Applied Science and Manufacturing, 63*, 133-148.

Guo, X., Zhang, J., & Huang, J. (2015). Poly(lactic acid)/polyoxymethylene blends: Morphology, crystallization, rheology, and thermal mechanical properties. *Polymer, 69*, 103-109.

Harper, C. A. (1999). *Modern Plastics Handbook.* New York, USA: McGraw Hill.

Ho, M., Wang, H., Lee, J., Ho, C., Lau, K., Leng, J., & Hui, D. (2012). Critical factors on manufacturing processes of natural fibre composites. *Composites Part B: Engineering, 43*(8), 3549-3562.

Hsu, C. I., Hwang, J. R., & Ting, P. H. (2010). Influence of Process Conditions on Tensile Properties Polyoxymethylene Composite. *Journal of Reinforced Plastics and Composites, 29*(16), 11.

Hu, K. H., Wang, J., Schraube, S., Xu, Y. F., Hu, X. G., & Stengler, R. (2009). Tribological properties of MoS_2 nano-balls as filler in polyoxymethylene-based composite layer of three-layer self-lubrication bearing materials. *Wear, 266*(11-12), 1198-1207.

Huang, C. Y., Kuo, M. C., & Roan, M. L. (2016). Increasing the Compatability of Self-Lubricated POM/PTFE Fiber Composite. *Academia Journal of Scientific Research, 4*(7), 168-179.

Huang, C. Y., & Tseng, C. I. (2000). The Effect of Interface Modification between POM and PTFE on the Properties of POM/PTFE Composites. *Journal of Applied Polymer Science, 78*, 800-807.

Huang, T., Lu, R., Wang, H., Ma, Y., Tian, J., & Li, T. (2011). Investigation on the Tribological Properties of POM Modified by Nano-PTFE. *Journal of Macromolecular Science, Part B, 50*(7), 1235-1248.

Huawei Zou, Wei Luo, Qianming Ding, Yi Li, Shengtai Zhou, & Liang, M. (2015). Effect of shape morphology on mechanical, rheological and tribological properties of polyoxymethylene/aramid composites. *Polymer Science Series A, 57*(2), 12.

Hunke, H., Soin, N., Shah, T., Kramer, E., Pascual, A., Karuna, M., & Siores, E. (2015). Low-Pressure H_2, NH_3 Microwave Plasma Treatment of Polytetrafluoroethylene (PTFE) Powders: Chemical, Thermal and Wettability Analysis. *Materials, 8*(5), 2258-2275.

Hunke, H., Soin, N., Shah, T., Kramer, E., Witan, K., & Siores, E. (2015). Influence of plasma pre-treatment of polytetrafluoroethylene (PTFE) micropowders on the mechanical and tribological performance of Polyethersulfone (PESU)–PTFE composites. *Wear, 328-329*, 480-487.

Jesson, D. A., & Watts, J. F. (2012). The Interface and Interphase in Polymer Matrix Composites: Effect on Mechanical Properties and Methods for Identification. *Polymer Reviews, 52*(3), 34.

Jones, F. R. (2012). Interphase in fiber-reinforced composites. *Wiley Encyclopedia of Composites*. NJ, USA: John Wiley & Sons.

Kalacska, G. (2012). An engineering approach to dry friction behaviour of numerous engineering plastics with respect to the mechanical properties. *Express Polymer Letters, 7*(2), 199-210.

Karger-Kocsis, J., Mahmood, H., & Pegoretti, A. (2015). Recent advances in fiber/matrix interphase engineering for polymer composites. *Progress in Materials Science, 73*, 1-43.

Kreivaitis, R., Zunda, A., Padgurskas, J., Zicans, J., Meri, R. M., Kokins, A., & Bochkov, I. (2015). Nanostructured zinc oxide filler for modification of polymer-polymer composites: structure and tribological properties. *Proceedings of the Estonian Academy of Sciences, 64*(1S), 82.

Krishna, B., Suresha, S. S., Kallesh, R., & Hemanth. (2016). Effect of Fillers on Erosive Wear behavior of Polyoxymethylene/Polytetrafluoroethylene Blend and their Composites: A Statistical Approach. *Indian journal of Advances in Chemical Science, S1*, 7.

Kuciel, S., Bazan, P., Liber-Knec, A., & Gadek-Moszczak, A. (2019). Physico-Mechanical Properties of the Poly(oxymethylene) Composites Reinforced with Glass Fibers under Dynamical Loading. *Polymers (Basel), 11*(12).

Kunnan Singh, J. S., Ching, Y., Abdullah, L., Ching, K., Razali, S., & Gan, S. (2018). Optimization of Mechanical Properties for Polyoxymethylene/Glass Fiber/Polytetrafluoroethylene Composites Using Response Surface Methodology. *Polymers, 10*(3), 338.

Kunnan Singh, J. S., Ching, Y. C., Liu, S., Ching, K. Y., Razali, S., & Gan, S. N. (2018). Effects of PTFE Micro-Particles on the Fiber-Matrix Interface of Polyoxymethylene/Glass Fiber/Polytetrafluoroethylene Composites. *Materials (Basel), 11*(11).

Lam, K. L., Abu Bakar, A., & Mohd Ishak, Z. A. (2004). Amorphous Copolyester/Polyoxymethylene Blends: Thermal, Mechanical and Morphological Properties. *KGK Kautschuk Gummi Kunststoffe, 57*(11), 9.

Laursen, J. L., Sivebaek, I. M., Christoffersen, L. W., Papsoee, M., Vigild, M. E., Brondsted, P., & Horsewell, A. (2009). Influence of tribological additives on friction and impact performance of injection moulded polyacetal. *Wear, 267*(12), 2294-2302.

Le Roy, L., Briani, G., Briois, C., Cottin, H., Fray, N., Thirkell, L., . . . Hilchenbach, M. (2012). On the prospective detection of polyoxymethylene in comet 67P/Churyumov–Gerasimenko with the COSIMA instrument onboard Rosetta. *Planetary and Space Science, 65*(1), 83-92.

Liang, C. Y., & Krimm, S. (1995). Infrared Spectra of High Polymers. III. Polytetrafluoroethylene and Polychlorotrifluoroethylene. *The Journal of Chemical Physics, 25*(3), 9.

Liu, B., Pei, X., Wang, Q., Wang, T., & Sun, X. (2012). Structural and Tribological Properties of Polytetrafluoroethylene Composites Filled with Glass Fiber and Al_2O_3 in Atomic Oxygen Environment. *Journal of Macromolecular Science, Part B, 51*(11), 2245-2254.

Liu, L., Wang, X., Zou, H., Yu, M., & Xie, W. (2017). Optimizing synthesis parameters of short carbon fiber reinforced polysulfonamide composites by using response surface methodology. *Polymer Testing, 59*, 355-361.

Liu, Z., Zeng, W., Yang, R., & Yang, F. (2015). Carbamate end-capped poly(oxymethylene) copolymer with enhanced thermal stability prepared by reactive extrusion. *Polymer Degradation and Stability, 111*, 131-141.

Luo, Y., Zhao, Y., Duan, Y., & Du, S. (2011). Surface and wettability property analysis of CCF300 carbon fibers with different sizing or without sizing. *Materials & Design, 32*(2), 941-946.

Marturano, V., Cerruti, P., & Ambrogi, V. (2017). Polymer additives. *Physical Sciences Reviews, 2*(6).

Mathurosemontri, S., Auwongsuwan, P., Nagai, S., & Hamada, H. (2014). The Effect of Injection Speed on Morphology and Mechanical Properties of Polyoxymethylene/Poly(Lactic Acid) Blends. *Energy Procedia, 56*, 57-64.

Mergler, Y. J., Schaake, R. P., & Huis in't Veld, A. J. (2004). Material transfer of POM in sliding contact. *Wear, 256*(3-4), 294-301.

Mihály, J., Sterkel, S., Ortner, H. M., Kocsis, L., Hajba, L., Furdyga, E., & Minka, J. (2006). FTIR and FT-Raman Spectroscopic Study on Polymer Based High Pressure Digestion Vessels. *Croatica Chemica Acta, 79*(3), 5.

Mohan Babu, K., & Mettilda, M. (2014). Studies on Mechanical, Thermal, and Morphological Properties of Glass Fibre Reinforced Polyoxymethylene Nanocomposite. *Journal of Applied Chemistry, 2014*, 1-8.

Montgomery, D. C. (2013). *Design and Analysis of Experiments* (8th ed.). NJ: John Wiley & Sons, Inc.

Myshkin, N. K., Pesetskii, S. S., & Grigoriev, A. Y. (2015). Polymer Tribology: Current State and Applications. *Tribology in Industry, 37*(3), 6.

Nirmal, U., Hashim, J., & Lau, S. T. W. (2011). Testing methods in tribology of polymeric composites. *International Journal of Mechanical and Materials Engineering, 6*(3), 6.

Olmos, D., Arroyo, J. M., & González-Benito, J. (2012). Interphase morphology in glass fiber/PMMA modified epoxy matrix composites. Effect of molecular weight of PMMA. *Polymer Testing, 31*(6), 785-791.

Papanicolaou, G. C., Paipetis, A. S., & Theocaris, P. S. (1978). The concept of boundary interphase in composite mechanics. *Composite and Polymer Science, 256*(7), 6.

Patrick, J. W., & Mark, J. A. (2005). *RSM Simplified: Optimizing Processes Using Response Surface Methods for Design of Experiments*: Productivity Press, a division of Karus Productivity.

Pedrazzoli, D., & Pegoretti, A. (2014). Expanded graphite nanoplatelets as coupling agents in glass fiber reinforced polypropylene composites. *Composites Part A: Applied Science and Manufacturing, 66*, 25-34.

Pesetskii, S. S., Bogdanovich, S. P., & Myshkin, N. K. (2013). Tribological behavior of polymer nanocomposites produced by dispersion of nanofillers in molten thermoplastics. 119-162.

Poulios, K., Drago, N., Klit, P., & De Chiffre, L. (2014). A reciprocating pin-on-plate test-rig for studying friction materials for holding brakes. *Wear, 311*(1-2), 40-46.

Prabhakar, K., Debnath, S., Ganesan, R., & Palanikumar, K. (2018). A review of mechanical and tribological behaviour of polymer composite materials. *IOP Conference Series: Materials Science and Engineering, 344*, 012015.

Rahman, M. S., Shaislamov, U., Yang, J.-K., Kim, J.-K., Yu, Y. H., Choi, S., & Lee, H.-J. (2016). Effects of electron beam irradiation on tribological and physico-chemical properties of Polyoxymethylene copolymer (POM-C). *Nuclear Instruments and Methods in Physics Research Section B: Beam Interactions with Materials and Atoms, 387*, 54-62.

Rye, R. R., & Arnold, G. W. (1989). Depth dependence of alkali etching of polytetrafluoroethylene: effect of X-ray radiation. *Langmuir, 5*, 4.

Saba, N., Paridah, M. T., & Jawaid, M. (2015). Mechanical properties of kenaf fibre reinforced polymer composite: A review. *Construction and Building Materials, 76*, 87-96.

Samyn, P., De Baets, P., Schoukens, G., & Quintelier, J. (2007). Wear transitions and stability of polyoxymethylene homopolymer in highly loaded applications compared to small-scale testing. *Tribology International, 40*(5), 819-833.

Sauer, B. B., & Carney, T. E. (1990). Dynamic contact angle measurement on glass fibers: Influence of fiber diameter on hysterisis and contact line pinning. *Langmuir, 6*(5), 1002-1007.

Schöneich, M., Zamanzade, M., & Stommel, M. (2015). Fiber-matrix interphase in applied short glass fiber composites determined by a nano-scratch method. *Composites Science and Technology, 119*, 100-107.

Siengchin, S., Karger-Kocsis, J., Psarras, G. C., & Thomann, R. (2008). Polyoxymethylene/polyurethane/alumina ternary composites: Structure, mechanical, thermal and dielectric properties. *Journal of Applied Polymer Science, 110*(3), 1613-1623.

Siengchin, S., Karger-Kocsis, J., & Thomann, R. (2008). Nanofilled and/or toughened POM composites produced by water-mediated melt compounding: Structure and mechanical properties. *Express Polymer Letters, 2*(10), 746-756.

Singh, G., & Verma, A. (2017). A Brief Review on injection moulding manufacturing process. *Materials Today: Proceedings, 4*(2), 1423-1433.

Sun, L.-H., Yang, Z.-G., & Li, X.-H. (2008a). Mechanical and tribological properties of polyoxymethylene modified with nanoparticles and solid lubricants. *Polymer Engineering & Science, 48*(9), 1824-1832.

Sun, L.-H., Yang, Z.-G., & Li, X.-H. (2008b). Study on the friction and wear behavior of POM/Al_2O_3 nanocomposites. *Wear, 264*(7-8), 693-700.

Suresha, B., Hemanth, R., & Sekar, M. (2014). Effects of Fibers and Fillers on Mechanical Properties of Thermoplastic Composites. *Indian journal of Advances in Chemical Science, 2*, 8.

Udenni Gunathilake, T., Ching, Y., Ching, K., Chuah, C., & Abdullah, L. (2017). Biomedical and Microbiological Applications of Bio-Based Porous Materials: A Review. *Polymers, 9*(12), 160.

Unal, H., Mimaroglu, A., & Demir, Z. (2010). Tribological Performance of POM, PTFE and PSU Composites Used in Electrical Engineering Applications. *International Journal of Polymeric Materials, 59*(10), 808-817.

Upadhyaya, P., & Kumar, S. (2015). Micromechanics of stress transfer through the interphase in fiber-reinforced composites. *Mechanics of Materials, 89*, 190-201.

Utracki, L. A. (1990). *Polymer Blends and Alloys: Thermodynamics and Rheology*: Hanser Gardner Publications.

Van de Velde, K., & Kiekens, P. (2000). Wettability and surface analysis of glass fibres. *Indian Journal of Fibre & Textile research, 25*(2000), 8-13.

Vesel, A., Kovac, J., Zaplotnik, R., Modic, M., & Mozetic, M. (2015). Modification of polytetrafluoroethylene surfaces using H_2S plasma treatment. *Applied Surface Science, 357*, 1325-1332.

Wacharawichanant, S., Thongyai, S., Phutthaphan, A., & Eiamsam-ang, C. (2008). Effect of particle sizes of zinc oxide on mechanical, thermal and morphological properties of polyoxymethylene/zinc oxide nanocomposites. *Polymer Testing, 27*(8), 971-976.

Wang, J., Hu, K. H., Xu, Y. F., & Hu, X. G. (2008). Structural, thermal, and tribological properties of intercalated polyoxymethylene/molybdenum disulfide nanocomposites. *Journal of Applied Polymer Science, 110*(1), 91-96.

Wang, M., Zhang, C., & Wang, X. (2017). The Wear Behavior of Textured Steel Sliding against Polymers. *Materials (Basel), 10*(4).

Wang, Y., Kim, J.-g., & Song, J.-i. (2014). Optimization of plastic injection molding process parameters for manufacturing a brake booster valve body. *Materials & Design (1980-2015), 56*, 313-317.

Xie, T., Feng, S., Qi, Y., & Cui, A. (2018). Effect of Self-Generated Transfer Layer on the Tribological Properties of PTFE Composites Sliding against Steel. *Coatings, 8*(11), 399.

Xie, X., Mai, Y., & Zhou, X. (2005). Dispersion and alignment of carbon nanotubes in polymer matrix: A review. *Materials Science and Engineering: R: Reports, 49*(4), 89-112.

Yan, L., Chouw, N., & Jayaraman, K. (2014). Flax fibre and its composites – A review. *Composites Part B: Engineering, 56*, 296-317.

Yao, S.-S., Jin, F.-L., Rhee, K. Y., Hui, D., & Park, S.-J. (2018). Recent advances in carbon-fiber-reinforced thermoplastic composites: A review. *Composites Part B: Engineering, 142*, 241-250.

Yu, N., He, L., Ren, Y., & Xu, Q. (2011). High-crystallization polyoxymethylene modification on carbon nanotubes with assistance of supercritical carbon dioxide: Molecular interactions and their thermal stability. *Polymer, 52*(2), 472-480.

Zhang, J., Deng, S., Wang, Y., Ye, L., Zhou, L., & Zhang, Z. (2013). Effect of nanoparticles on interfacial properties of carbon fibre–epoxy composites. *Composites Part A: Applied Science and Manufacturing, 55*, 35-44.

Zhang, L., Qi, H., Li, G., Zhang, G., Wang, T., & Wang, Q. (2017). Impact of reinforcing fillers' properties on transfer film structure and tribological performance of POM-based materials. *Tribology International, 109*, 58-68.

Zhao, X., & Ye, L. (2011a). Structure and mechanical properties of polyoxymethylene/multi-walled carbon nanotube composites. *Composites Part B: Engineering, 42*(4), 926-933.

Zhao, X., & Ye, L. (2011b). Structure and properties of highly oriented polyoxymethylene/multi-walled carbon nanotube composites produced by hot stretching. *Composites Science and Technology, 71*(10), 1367-1372.

Zsidai, L., De Baets, P., Samyn, P., Kalacska, G., Van Peteghem, A. P., & Van Parys, F. (2002). The tribological behaviour of engineering plastics during sliding friction investigated with small-scale specimens. *Wear, 253*(5-6), 673-688.

LIST OF PUBLICATIONS AND PAPERS PRESENTED

Journals

1. **Kunnan Singh, J. S., Ching, Y.C., Abdullah, L., Ching, K.Y., Razali, S., & Gan, S.N. (2018). Effects of PTFE Micro–Particles on the Fiber–Matrix Interface of Polyoxymethylene/Glass Fiber/Polytetrafluoroethylene Composites;** *Materials,* Vol. 11(11), 2164

2. **Kunnan Singh, J. S., Ching, Y. C., Liu, S., Ching, K. Y., Razali, S., & Gan, S. N. Optimization of Mechanical Properties for Polyoxymethylene/Glass Fiber/Polytetrafluoroethylene Composites using Response Surface Methodology;** (2018) Polymers, Vol. 10(3), 338

Proceedings

1. **Kunnan Singh, J.S. Effects of Polytetrafluoroethylene Micro Powder Adhesion on Glass Fiber Reinforced Polyoxymethylene.** *International Symposium on Advanced Polymeric Materials (ISAPM 2016)*